

METAHEURISTIC BASED SOIL PARAMETER IDENTIFICATION IN DEEP  
EXCAVATIONS

A THESIS SUBMITTED TO  
THE GRADUATE SCHOOL OF NATURAL AND APPLIED SCIENCES  
OF  
MIDDLE EAST TECHNICAL UNIVERSITY

BY

ABDÜLSAMED AKGÜL

IN PARTIAL FULFILLMENT OF THE REQUIREMENTS  
FOR  
THE DEGREE OF MASTER OF SCIENCE  
IN  
CIVIL ENGINEERING

SEPTEMBER 2019



Approval of the thesis:

**METAHEURISTIC BASED SOIL PARAMETER IDENTIFICATION IN  
DEEP EXCAVATIONS**

submitted by **ABDÜLSAMED AKGÜL** in partial fulfillment of the requirements for the degree of **Master of Science in Civil Engineering Department, Middle East Technical University** by,

Prof. Dr. Halil Kalıpçılar  
Dean, Graduate School of **Natural and Applied Sciences**

\_\_\_\_\_

Prof. Dr. Ahmet Türer  
Head of Department, **Civil Engineering**

\_\_\_\_\_

Assist. Prof. Dr. Onur Pekcan  
Supervisor, **Civil Engineering, METU**

\_\_\_\_\_

**Examining Committee Members:**

Prof. Dr. Oğuzhan Hasaebi  
Civil Engineering, METU

\_\_\_\_\_

Assist. Prof. Dr. Onur Pekcan  
Civil Engineering, METU

\_\_\_\_\_

Assoc. Prof. Dr. Zeynep Gülerce  
Civil Engineering, METU

\_\_\_\_\_

Assoc. Prof. Dr. Ercan Gürses  
Aerospace Engineering, METU

\_\_\_\_\_

Assist. Prof. Dr. Ebru Akış  
Civil Engineering, Atılım University

\_\_\_\_\_

Date: 20.09.2019

**I hereby declare that all information in this document has been obtained and presented in accordance with academic rules and ethical conduct. I also declare that, as required by these rules and conduct, I have fully cited and referenced all material and results that are not original to this work.**

Name, Surname: Abdülsamed Akgül

Signature:

## **ABSTRACT**

### **METAHEURISTIC BASED SOIL PARAMETER IDENTIFICATION IN DEEP EXCAVATIONS**

Akgül, Abdülsamed  
Master of Science, Civil Engineering  
Supervisor: Assist. Prof. Dr. Onur Pekcan

September 2019, 123 pages

Attaining accurate ground parameters in the design of cost- efficient underground structures is essential due to the level of complexity and uncertainty in soil- structure interactions and ground conditions. Backcalculation methods have an increasing popularity in the field of geotechnical engineering due to the fact that these methods rely on laboratory and field tests in addition to field monitoring and field information which delivers genuine structure conditions. Therefore, the use of this method provides much more accurate geomechanical parameters of materials in deep excavations when compared to conventional methods. Moreover, acquiring these parameters in a faster method aids in the calibration of the parameters during fast track construction projects. In this study, a finite element based backcalculation is developed through the use of Particle Swarm Optimization algorithm (PSO). The PSO algorithm, which is embedded in the back-analysis platform, acts as an intelligent parameter selection process which provides data for the finite element method. The reaction of the deep excavation structure is attained through two-dimensional finite element analyses. This developed back analysis framework is then tested using the ground deformation data obtained from the deep excavation case study in Ankara/Turkey. The parameters of soil are backcalculated and these parameters are

then used for future predictions of deep excavation response. The attainment of the successful results has been observed due to the use of the optimization algorithm and the sensitivity of the measured values. This backcalculation using the PSO algorithm can be used to create more realistic models for the construction of underground structures which share the same properties and ground conditions.

Keywords: Deep Excavations, Backcalculation, Particle Swarm Optimization, Metaheuristic, Soil Parameter Identification

## ÖZ

### **DERİN KAZILARDAKİ PARAMETRELERİN SAPTANMASINDA METASEZGİSEL TABANLI GERİ HESAPLANMA YÖNTEMİ**

Akgül, Abdülsamed  
Yüksek Lisans, İnşaat Mühendisliği  
Tez Danışmanı: Dr. Öğr. Üyesi Onur Pekcan

Eylül 2019, 123 sayfa

Zemin koşullarındaki belirsizlikler ve zeminin karmaşık yapısı nedeniyle, derin kazılar gibi yapıların tasarımlarında kullanılan geoteknik parametrelerinin doğru belirlenmesi, imalatların ekonomik olması hususunda büyük önem taşımaktadır. Laboratuvar ve saha deneylerinin yanı sıra arazide gözlem verilerine dayanan ve saha şartlarını daha gerçekçi yansıtan geri hesaplama yöntemleri, özellikle geoteknik mühendisliği alanında son dönemlerde popülerliğini artırmaktadır. Geri hesaplama yöntemi kullanılarak, derin kazı inşaat aşamasında yapılan deplasman gözlemleri sayesinde, kazı çevresinde bulunan malzeme parametreleri standart tekniklere göre daha gerçekçi olarak elde edilebilmektedir. Zemin parametrelerinin pratik şekilde elde edilmesi, derin kazı inşaat aşamasında kullanılacak parametrelerin kalibrasyonu açısından da büyük önem taşımaktadır. Bu çalışmada, sürü optimizasyonu yöntemi kullanılarak sonlu elemanlara dayanan bir geri hesaplama yöntemi geliştirilmiştir. Geliştirilen platformda, metasezgisel optimizasyon algoritması, sonlu elemanlar yöntemine veri sağlayan akıllı bir parametre seçim yöntemi olarak geri hesaplama yönteminin içine gömülmüştür. İksa yapılarının tepkileri ise 2 boyutlu sonlu elemanlar analizleri ile elde edilmiştir. Geliştirilen geri hesaplama platformu, örnek bir iksa projesi sırasında ölçülen deformasyon verileri kullanılarak test edilmiş ve böylelikle derin kazı çevresindeki malzeme parametrelerinin geri hesaplanması da sağlanmıştır.

Daha sonra bu parametreler ileri hesaplama yöntemi kullanılarak, sonraki kazı aşamaları tahmin edilmeye çalışılmıştır. Elde edilen sonuçların başarısının, ölçüm verilerinin hassasiyetine ve kullanılan optimizasyon algoritmasının seçimine bağlı olduğu gözlenmiştir. Raporlanan parametreler aynı zemin yapısına sahip birimlerde açılacak olan yeni yer altı yapılarının gerçekçi modellenmesinde kullanılabilir.

Anahtar Kelimeler: Derin Kazılar, Geri Hesaplama, Parçacık Sürü Optimizasyonu, Metasezgisel, Parametre Saptanması

To my dear family...

## ACKNOWLEDGEMENTS

My greatest gratitude goes to my supervisor Asst. Prof. Dr. Onur Pekcan without whom the completion of this study would be unachievable. I always felt your endless support both for academic and personal life. I am THANKFUL to him from my heart.

I am also grateful to *Toker Drilling and Construction Co.* for sharing the case study and providing reliable field data for this study.

I would also like to thank my colleagues and dear friends Gönç Berk Güneş, Muhammed Fadi Anzarouti and Berkan Söylemez for their technical supports and assistance in many instances during my thesis journey.

I express my sincere thanks to my partners in *Geoda Technical Instrumentation Co.*

Last but not least, I am GRATEFUL to my parents and my brothers for their eternal faith and patience until the end.

## TABLE OF CONTENTS

ABSTRACT .....	v
ÖZ .....	vii
ACKNOWLEDGEMENTS .....	x
TABLE OF CONTENTS .....	xi
LIST OF TABLES .....	xiv
LIST OF FIGURES .....	xv
LIST OF ABBREVIATIONS .....	xx
LIST OF SYMBOLS .....	xxii
CHAPTERS	
1. INTRODUCTION .....	1
1.1. General .....	1
1.2. Research Objective .....	4
1.3. Scope .....	5
1.4. Thesis Outline.....	6
2. LITERATURE SURVEY .....	7
2.1. Introduction .....	7
2.2. Commonly Used Design Approaches for Estimating Deep Excavation-induced Movements .....	8
2.3. Deep Excavation Monitoring .....	22
2.3.1. Inclinometers .....	23
2.4. Numerical analysis of Deep Excavations .....	25
2.4.1. Finite Element Method (FEM) .....	26

2.4.1.1. PLAXIS Software .....	27
2.4.2. Conventional Constitutive Modeling for Deep Excavations.....	28
2.5. Back Analysis in Geotechnical Engineering.....	30
2.5.1. Assessment on Measured and Calculated Displacement using Back Analysis .....	33
2.6. Observational Method.....	36
2.6.1. Optimization Techniques .....	37
2.6.1.1. Nature-inspired (Metaheuristic) Search Methods.....	40
2.6.1.2. Particle Swarm Optimization (PSO).....	41
3. BACK ANALYSIS PLATFORM.....	43
3.1. Introduction.....	43
3.2. Development of Back-analysis Platform for Deep Excavation-induced Movements.....	43
3.2.1. Finite Element Analysis Configuration.....	45
3.2.2. Particle Swarm Optimization Algorithm.....	49
4. CASE STUDY: DEEP EXCAVATION OF MAIDAN OFFICE – HOME OFFICE - SQUARE .....	55
4.1. Introduction.....	55
4.2. Project Description.....	55
4.2.1. Geological and Geotechnical Information .....	57
4.2.2. Construction and Monitornig .....	63
4.3. Finite Element Model.....	65
4.4. Application and the Performance of Particle Swarm Optimization.....	77
4.4.1. Initial Design Performance.....	78
4.4.2. Optimization based on Stage 1 Observations.....	81

4.4.3. Optimization based on Stage 2 Observations .....	83
4.4.4. Optimization based on Stage 3 Observations .....	85
4.4.5. Optimization based on Stage 4 Observations .....	87
4.4.6. Optimization based on Stage 5 Observations .....	89
4.5. Forward Predictions with Optimized Parameters.....	91
4.5.1. Horizontal Displacement Prediction of Stage 2.....	91
4.5.2. Horizontal Displacement Prediction of Stage 3.....	92
4.5.3. Horizontal Displacement Prediction of Stage 4.....	93
4.5.4. Horizontal Displacement Prediction of Stage 5.....	94
4.6. Results and Comparisons .....	95
5. SUMMARY AND CONCLUSION .....	103
5.1. Summary .....	103
5.2. Findings of the Study .....	104
5.3. Recommendations for Future Study .....	108
REFERENCES.....	109
APPENDICES	
A. Borehole Logs.....	119
B. Inclinator #2 Readings .....	122
C. Laboratory Test Results .....	123

## LIST OF TABLES

### TABLES

Table 2.1. Comparison of Wall Displacements Measured in Worldwide Case Histories (Wang et al., 2009) .....	20
Table 3.1. Parameters of Hardening Soil Model .....	47
Table 4.1. Initial Design Parameters of Soil Materials.....	57
Table 4.2. $\alpha' - \tan\phi'$ Relationship (Lunne, 1997).....	58
Table 4.3. Search Range of Optimized Parameters .....	66
Table 4.4. Construction Stages and Calculation Phases in Numerical Model.....	77
Table 4.5. Optimized Parameters after Stage 1 .....	83
Table 4.6. Optimized Parameters after Stage 2 .....	85
Table 4.7. Optimized Parameters after Stage 3 .....	87
Table 4.8. Optimized Parameters after Stage 4 .....	89
Table 4.9. Optimized Parameters after Stage 5 .....	91
Table 4.10. Best-fit Values of Parameters at Each Optimization Stages.....	96
Table 4.11. Calculated Fitness Values at Each Optimization Stages .....	99
Table 4.12. Completion Period of Each Optimization Stages .....	102

## LIST OF FIGURES

### FIGURES

Figure 1.1. Özdilek Shopping Mall (24 m of Diaphragm Wall) – Bursa, Turkey – The Fourth Highest Population in Turkey with 2.9 Million .....	1
Figure 1.2. Ankara Metro 3. Stage Kızılay Retaining System (35 m Deep Station) – Ankara, Turkey – The Second Highest Population in Turkey with 5.5 Million .....	2
Figure 2.1. Relationship between Factor of Safety against Basal Heave and Maximum Lateral Wall Movements (Mana and Clough, 1981) .....	10
Figure 2.2. Relationship between Time and Maximum Lateral Wall Movements (Mana and Clough, 1981) .....	10
Figure 2.3. Relationship between Maximum Ground Settlements and Maximum Lateral Wall Movements (Mana and Clough, 1981).....	11
Figure 2.4. Relationship Factor of Safety against Basal Heave and Maximum Lateral Wall Movements (Mana and Clough, 1981).....	11
Figure 2.5. Relationship between Maximum Surface Settlements and Maximum Lateral Wall Movement (Mana and Clough, 1981).....	12
Figure 2.6. Monitored Maximum Lateral Movements for In-situ Walls in Stiff Clays, Residual Soils and Sands (Clough and O’Rourke, 1990) .....	13
Figure 2.7. Monitored Maximum Settlements in the Soil Retained by In-situ Walls (Clough and O’Rourke, 1990).....	14
Figure 2.8. Maximum Horizontal Wall Movement in Stiff Soils (Obtained by using Finite Element Analyses) (Clough and O’Rourke, 1990).....	14
Figure 2.9. Design Curves for Maximum Horizontal Wall Movement for excavations in Soft to Medium Clays (Clough and O’Rourke, 1990).....	15
Figure 2.10. Movement Patterns of Braced and Tied-Back Walls (Clough and O’Rourke, 1990) .....	16

Figure 2.11. Relationship between Lateral Movement of Wall and Excavation Depth for Different Supporting System (Wang et al., 2009).....	19
Figure 2.12. Deflection Paths of Diaphragm Walls with Different Thickness (Wang et al., 2009) .....	21
Figure 2.13. Relationship between System Stiffness and Normalized Maximum Horizontal Movement (Wang et al., 2009) .....	22
Figure 2.14. Deep Excavation Monitoring Instruments (source: <a href="http://www.recordtek.com/solutions/geotechnical-solution/">http://www.recordtek.com/solutions/geotechnical-solution/</a> ) [last accessed on 13.09.2019].....	23
Figure 2.15. Inclinator Casing (source <a href="http://www.geotechnicaltrade.com/product-detail/pvc-inclinometer-casing">http://www.geotechnicaltrade.com/product-detail/pvc-inclinometer-casing</a> ) [last accessed on 14.05.2019] .....	24
Figure 2.16. Typical Inclinator System including Probe, Cable, Readout Unit (source: <a href="http://www.geodata.com/geodata-aletsel-gozlem-cihazlari.html">http://www.geodata.com/geodata-aletsel-gozlem-cihazlari.html</a> ) [last accessed on 04.05.2019].....	24
Figure 2.17. Schematic of Inclinator Probe placed in Casing (Mikkelsen, 1996)	25
Figure 2.18. Non-linear Stress-Strain Curve and Inconstant Soil Stiffness (Liong, 2014).....	28
Figure 2.19. Common Approach to Modeling of Geomechanics Problems (Hashash et al., 2003) .....	30
Figure 2.20. Difference between Forward Analysis and Back Analysis (Sakurai, 1997) .....	31
Figure 2.21. Schema of Iterative Back Analysis Procedure (Calvello and Finno, 2004) .....	32
Figure 2.22. Comparison of Predicted and Measured Lateral Wall Deflections (Whittle, Hashash, and Whitman, 1993) .....	35
Figure 3.1. Back Analysis Platform Flowchart .....	44
Figure 3.2. Generated Mesh Example of Deep Excavation with Supported Wall ....	46
Figure 3.3. Hyperbolic Stress-Strain relation in Primary Loading for a Standard Drained Triaxial Test (PLAXIS 2D User's Manual, 2010).....	48
Figure 3.4. Position Update Process using PSO .....	52

Figure 3.5. PSO Algorithm Flow Chart .....	52
Figure 4.1. The location of the Project (retrieved from soil investigation report “Ankara İli, Çankaya İlçesi, 25389 Ada, 3 Parsel Jeolojik – Jeoteknik Etüt Raporu” by Toker Drilling and Construction Engineering Consultancy CO).....	56
Figure 4.2. $\sigma'$ -PI Relationship (Gibson, 1953).....	58
Figure 4.3. SPT- $N_{60}$ - $C_u$ – PI Relationship (Stroud,1974) .....	59
Figure 4.4. Project Layout and Instrumentation Plan (retrieved from soil investigation report “Ankara İli, Çankaya İlçesi, 25389 Ada, 3 Parsel Jeolojik – Jeoteknik Etüt Raporu” by Toker Drilling and Construction Engineering Consultancy CO) .....	60
Figure 4.5. SPT-N values of SK-14 and Geological Section up to 40 m (retrieved from Toker Drilling and Construction Engineering Consultancy CO).....	62
Figure 4.6. Ground Profile and Deep Excavation Geometry .....	63
Figure 4.7. Inclinomometer #2 Cumulative Readings .....	64
Figure 4.8. Numerical Model Properties.....	65
Figure 4.9. Finite Element Mesh.....	67
Figure 4.10. (a) Groundwater Level Definition; (b) Groundwater Flow through the Pile .....	69
Figure 4.11. Initial Phase .....	70
Figure 4.12. Phase 1 .....	70
Figure 4.13. Phase 2 .....	71
Figure 4.14. Phase 3 .....	71
Figure 4.15. Phase 4 .....	72
Figure 4.16. Phase 5 .....	72
Figure 4.17. Phase 6 .....	73
Figure 4.18. Phase 7 .....	73
Figure 4.19. Phase 8 .....	74
Figure 4.20. Phase 9 .....	74
Figure 4.21. Phase 10 .....	75
Figure 4.22. Phase 11 .....	75
Figure 4.23. Phase 12 .....	76

Figure 4.24. Measured versus Computed Deflections: Initial Design Parameters ....	80
Figure 4.25. Evolution of Particle's Best Positions pBest in Different Iterations for Stage 1: (a) 1 <sup>st</sup> iteration; (b) 10 <sup>th</sup> iteration; (c) 15 <sup>th</sup> iteration;(d) 20 <sup>th</sup> iteration .....	81
Figure 4.26. gBest Fitness Values of Best Parameter in 20 Iterations for Stage 1 ....	82
Figure 4.27. Measured versus Computed Deflections: Parameters Optimized based on Stage 1 Observations .....	82
Figure 4.28. Evolution of Particle's Best Positions pBest in Different Iterations for Stage 2: (a) 1 <sup>st</sup> iteration; (b) 10 <sup>th</sup> iteration; (c) 15 <sup>th</sup> iteration;(d) 20 <sup>th</sup> iteration .....	83
Figure 4.29. gBest Fitness Values of Best Parameter in 20 Iterations for Stage 2 ....	84
Figure 4.30. Measured versus Computed Deflections: Parameters Optimized based on Stage 2 Observations .....	84
Figure 4.31. : Evolution of Particle's Best Positions pBest in Different Iterations for Stage 3: (a) 1 <sup>st</sup> iteration; (b) 10 <sup>th</sup> iteration; (c) 15 <sup>th</sup> iteration;(d) 20 <sup>th</sup> iteration .....	85
Figure 4.32. gBest Fitness Values of Best Parameter in 20 Iterations for Stage 3 ....	86
Figure 4.33. Measured versus Computed Deflections: Parameters Optimized based on Stage 3 Observations .....	86
Figure 4.34. Evolution of Particle's Best Positions pBest in Different Iterations for Stage 4: (a) 1 <sup>st</sup> iteration; (b) 10 <sup>th</sup> iteration; (c) 15 <sup>th</sup> iteration;(d) 20 <sup>th</sup> iteration .....	87
Figure 4.35. gBest Fitness Values of Best Parameter in 20 Iterations for Stage 4 ....	88
Figure 4.36. Measured versus Computed Deflections: Parameters Optimized based on Stage 4 Observations .....	88
Figure 4.37. Evolution of Particle's Best Positions pBest in Different Iterations for Stage 5: (a) 1 <sup>st</sup> iteration; (b) 10 <sup>th</sup> iteration; (c) 15 <sup>th</sup> iteration;(d) 20 <sup>th</sup> iteration .....	89
Figure 4.38. gBest Fitness Values of Best Parameter in 20 Iterations for Stage 5 ....	90
Figure 4.39. Measured versus Computed Deflections: Parameters Optimized based on Stage 5 Observations .....	90
Figure 4.40. Measured versus Predicted Deflections of Stage 2: Parameters Optimized based on Stage 1 Observations .....	92
Figure 4.41. Measured versus Predicted Deflections of Stage 3: Parameters Optimized based on Stage 2 Observations .....	93

Figure 4.42. Measured versus Predicted Deflections of Stage 4: Parameters Optimized based on Stage 3 Observations.....	94
Figure 4.43. Measured versus Predicted Deflections of Stage 5: Parameters Optimized based on Stage 4 Observations.....	95
Figure 4.44. Comparison of Field Observed and Computed Deflections at each Stage using Initial Design Parameters and Best-fit Estimates of Parameters .....	98
Figure 4.45. Comparison of Field Observed and Predicted Deflections for Stages 2-5 using Optimized Parameters from the Previous Stage and Initial Design Parameters .....	100
Figure A.1. Borehole Log 1/3 .....	119
Figure A.2. Borehole Log 2/3 .....	120
Figure A.3. Borehole Log 3/3 .....	121
Figure B.1. Inclinator #2 Readings .....	122
Figure C.1. Laboratory Test Results .....	123

## LIST OF ABBREVIATIONS

### ABBREVIATIONS

ANN	:	Artificial Neural Networks
CDSM	:	Compound Deep Soil Mixing Columns
CSN	:	Compound Soil Nail
CPW	:	Contiguous Pile Wall
DE	:	Differential Evolutions
DSM	:	Deep Soil Mixing
DW	:	Diaphragm Wall
ES	:	Evolution Strategy
FE	:	Finite Element
FEM	:	Finite Element Method
FOS	:	Factor of safety
GA	:	Genetic Algorithm
HS	:	Hardening Soil
JR	:	Jointed Rock
MC	:	Mohr-Coulomb
MCC	:	Modified Cam-Clay
PI	:	Plasticity index
PMT	:	Pressuremeter Tests
PSO	:	Particle Swarm Optimization

PVC	:	Polyvinyl Chloride
SPT	:	Standard Penetration Tests
SPW	:	Sheet Pile Wall
SSC	:	Soft Soil Creep
UD	:	User Defined

## LIST OF SYMBOLS

### SYMBOLS

$\nu$	:	Poisson's ratio
$\nu_{ur}$	:	Poisson's ratio for unloading-reloading
$\psi$	:	Angle of dilatancy
$\gamma$	:	Unit weight of soil
$\delta h$	:	Lateral displacement
$\delta h_{max}$	:	Maximum lateral displacement
$\epsilon_z$	:	Strains in the longitudinal axis
$\sigma_n'$	:	Normal effective stress
$c$	:	Cohesion
$c'$	:	Effective cohesion
$c_u$	:	Undrained shear strength
$E_{50}^{ref}$	:	The reference secant Young's modulus at the 50% stress level
$E_{oed}^{ref}$	:	Tangent stiffness for primary oedometer loading
$E_{ur}^{ref}$	:	Unloading-reloading stiffness
$E_i$	:	Initial stiffness (Young's) modulus
$E_s$	:	Deformation modulus
$f$	:	Fitness function
$f_1$	:	Constant dependent on Plasticity Index, PI.

$H$	:	Depth of excavation
$I$	:	Moment of inertia
$K_0$	:	Coefficient of earth pressure
$m$	:	Power for the stress-level dependency of stiffness
$n$	:	Number of selected points on the model
$\emptyset$	:	Angle of friction
$\emptyset'$	:	Effective angle of friction
$R_{inter}$	:	Strength reduction factor interface
SPT-N	:	SPT blow count number
$T_{top,max}$	:	Allowable skin resistance
$v$	:	Velocity of particle
$w$	:	The inertia weight
$X_{fem}$	:	Calculated lateral deflection
$X_{measured}$	:	Measured lateral deflection



## CHAPTER 1

### INTRODUCTION

#### 1.1. General

In developed countries, especially in urbanized areas, buildings have to be constructed in the neighborhood of existing structures due to limited space. This has resulted in the tendency towards having prevalent underground constructions, which naturally brings deep excavations into the picture. Figure 1-1 and Figure 1-2 show typical deep excavation applications supported by anchorages and struts, respectively, built in two major city centers of Turkey.



*Figure 1.1.* Özdilek Shopping Mall (24 m of Diaphragm Wall) – Bursa, Turkey –  
The Fourth Highest Population in Turkey with 2.9 Million



*Figure 1.2.* Ankara Metro 3. Stage Kızılay Retaining System (35 m Deep Station) – Ankara, Turkey – The Second Highest Population in Turkey with 5.5 Million

Constructions of deep excavations are often a significant concern due to ground movements and structural effects on the adjacent structures. From engineering point of view, it is crucial to estimate these effects and monitor them during the lifetime of open cuts. For this purpose, there has been significant number of theoretical and case studies performed in the literature. As a result, empirical settlement envelopes and other semi-empirical methods (e.g., Goldberg et al. 1976; Mana and Clough 1981; Clough and O'Rourke 1990) have been used by the designers in order to predict ground movements induced by deep excavations.

In addition to so called conventional approaches based on empirical works, the finite element method (FEM) of analysis has been popular to estimate the wall and ground movements accurately. For example, Whittle et al. (1993) studied the application of FEM analysis for modeling top-down constructions and analyzed them through comparing the differences between predicted and measured wall displacements. With time, the rate of increase in the use of FEM proves that more accurate results have been obtained lately. However, there are several factors that may affect the accuracy of results of this type of numerical tools, including appropriate soil material parameters, initial conditions of the ground, groundwater flow, boundary conditions, pre-history of the construction site, etc. Linking the field data with the numerical modeling reflects the soil behavior during the construction and increases the performance of solving even extremely complex excavation problems (Finno and Harahap 1991). Such an attempt is also useful for future displacement predictions.

Most of the well-documented assessment on measured and calculated displacement in the literature has been done by using back analyses (Whittle et al., 1993). In back analyses cases, geotechnical input parameters of a model such as elastic modulus, friction angle, and cohesion of the soil are calibrated against the field data which results in more accurate soil and wall movement estimations. It has been confirmed that back analysis is very beneficial in order to get information regarding the geotechnical parameters (Du et al., 2006). If the estimations and field data are linked together, the analyses are improved, and the results approach the measured

deflections. However, due to complex nonlinear behavior of soil structures, back analysis processing becomes grueling most particularly when back-calculated parameters are high in number. Moreira et al. (2012) state that optimization algorithms are used in the back analysis in order to minimize the number of iterations and find the best results of parameters.

Shao and Macari (2008) argue that the optimization algorithms are used to yield the optimal possible results of soil parameters. These results are then used to forecast the deformation of the ground at separate stages throughout the excavation period while constantly inputting the results into the system. This, in turn, allows for increasing accuracy of soil deformation forecasting. This method provides acceptable benefits over the conventional analysis. Unlike conventional modeling, entering continuously updated field data into the system leads to more precise estimations and enables to find the global response of the deep excavation system. Since the results are continuously updated throughout the excavation period, any variation from the original design will be noticeable and possibly dealt with. In order to reach the optimal solution, numerical model and optimization algorithm are coupled to apply back-analysis for deep excavation problem.

In this thesis, the back-analysis platform is established which combines the finite element model and the optimization algorithm in order to find the actual, i.e., in-situ, soil material parameters. The developed platform is then applied to back-calculate the soil material parameters of deep excavation of Maidan Office-Home Office-Square project constructed in Ankara/Turkey. The forecasted behavior of deep excavation and its conformity with measured field data are discussed thoroughly.

## **1.2. Research Objective**

Most of the previous studies in the literature on back analysis are performed to evaluate the effectiveness of the preliminary designs. However, in light of continuous monitoring, precautions can be taken during construction. Entering continuously

updated field data into the system leads to more precise estimations and enables designers to find the global response of the deep excavation system. Nowadays, systematically calibrating the outcome of numerical simulation using perceived ground movements is problematic without expending hefty resources. Back analysis of such systems requires an optimization algorithm to get faster and accurate results.

Within the above framework, calibration of soil parameters for selected stages by comparing measured field data and FEM results and thus extracting constitutive model parameters that reflects the soil behavior in a deep excavation case study is the primary interest of this study. In this sense, the set of soil material parameters are obtained by using a developed back analysis platform for selected stages of construction, and the alteration of the material parameters set are observed. The study hopes to clarify whether the upcoming stages' behavior can be predicted or not by using calibrated parameters obtained by using the combination of FEM and Particle Swarm Optimization (PSO) algorithm. This work is also intended to encourage possible future studies for ways of finding the actual soil material parameters that contribute to a safe and economical geotechnical design.

### **1.3. Scope**

Within scope of this thesis, a back analysis platform is developed for modeling deep excavations, in which the field measurements are used to acquire the constitutive model parameters for both FE model and therefore the in-place properties of soils. Other types of field data such as the ones obtained from the extensometers are not taken into account within the scope. For modeling purposes, the commercial finite element program PLAXIS is preferred to compute displacements of the wall at selected construction stages. Computed displacements by the numerical model and inclinometer readings at corresponding stages are compared, and the difference between them is minimized through the metaheuristic-based optimization method named PSO.

Constitutive parameters of soil layers are identified using Hardening-soil model. Only the reference secant Young's modulus at the 50% stress level ( $E_{50}^{ref}$ ), cohesion ( $c'$ ) and effective angle of friction ( $\phi'$ ), the three material parameters that are having weighty effects on horizontal deflections at the site, are considered and calibrated during the optimization process.

#### **1.4. Thesis Outline**

This chapter contains the problem statement, objectives and the scope of the study. Then, the literature survey is provided in Chapter 2 including the studies related to deep excavations, numerical analysis, back calculation, and optimization techniques. Chapter 3 contains the main work; where the back analysis platform is described including the development of numerical model and optimization algorithm used in the thesis. In Chapter 4, the application of a back analysis platform on the deep excavation of a recently constructed set of buildings named Maidan Office – Home Office – Square, and the performance of PSO algorithm is presented. Following this, comparison of inclinometer measurements and FEM calculations and the deflection predictions are revealed. In conclusion, the findings of the study are highlighted and the recommendations for future studies are presented in Chapter 5.

## CHAPTER 2

### LITERATURE SURVEY

#### 2.1. Introduction

Deep excavations are a necessity when it comes to the development and construction in urban environments. This is due to the fact that existing structures in urban areas take up much of the space on the surface and therefore engineers have to utilize underground expanses. When dealing with deep excavations; it is of utmost importance that existing structures are not affected before, during and after the excavation is complete. Hence, estimation of the magnitude and distribution of the ground movements and minimizing these movements is absolutely critical (Marulanda 2005). Support systems are usually designed and constructed to prevent and/or minimize critical ground movements. According to Marulanda (2005), when designing support systems, three conditions have to be met:

- 1- Stability against bottom heave and piping
- 2- Failure of the support system
- 3- Limitation of ground lateral movements that may damage neighboring existing structures.

In light of these conditions, the engineer must include stability and deformation in the analysis of deep excavations.

Commonly used design approaches for estimation of deep excavation induced movements in the literature reviewed in Section 2.2. Monitoring of deep excavation is reviewed in Section 2.3. Section 2.4 includes previous works related to numerical analyses and common modeling approaches for solving geomechanics problems. In section 2.5, back analysis concept in geotechnical engineering and assessment on

measured and calculated displacement using back analysis is discussed. Section 2.6 presents a description of the observational method. Optimization techniques for solving inverse problems and studies in the literature are briefly overviewed in the same section.

## **2.2. Commonly Used Design Approaches for Estimating Deep Excavation-induced Movements**

When designing support systems in deep excavations, lateral ground movements are the key aspect of design. Therefore, the prediction of ground movements is also significant regarding the design of support systems. After investigating sheet pile support systems in an excavation, Peck (1969) came to the conclusion that the property of the soil around the support system is the main aspect that affects the soil deformations. He further elaborates that lateral movements even occur under the excavation level and that the extent of these movements is governed by the depth of the excavation.

Mana and Clough (1981) investigated the correlation between soil lateral movements and important soil parameters by using a combination of field tests and finite element analyses. After studying 11 case histories with field data, they constructed a graph that illustrates the correlation between the factor of safety and movement. It was concluded after plotting maximum wall movement over excavation depth and the factor of safety against basal heave that there is a significant correlation between the movement of the soil and factor of safety where movements promptly increase as factor of safety decreases (See Figure 2-1). Additionally, as the factor of safety increases, movements tend to decrease and remain constant at around 0.5%.

Mana and Clough (1981) further investigated the effects of time on maximum lateral wall movements as seen in Figure 2-2. This investigation concluded that as time passes, the rate of movement decreases rapidly. Moreover, Figure 2-3 plots maximum

settlement values against lateral wall movements. The graph shows an almost linear correlation where settlements are 0.5 to 1.0 times the horizontal wall displacements.

Mana and Clough (1981) also performed over 70 finite element analyses taking in factors such as wall and strut stiffness, strut spacing, preloading, excavation width and depth, soil stiffness and stress distribution. To confirm their field measurements, they plotted the finite element values of maximum wall movement over excavation depth versus the basal heave safety factor as shown in Figure 2-4. Moreover, the correlation resembled that of the field measurements. Additionally, Figure 2-5 shows that also when using finite element studies, correlations similar to the field data suggests that settlements become a larger percentage of lateral movements at 1.0 to 1.5 factor of safety values.

Mana and Clough (1981) concluded the following in their finite element studies:

- 1- As strut stiffness increases, soil movements decrease.
- 2- Increasing the stiffness of the wall and increasing the number of struts in an excavation prompts a decrease in soil movements. This effect is increasingly significant at a lower factor of safety values.
- 3- With an increase in the width and depth of excavation, movements also increase.
- 4- Soil modulus of elasticity radically disturbs the movements of the soil where increasing measurements of elasticity modulus produce smaller movements and vice versa.
- 5- Preloaded struts decrease the movements in the soil, however; the effects also fade at higher preloads.

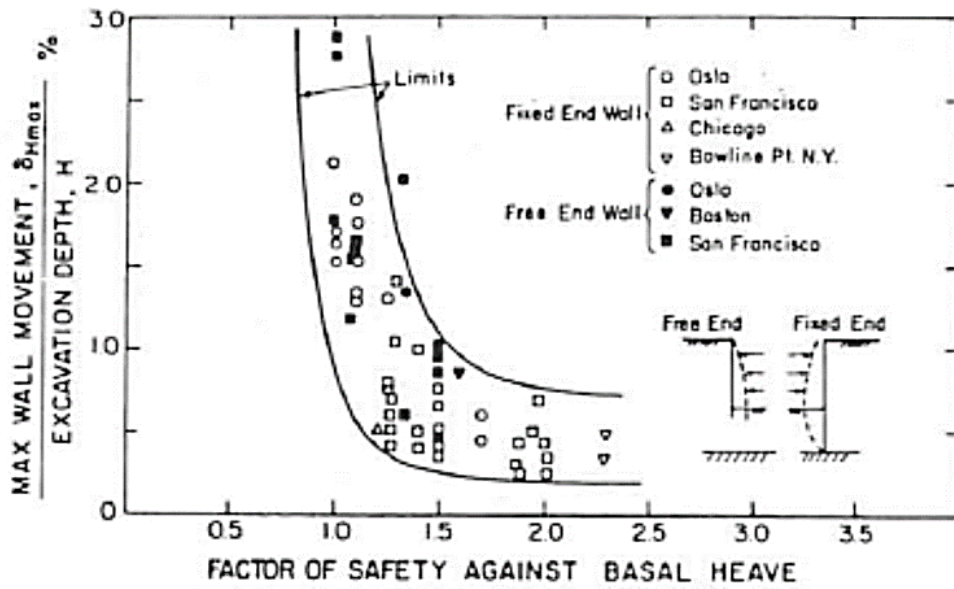


Figure 2.1. Relationship between Factor of Safety against Basal Heave and Maximum Lateral Wall Movements (Mana and Clough, 1981)

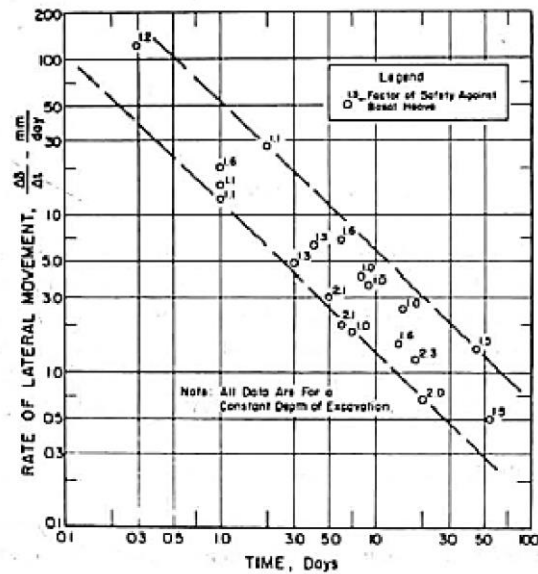


Figure 2.2. Relationship between Time and Maximum Lateral Wall Movements (Mana and Clough, 1981)

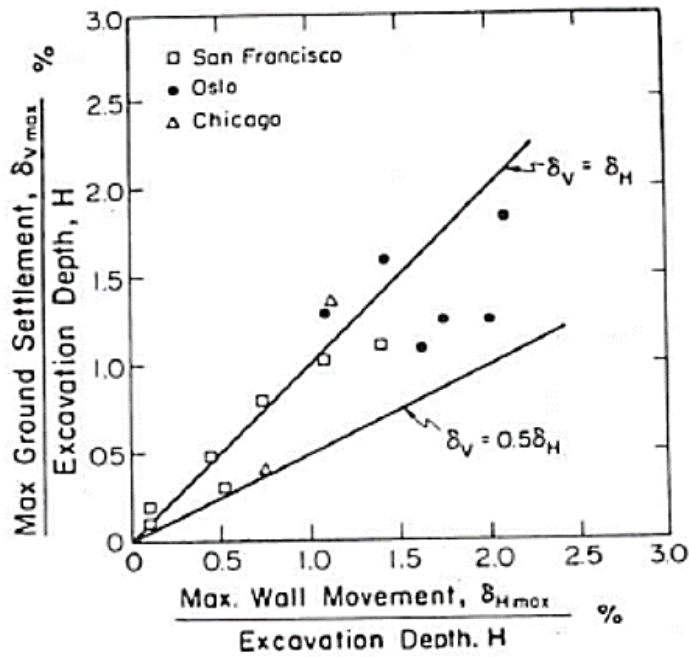


Figure 2.3. Relationship between Maximum Ground Settlements and Maximum Lateral Wall Movements (Mana and Clough, 1981)

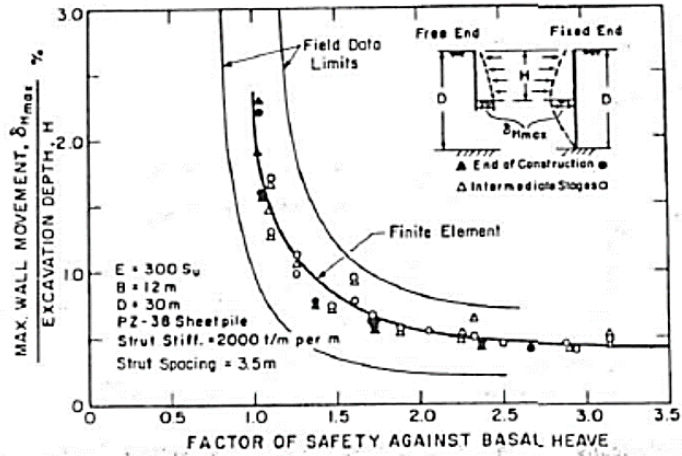


Figure 2.4. Relationship Factor of Safety against Basal Heave and Maximum Lateral Wall Movements (Mana and Clough, 1981)

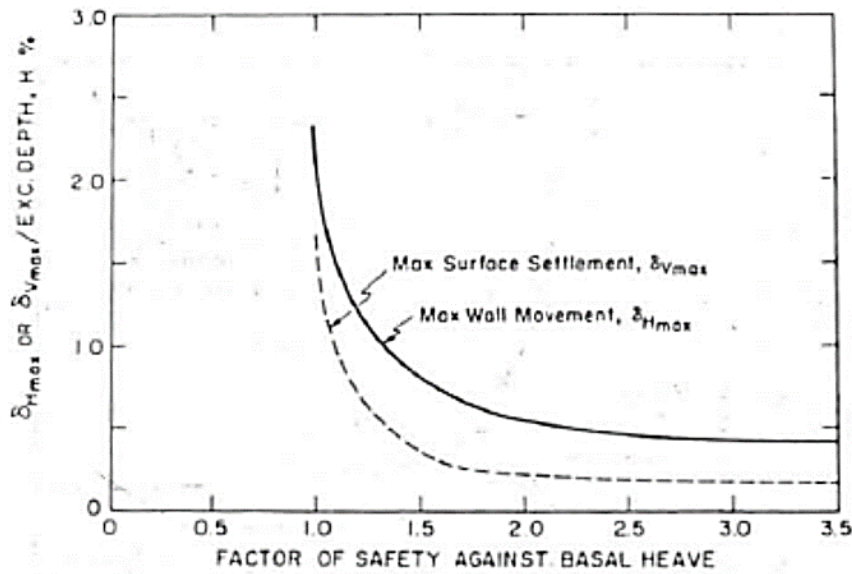


Figure 2.5. Relationship between Maximum Surface Settlements and Maximum Lateral Wall Movement (Mana and Clough, 1981)

Clough and O'Rourke (1990) studied existing ways to forecast ground movement patterns and settlement distributions by investigation of the movements of in-situ walls. They also used updated existing data bearing in mind the effects of construction activities, excavation and support process. As stated by them, movements in in-situ walls are affected and caused by aspects like groundwater and soil settings, depth and shape of excavation, wall support condition, surcharge loads, wall stiffness, groundwater level undulation and the construction technique of the wall with its period of exposure. However, one of the chief reasons of wall movements is related with the support and excavation method. Figures 2-6 and 2-7 investigate the wall and soil movements in residual soils, sand and stiff clays where maximum displacements and settlements are plotted against the depth of excavation. Looking at the graphs, it can be said that there are no significant dissimilarities between maximum movement tendencies of different walls. Therefore, Clough and O'Rourke (1990) considered wall and soil stiffness, the coefficient of lateral earth pressure and support spacing in their implemented finite element analyses as seen in Figure 2-8. The linear graph resembles



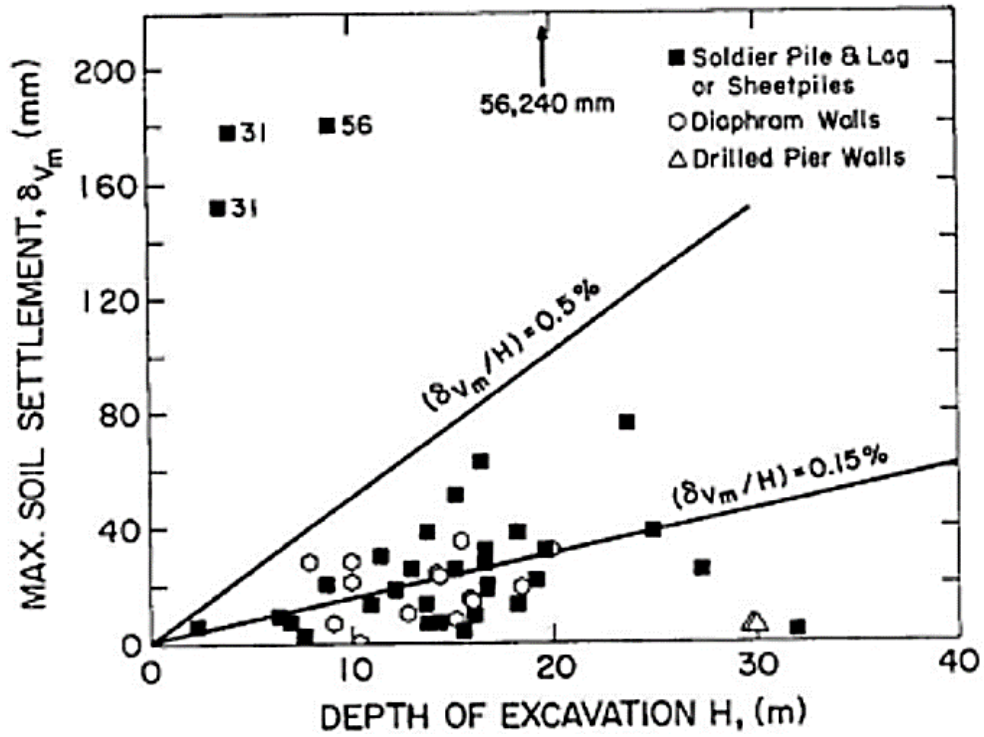


Figure 2.7. Monitored Maximum Settlements in the Soil Retained by In-situ Walls (Clough and O'Rourke, 1990)

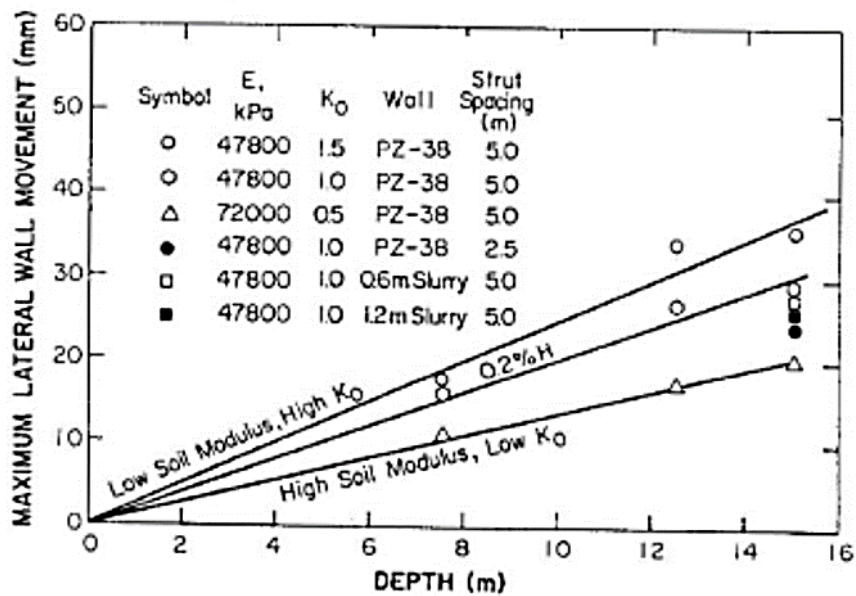


Figure 2.8. Maximum Horizontal Wall Movement in Stiff Soils (Obtained by using Finite Element Analyses) (Clough and O'Rourke, 1990)

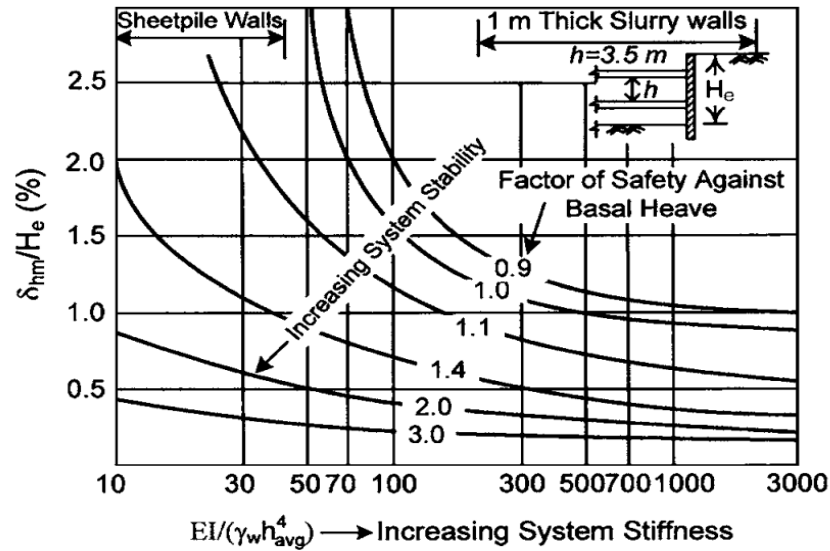


Figure 2.9. Design Curves for Maximum Horizontal Wall Movement for excavations in Soft to Medium Clays (Clough and O'Rourke, 1990)

Cough and O'Rourke (1990) generalized wall and ground movement patterns of braced and tied-back walls as illustrated in Figure 2-10 using inclinometer and settlement values. Moreover, Figure 2-10a demonstrates a cantilever movement where soil settlements increase inversely with respect to the distance from the excavation edge. With deeper excavations, movements at lower levels of the excavation are formed when higher elevations are restrained with a support system as seen in Figure 2-10b. The combination of these two cases is presented in Figure 2-10c to further illustrate the general movement in such a case.

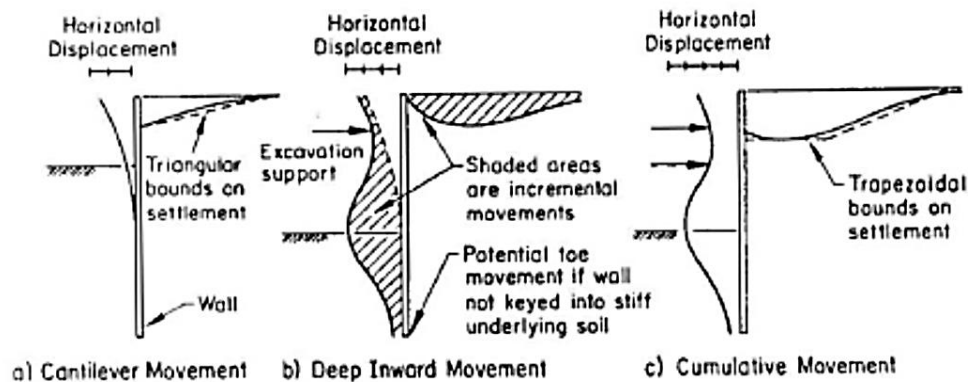


Figure 2.10. Movement Patterns of Braced and Tied-Back Walls (Clough and O'Rourke, 1990)

The authors associated wall displacements with the construction method of the wall itself and identified the main causes of these movements. These causes fall under the following criteria:

- 1- Construction technique: Less experienced contractors and geotechnical engineers may lead to poor wall construction quality which may cause large movements of the wall.
- 2- Wall installation method: Driving method of in-situ walls and their placements can produce ground movements.
- 3- Deep excavation below supports: Extending the excavation depth way below the support location can increase wall movements.
- 4- Construction and removal of deep foundations: In demolition or renovation cases, old deep foundations have to be replaced with new ones and that may cause movements.

Moreover, the designer controls the support system of the excavation which can affect wall movements significantly. The designer can increase wall stiffness in order to reduce wall movements. Additionally, increasing the support spacing and stiffness both horizontally and/or vertically will reduce wall movements. Preloading of the in-situ wall may also be applied to diminish the soil movements. Furthermore, wall

settlement, earth berms, piezometric pressure and movements in the anchored wall are special geotechnical factors that affect in-situ wall movements.

Clough and O'Rourke (1990) concluded that in-situ wall displacements can be approximated rationally given that the primary causes of displacements are considered. They also concluded that the wall movements are primarily affected by the method of excavation and support system, construction activities, and geotechnical respects. Additionally, horizontal and vertical settlements are caused by excavations at the front end of an in-situ wall. Finally, to investigate the damage to structures, it is important to consider a structure's response to ground movements based on the nature and condition of the building.

Wang et al. (2009) studied the wall and soil movements because of deep excavations in Shanghai by collecting and analyzing 300 case histories including diaphragm wall, contiguous pie walls, sheet pile walls and deep soil mixing walls. He questioned the reasons affecting the wall deformation and confirmed that when the system stiffness and the basal heave safety factor increase, the wall displacement decreases as Mana and Clough (1981) suggested. He also associated the wall and ground deformations with worldwide case histories.

In the analysis, Wang (2009) classified the results according to wall type and the method of construction. 32 cases were constructed by the top-down method of which 4 were contiguous pile wall (CPW), 28 were diaphragm wall (DW). 92 cases were bottom-up DW, 78 cases were CPW and 30 cases of compound deep soil mixing columns (CDSM). 11 cases of sheet pile wall (SPW), 23 cases of compound soil nail (CSN) wall and 34 cases were retained by deep soil mixing (DSM) columns. Figure 2-11 demonstrates the relationship between the horizontal movement of the wall ( $\delta_{hm}$ ) and the depth of excavation (H) for all the cases.

Wang (2009) concluded the following in his study:

- 1- As the depth of excavation increases, wall movements increase.

- 2- For the top-down method of constructions,  $\delta_{hm}$  values vary between 0.1%H and 0.55%H; an average of 0.27%H (see Figure 2.11a).
- 3- For the bottom-up method of constructions and stiff walls (DW, CPW, and CDSM),  $\delta_{hm}$  values vary between 0.1%H and 1.0%H; an average of 0.4%H (see Figure 2.11b).
- 4- For SPW, wall displacement becomes larger up to 3.2%H; an average of 1.5%H (see Figure 2.11c).
- 5- For CSN walls,  $\delta_{hm}$ -values vary between 0.2%H and 0.9%H; an average of 0.55%H (see Figure 2.11d).
- 6- For DSM walls,  $\delta_{hm}$ -values vary between 0.3%H and 2.4%H; an average of 0.91%H (see Figure 2.11e).
- 7- The maximum horizontal movement of walls heavily depends on the wall type. In other words, the stiffness of the system plays an important role on the lateral displacement.

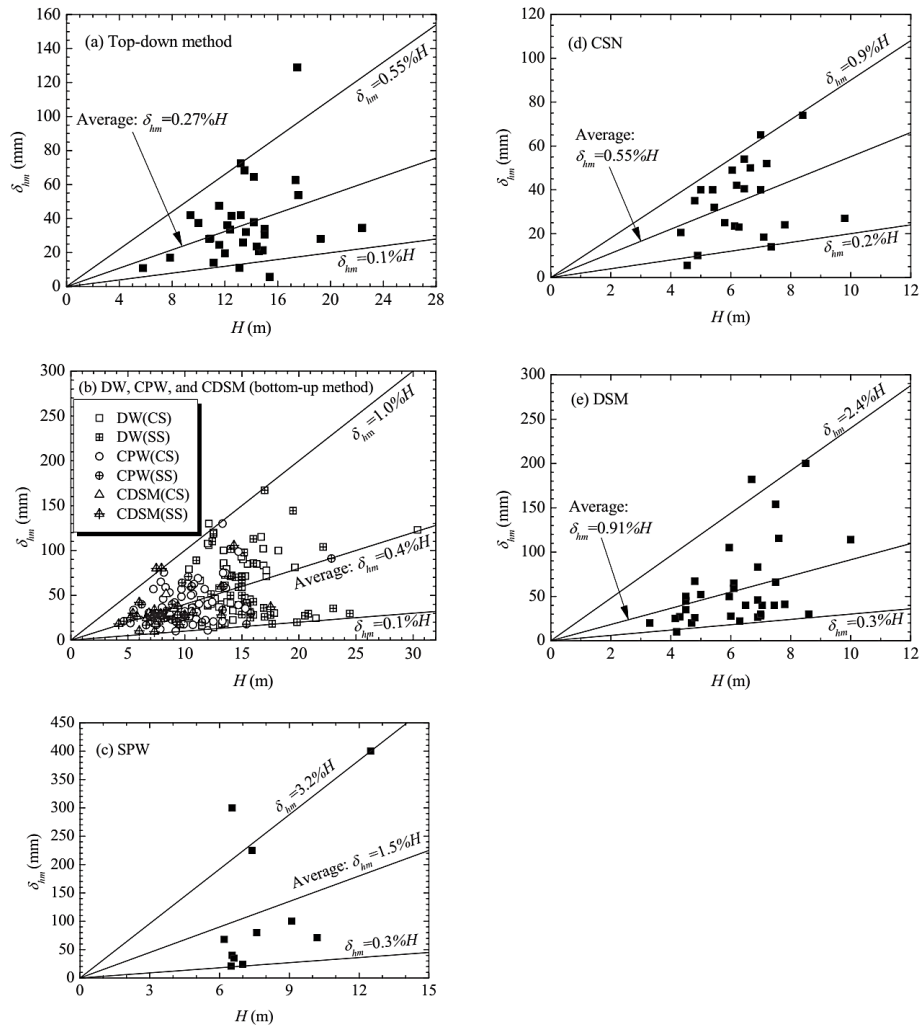


Figure 2.11. Relationship between Lateral Movement of Wall and Excavation Depth for Different Supporting System (Wang et al., 2009)

In Table 2.1, the comparison of the maximum deformation of the wall studied by different authors for different ground condition and wall type is shown.

Table 2.1. Comparison of Wall Displacements Measured in Worldwide Case Histories (Wang et al., 2009)

Study	Ground condition	Wall type/construction method	Case number	Average $\delta_{im}/H$ (%)
Mana and Clough (1981)	Saturated soft to medium clay	SPW	10	1.32
Ou et al. (1993)	Taipei soft soil	Most were DWs and most were constructed by the bottom-up method	10	0.4
Masuda (1993)	Clay	DW constructed by the top-down method or semi-top-down method	17	0.2
		DW constructed by the bottom-up method	21	0.23
Wong et al. (1997)	Stiff residual soils and weathered rocks overlaid with soft deposit of thickness of $0.6 \sim 0.9H$	DW and CPW with struts or anchors	24	0.16
		SPW with struts or anchors	13	0.23
Long (2001)	Stiff soils overlaid with soft soils of thickness $>0.6H$	DW and CPW constructed by the bottom-up method	22	0.47
		SPW constructed by the bottom-up method	14	1.56
Kung et al. (2007)	Taipei clay	DW constructed by the top-down method or semi-top-down method	7	0.39
		DW constructed by the bottom-up method	23	0.32
This study	Shanghai soft soil	DW and CPW constructed by the top-down method	32	0.27
		DW, CPW, and compound DSM wall constructed by the bottom-up method	200	0.40
		SPW with internal strut or anchors	11	1.5

Wang et al. (2009) also mentioned the parameters that affect the wall displacement. Although the data are quite limited, it can be said that the wall movements decrease as the thickness of the wall increase. Figure 2-12 represents deflection paths of diaphragm walls with a thickness of 600 mm, 800 mm and 1,000 mm. Another parameter that affects the wall displacement is the system stiffness. Many researchers pointed out that stiffness of a supporting system is one of the most essential parameters for the excavation performance. Location, spacing and axial stiffness of support and wall bending stiffness are counted as system stiffness. Figure 2-13 is the graph of system stiffness vs. normalized maximum horizontal movement defined by Clough et al. (1989) for top-down and bottom-up construction method including diaphragm walls and contiguous pile walls. The factor of safety against basal heave (FOS) suggested by Clough and O'Rourke (1990) are shown as design curves in the figure. It can be deduced that as system stiffness increases, normalized maximum horizontal

movements of the wall decrease. This conclusion is consistent with other researchers' findings on the influence of system stiffness.

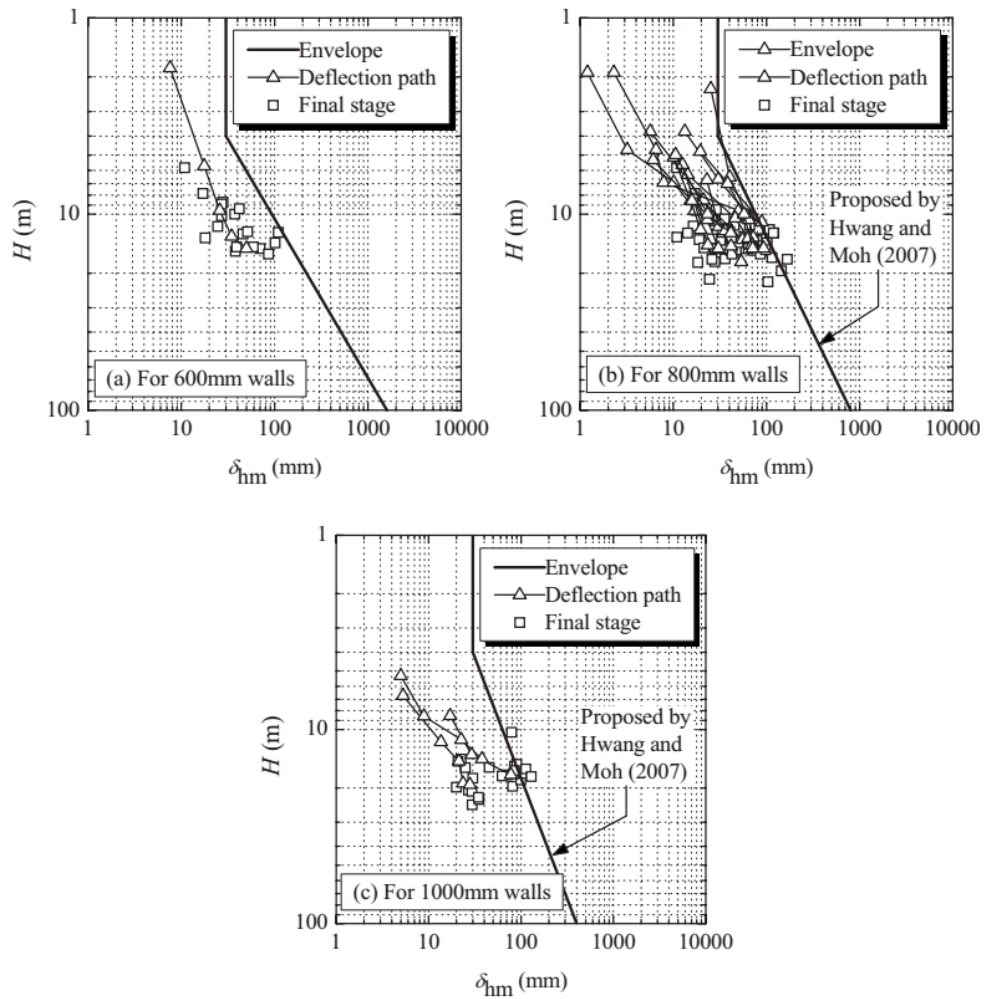


Figure 2.12. Deflection Paths of Diaphragm Walls with Different Thickness (Wang et al., 2009)

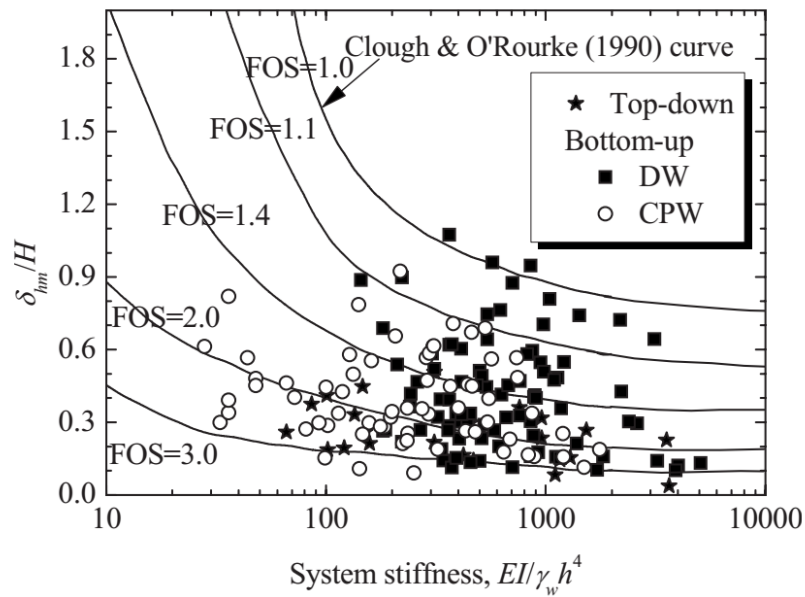


Figure 2.13. Relationship between System Stiffness and Normalized Maximum Horizontal Movement (Wang et al., 2009)

Executing numerical analyses that are able to model real constructions helped many engineers to avoid retrieving and studying a hefty number of empirical relations as it is problematic and time-consuming. These analyses are mentioned in section 2.4.

### 2.3. Deep Excavation Monitoring

Recently, monitoring of deep excavation has become a vital issue in order to control the risks of failure which causes loss of life. Monitoring is one of the most important parts to complete geotechnical projects. Especially for the projects in the district of the existing structures, instrumentation becomes more essential. In deep excavation projects, instruments are installed to control displacements of the wall and surrounding soil, stresses on the wall and water pressures. Figure 2-14 shows commonly used geotechnical instruments for deep excavation monitoring purposes.

Information gathered from the instruments are also used for back-analysis calculations in order to improve design quality by calibrating the soil parameters and thus predict upcoming stages' behavior for safety and financial purposes. Geotechnical input parameters of a model are altered by using the field data which results in more accurate soil and wall movement estimations. Inclinometers are the most commonly used instrument for the purpose of measuring horizontal displacements of the wall.

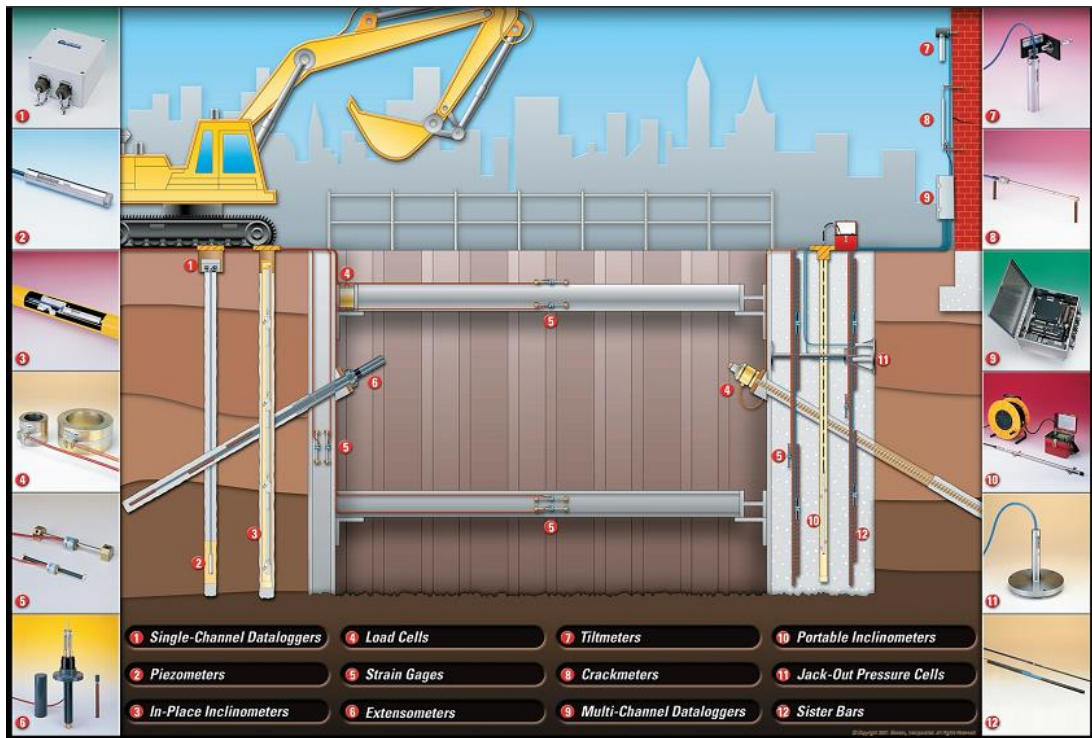


Figure 2.14. Deep Excavation Monitoring Instruments (source: <http://www.recordtek.com/solutions/geotechnical-solution/>) [last accessed on 13.09.2019]

### 2.3.1. Inclinometers

Inclinometers are used to measure horizontal displacements in underground structures. In order to drive the inclinometer probe, firstly vertical boreholes, mostly made of polyvinyl chloride (PVC) materials, are placed in the ground or inside the wall. After

placing the inclinometer casing (Figure 2.15) by grouting, inclinometer probe (Figure 2.16) is driven and gets angular measurements at specified points in a casing by tilt-sensors in it. Displacements are compared with the initial reading each time to calculate the relative movements. This procedure is done periodically while the construction takes place. Schematic of inclinometer probe placed in casing is shown in Figure 2.17.



Figure 2.15. Inclinometer Casing (source <http://www.geotechnicaltrade.com/product-detail/pvc-inclinometer-casing>) [last accessed on 14.05.2019]



Figure 2.16. Typical Inclinometer System including Probe, Cable, Readout Unit (source: <http://www.geodata.com/geodata-aletsel-gozlem-cihazlari.html>) [last accessed on 04.05.2019]

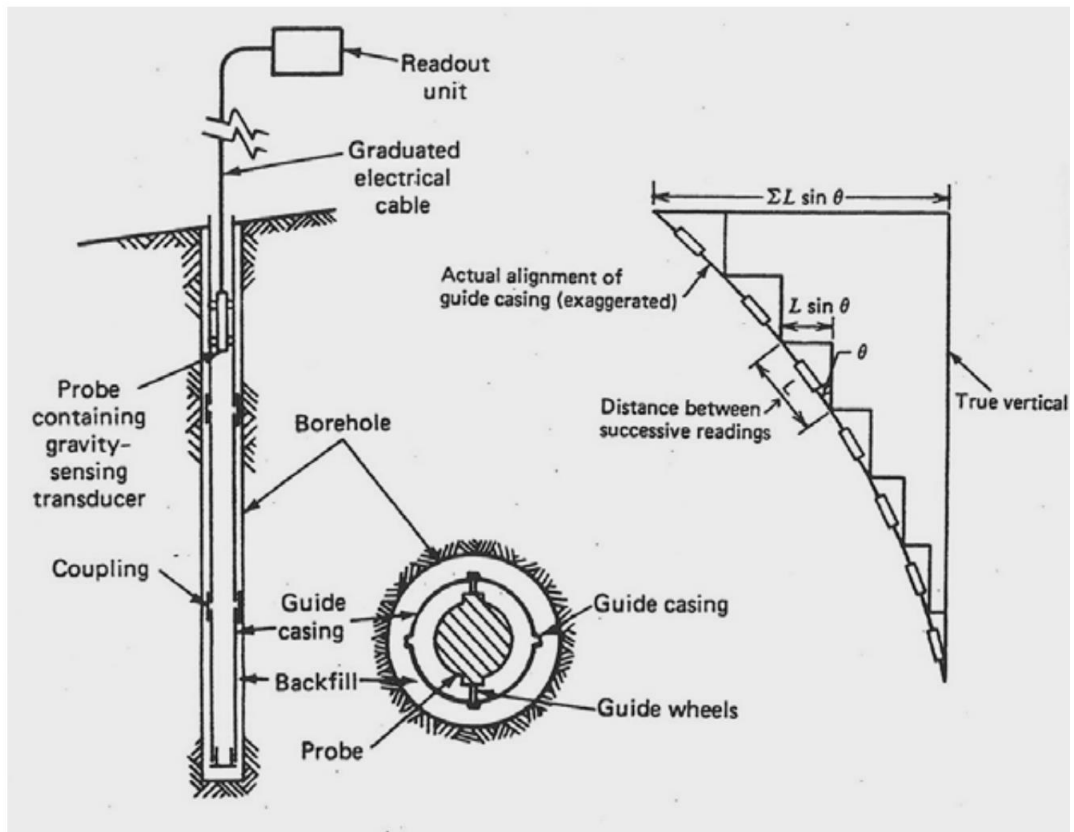


Figure 2.17. Schematic of Inclinometer Probe placed in Casing (Mikkelsen, 1996)

#### 2.4. Numerical analysis of Deep Excavations

Recently, there has been a significant rate of increase of using numerical modeling techniques by designers while dealing with deep excavations in order to predict more reliable ground movements. Finite element method (FEM) is one of the most common techniques for solving the equilibrium equations boundary value problem including many significant analysis programs (Hashash et al., 2003). These programs such as ABAQUS, FLAC, and PLAXIS are used in the analysis of deep excavations to estimate the ground movements.

The widely use of numerical analysis to calculate ground deformations in deep excavation started in the early 1970s. Clough and Duncan (1971) analyzed the

behavior of the interface between soil and the wall using finite element analysis. Mana and Clough (1981) provided envelope curves to represent the maximum wall movement over excavation depth against the basal heave safety factor by using FEM. Clough et al. (1989) studied the relation between the system stiffness and the maximum horizontal wall movement. Many other studies on numerical analysis of deep excavations can be found in the literature counting Finno and Harahap (1991); Hashash (1992); Ou et al. (1996); Yoo and Lee (2008) as a significant number of designers tend to use the finite element method to analyze deep excavations. That is because the finite element method provides the ability to model the complex nonlinear behavior of the soil through various geometrics with diverse boundary limits and constitutive model.

#### **2.4.1. Finite Element Method (FEM)**

Use of the finite element method is dramatically increased in the studies of numerical analysis in geomechanics (Sloan and Randolph, 1982). It is practical to use the finite element method in geotechnical engineering since it simplifies the calculations. This method estimates the stress, deformation and pore pressures and analyzes the system stability throughout the excavation (step by step) for several geometries and boundary conditions. The soil is modeled as a continuum and decoupled into meshes (the specified number of elements). The meshes can be formed in different shape and size. As the size of mesh increases, the execution time of the analysis shortens but the accuracy decreases. Therefore, the designer should choose the proper size of the mesh to balance the execution time and the accuracy of the results. Recently, PLAXIS is commonly used finite element program for deep excavation analyses in Turkey and Europe.

#### 2.4.1.1. PLAXIS Software

PLAXIS 2D is developed by the Delft University of Technology and nowadays is used for deformation and stability analyses, two-dimensional finite element analysis software. It allows the user to solve non-linear finite element calculations efficiently. The software enables to view the analysis solutions for the selected phase. The user can view the outputs such as total displacements, total strains, effective stresses, total stresses, pore pressures and internal forces of the structural elements. Eight different constitutive models for soil behavior may be used for analysis; Mohr-Coulomb model (MC), Jointed Rock model (JR), Hardening Soil model (HS), Hardening Soil model with Small-Strain Stiffness (HSsmall), Soft Soil Creep model (SSC), Soft Soil model (SS), Modified Cam-Clay model (MCC), and User Defined (UD) model. Drained, undrained and non-porous behaviors are available for pore pressure behavior simulation. Mohr-Coulomb model is a linear elastic, perfectly plastic model. Soil parameters used in this model  $E$ ,  $\nu$ ,  $\phi$ ,  $c$ , and  $\psi$  and average stiffness. Stress dependency, the stress path dependency of stiffness and anisotropic stiffness are not involved in this model (Brinkgreve et al., 2009). Therefore, this model can only be used for the initial estimate (PLAXIS 2D User Manual). On the other hand, the stress dependence on soil stiffness is considered in hardening soil constitutive model. The soil behavior is non-linear, and the stiffness of soil is never constant. It is inversely proportional with the stress level within the soil. The stiffness modulus decreases as the load increases as illustrated in Figure 2-18. Considering the theory of plasticity, including soil dilatancy and yield cap makes hardening soil model more thematic. This model is an elastoplastic form of hyperbolic model, expressed in the framework of shear hardening plasticity. Soil parameters used in this model are  $E_{50}$ ,  $E_{oed}$ ,  $E_{ur}$ ,  $\phi$ ,  $c$ ,  $\psi$ ,  $K_0$ ,  $\nu_{ur}$ . The difference between two models is that the Mohr-Coulomb model uses constant soil stiffness while the soil has effective stress dependent stiffness as used in hardening soil model (PLAXIS 2D User Manual). Not only the loading stiffness ( $E_{50}$ ), but also the unloading-reloading modulus ( $E_{ur}$ ) and oedometer modulus ( $E_{oed}$ ) are considered in the HS model. Details about the HS model are given in Section 3.2.1.

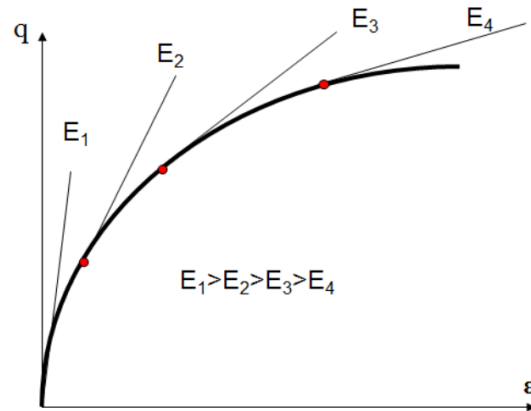


Figure 2.18. Non-linear Stress-Strain Curve and Inconstant Soil Stiffness (Liong, 2014)

#### 2.4.2. Conventional Constitutive Modeling for Deep Excavations

Mostly, constitutive models used in geotechnical engineering are based on elasticity and plasticity theories (Marulanda, 2005). Material failure was represented by Tresca and von Mises yield criteria (Hill 1950) which contained by initial forms of yield criterion. Recent plasticity models that contained by constitutive relations used for geological materials are studied by Prevost and Popescu (1996). These models are adjusted by common laboratory tests.

As a common method to update constitutive models in deep excavation, linear process with ad hoc loops are followed as represented in Figure 2-19 (Hashash et al., 2006).

1. Description of problem and model idealization: For deep excavations, ground movements are assessed by model simulation.
2. Description of material property, field and laboratory testing: Soil parameters used in the model are defined by in-situ and laboratory tests.

3. Material constitutive behavior, model and property selections: Information acquired from Step-2 is used for material constitutive behavior. Model signify soil stress-strain-strength characteristics.

4. Boundary value problem solution: Finite element programs are used to predict stress and deformations of the system for numerous geometrics with different boundary conditions.

5. Comparing with actual field behavior: Lateral wall movements and surface settlements are generally used field data to link with the calculated results during construction. If the compared results are not satisfied, the model and soil properties are adjusted by repeating Step 3 and solve the boundary value problem (Step 4). This loop repeats until satisfactory criteria have been met (Step 5).

6. Analysis of upcoming excavations/stages: The model simulations are used for soil and wall movement prediction for future excavation stages or another project.

This common approach to modeling geomechanics was first demonstrated by Mana and Clough (1981) and Whittle et al. (1993).

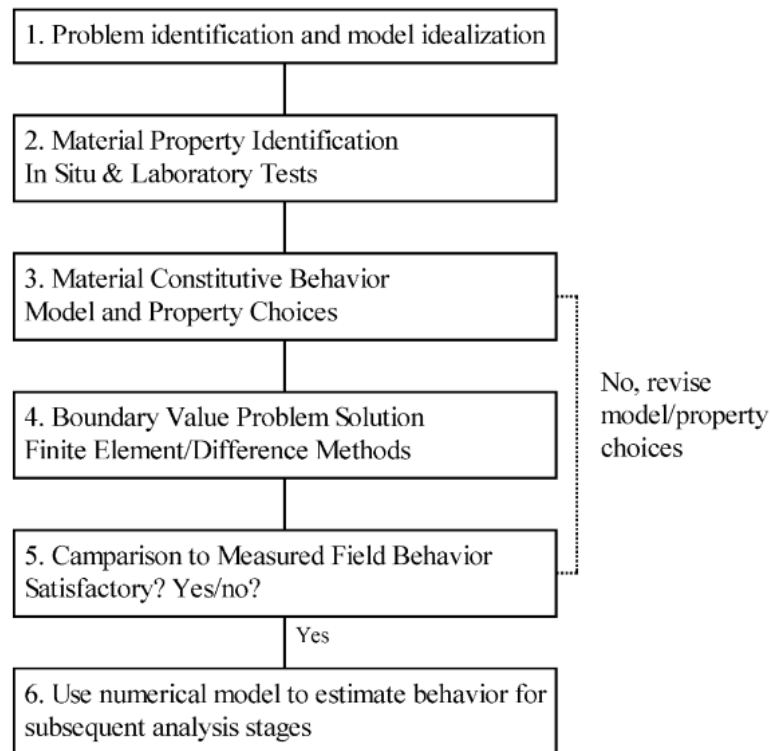


Figure 2.19. Common Approach to Modeling of Geomechanics Problems (Hashash et al., 2003)

Inverse analysis concept with its capability to automatically estimate the appropriate parameters that give comparable predicted and calculated outcomes is discussed in the following section.

## 2.5. Back Analysis in Geotechnical Engineering

Back analysis concept is to match the estimated performance of the results of the analysis of numerically denoted parameters and the hypotheses of a problem by any means necessary (Vardakos, 2007). For geomechanics point of view, calculation procedure is reverse of forward analysis such that the measured stress and displacement values are input while mechanical properties of soil are output in the back analysis (Sakurai, 1997). Figure 2-20 illustrates the difference between forward and back analysis.

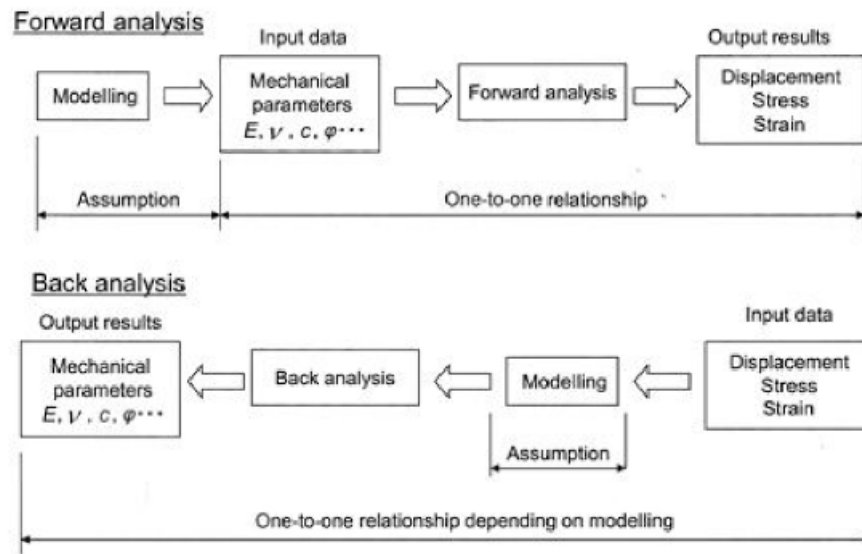


Figure 2.20. Difference between Forward Analysis and Back Analysis (Sakurai, 1997)

Inverse approach and direct (minimization) method are two common back-analysis approaches in geotechnical engineering practice. In the former, the known performance converts an input parameter and the output becomes the original parameters since all equations of the numerical model are reversed. This method is applicable when the numerical model can be reversible and therefore can only be useful for some engineering problems under good control of test implementation (Vardakos, 2007). Sakurai (1993) states that this approach is only valid for the linear elastic materials where the stress-strain relationship is expressed in a linear form. The latter's goal is to minimize the difference between observed and estimated quantities (e.g., deformations and stresses) of numerical analysis. The iterative procedure continues until the difference between observed and estimated results is a tolerable range. The direct method is applicable to many engineering problems including numerous unknowns, non-linear equations and procedures (Vardakos, 2007). It consists of three key elements which are the error (fitness) function, the numerical model, and the optimization algorithm. The numerical model reflects the structure's response by including soil characteristics and excavation scheme. Error function

represents the difference between observed and estimated values. The optimization algorithm is used for modification of the material parameters in order to minimize the error function. According to Cividini et al. (1981), any standard algorithms such as the Simplex method (Nelder & Mead, 1965), Powell method (Powell, 1964), Conjugate Gradient method (Fletcher & Reeves, 1964), etc. can be used in direct method for the numerical solution which counted as an advantage for this method. Shao (1999) indicates that using the direct approach sets better for excavation problems due to the order of construction and the boundary conditions. Figure 2-21 illustrates the schema of the iterative back analysis procedure.

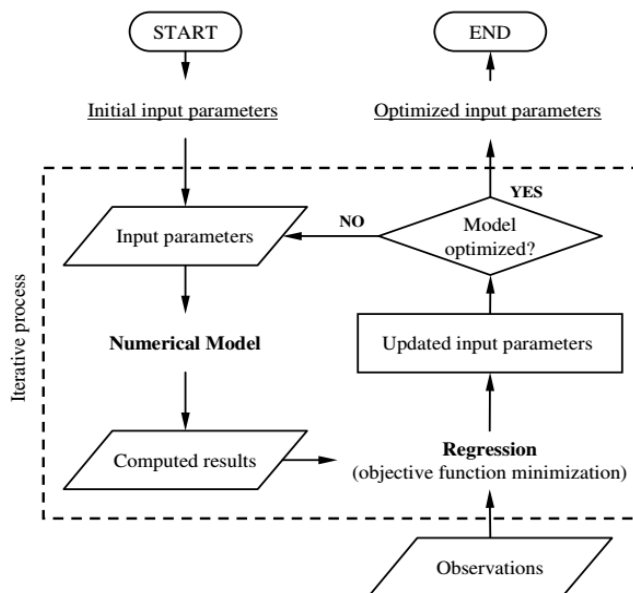


Figure 2.21. Schema of Iterative Back Analysis Procedure (Calvello and Finno, 2004)

Many studies on back-analysis have been published in the literature using both approaches. Gioda and Maier (1980) applied the direct method to back calculation problem using a tunnel case study. Cividini et al. (1981) reviewed back analysis philosophy together with examples of both inverse and minimization methods. Gioda (1985) studied an embankment problem using both approaches. Sakurai and Abe

(1981), Sakurai and Takeuchi (1983) studied displacement based back analysis method. Sakurai et al. (2003) compared different methods of back analysis and showed the significance of the assumptions.

### **2.5.1. Assessment on Measured and Calculated Displacement using Back Analysis**

Applying the back-analysis concept in geotechnical engineering is useful in order to minimize the uncertainty of design parameters for geotechnical projects (Gioda and Sakurai, 1987). In situ measurements (displacements etc.) are provided by design made by actual soil parameters. According to Finno and Calvello (2005), the essential advantage of inverse analysis is its capability to automatically estimate the appropriate parameters that give comparable predicted and calculated outcomes. Even when the problem has high complexity, the inverse analysis provides a valuable aid to designers (Keidser and Rosjberg, 1991; Ou and Tang, 1994; Poeter and Hill, 1997)

Most of the well-documented assessment on measured and calculated displacement in the literature has been done by using back analyses method (Whittle et al., 1993). In these assessments, geotechnical input parameters of a model such as elastic modulus, friction angle, the cohesion of the soil and Young Modulus, etc. are calibrated by using the field data which results in more accurate soil and wall movements. If the estimations and field data are linked together, the analyses are improved, and the results approach the measured deflections. It has been confirmed that back analysis is very beneficial in order to get information regarding the geotechnical parameters (Du et al., Chi, 2006). Calvello and Finno (2004) state that the inverse analysis method is an effective and more objective way of choosing soil parameters for constitutive models since they do not require subjective judgment.

Whittle et al., (1993) applied FE analysis to model seven-story top-down construction in Boston to compare the measured and estimated wall movements by using back analysis concept. The aim of the back analysis is to observe the finite element model's

success rate for interpretation of geotechnical parameters such as displacement of wall and ground movements. ABAQUS finite element program is used to model the case study. The major uncertainty in the finite element analysis is soil input parameters because of the deficiency of laboratory tests. The field data contain 13 inclinometers for monitoring the horizontal movement of the wall and 11 inclinometers for monitoring horizontal ground movement. The observed data are compared with estimations from the back-case analysis at three different stages of construction. The phases of finite element match up with the history of construction activities. Figure 2-22 illustrates the comparison of predicted and measured horizontal wall deformations including modified analysis. While base case analysis underestimates the maximum deflections by approximately 20 mm, modified analysis predictions are compatible with the measured lateral wall deflections. The authors indicate that the description of a constant pore pressure boundary condition can improve the reliability of base case analysis. The key benefits of using finite element analyses in the mentioned study are that time-dependent displacements related with the temporary groundwater flow, and nonlinear and inelastic effective stress, strain and strength properties of soil can be described by these analyses. The major outcome of the study is that it is conceivable to estimate deep excavation-induced movements during construction. However, as the complexity of the model increases, the characterization of soil properties becomes harder with an increasing amount of uncertainties. The quality and amount of laboratory tests need to be increased to minimize uncertainties.

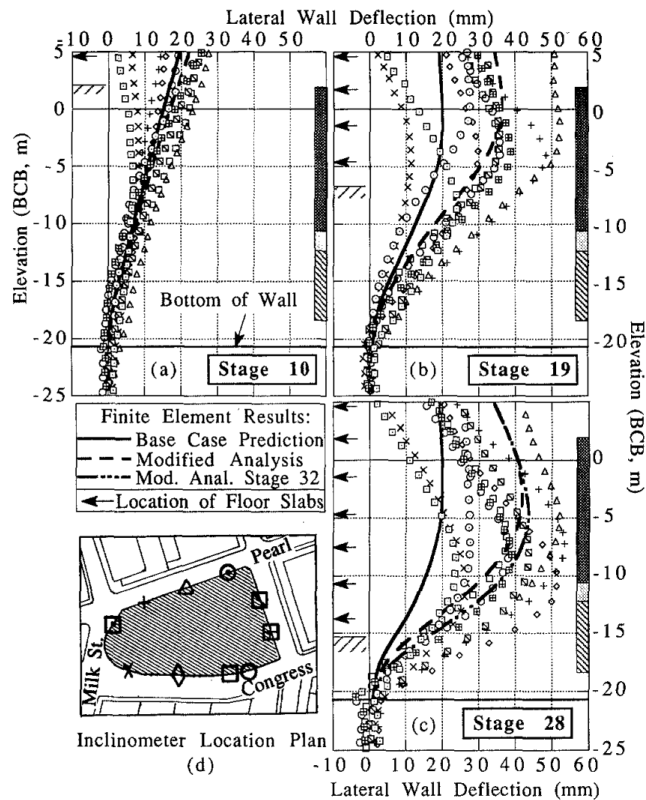


Figure 2.22. Comparison of Predicted and Measured Lateral Wall Deflections (Whittle, Hashash, and Whitman, 1993)

Gioda and Locatelli (1999) exemplify the back-analysis case in order to minimize the difference between measured and calculated displacements of Monteolimpino 2 tunnel on the railway connecting Milan (Italy) to Chiasso (Switzerland). Firstly, the average secant elastic modulus of the soil around the tunnel was intended to find and secondly, the authors want to assess the success of preliminary design by comparing observed and estimated displacements. SPT and dilatometer tests were completed for estimating the in-situ elastic modulus and topographic surveys and sliding micrometers were used to record displacements. Authors point out the finite element model provides a realistic estimate of vertical movements compared to measured ones. The study shows that reasonable results and tunnels' performance can be provided by back analyses during construction.

Many other studies published in the literature including Horodecki et al. (2004), Vogt and Totsev (2006), Ma et al. (2006), Becker et al. (2008), Hsiung (2008), Ma'ruf and Darjanto (2017), etc. using back-analysis concept. The studies aided for the evaluation of estimated displacement of wall or soil movements for the different type of excavations and support systems. All of these studies on back-analysis evaluate the effectiveness of preliminary design instead of mentioning about modification of the design during construction. Information obtained from back-analyses should be used during construction to predict upcoming stages' behavior for safety and financial purposes.

Peck (1969) suggests that back-analysis is positively linked to the observational method in geotechnical engineering. Observational method and optimization techniques for solving inverse problems are discussed in the following section.

## **2.6. Observational Method**

When perilous ground movements are detected in a certain excavation, the need for approximating these movements arises (Marulanda, 2005). These approximations can be obtained through either similar experiences or semi-empirical methods (Clough and O'Rourke, 1990). Model simulation can also be used for estimation of the ground movements in excavations (Clough and Tsui 1974; Potts and Flourie 1984; Mana and Clough 1981; Whittle et al. 1993).

Model simulations rely on the usage of numerical programs such as the FEM whereas semi-empirical methods partly include past performance data. Nonetheless, the application of a monitoring program that registers ground movements, and reactions of nearby structures is of utmost significance due to the uncertainties associated with soil properties, construction methods, and support system details. The monitoring program produces interpretations which are used to assess the performance of the construction and compares it with original design expectations. In case a substandard performance is observed, modifications to the construction and support system can be

made (Marulanda, 2005). This procedure is called the observational method (Peck 1969) which is usually implemented in the engineering practice (Institution of Civil Engineers GB 1996).

The observational method comprises of a design based on the most likely conditions coupled with estimates of behavior and a system monitoring performance through the construction process. Past projects can provide valuable information which would aid engineers, especially geotechnical engineers, in the design and construction of a new yet similar project. Hence, noting deformations in structures and soil surface settlements during an excavation construction provide useful information on the stress-strain response of the soil due to the fact that these deformations and settlements occur as a result of complex shearing of the soil surrounding the excavation (Marulanda, 2005). Knowledge from precedence characterizes a classic inverse analysis problem intending to understand the soil-stress response implied by field measurements. Ad-hoc approaches are frequently used to unravel this inverse problem whereby soil model parameters are adjusted to narrowly duplicate numerical analyses with field measurements. However, the ad-hoc methods for the model update are not adequately wide-ranging. (Marulanda, 2005)

### **2.6.1. Optimization Techniques**

Gioda and Sakurai (1987); Ou and Tang (1994); Zentar et al. (2001); Calvello and Finno (2004) suggest a substitute to ad-hoc procedures in determining the solution of inverse problems and learning from precedence, named optimization techniques. If one is provided with a numerical model, unidentified properties of the material in the constitutive model are analytically tinkered with to diminish the discrepancy between numerical model estimations and the observational response. Optimization techniques can be quite helpful in model calibration although there are some setbacks. (Hashash et al., 2006). Moreira et al. (2013) state that optimization algorithms are used in the

back analysis in order to minimize the number of iterations and find the best results of parameters.

Many authors combined inverse analysis with the use of different optimization techniques in their studies. Zentar et al. (2001) used back-analysis concept based on an optimization code SiDoLo (Simulation and identification of constitutive models) in order to minimize the function indicating the discrepancy between experimental data and the in-situ test results. Finno and Calvello (2005) combined observational method and inverse modeling based on the Gauss-Newton method using UCODE (Poeter and Hill, 1998) computer code that is used for parameter estimation. Numerical analysis is used to optimize the FEM of a deep excavation in order to minimize the observed and estimated horizontal displacements of Chicago clays. Rechea et al. (2008) compared the gradient-based method and genetic algorithm (GA) by simulating excavation support systems. Both synthetic and real excavation displacement results are used to demonstrate the performance of the algorithms. The reason for using synthetic excavation is to prevent the algorithms being affected by complexity and errors in in-situ measurements. The authors also want to show some of the findings to apply the approaches in the field by using a well-documented case. In spite of the high calculation costs, GA gives better solutions. On the other hand, the gradient method showed higher performance from the point of view of time. Shao and Macari (2008) studied a systematic process called “information feedback analysis” with the purpose of estimate excavation-induced ground deformations by using a combination of “downhill simplex method” and “the conjugate direction method” optimization algorithms in deep excavation case (Subway station in Shanghai City, China). The authors think that their study encourages the use of inverse-analysis-based “computer observational method” in practice. Another work done for learning deep excavation response is by Hashash et al. (2009) by comparing two inverse analysis techniques. The first technique GA is a parameter optimization method while the second technique SelfSim is a back-analysis method which bonds the finite element method with an unceasingly evolving material model (Ghaboussi et al., 1998). Two

techniques are compared for real deep excavation case in Chicago. They concluded that the accuracy performance of SelfSim is better in surface settlement prediction. GA predicts higher values of settlement. Miranda et al. (2011) applied two optimization techniques using the back-analysis concept in order to estimate soil parameters during the construction phase of an underground structure by using 3D numerical model. Classical optimization algorithm and the evolutionary optimization algorithm are used in their study. The performances of both approaches are found well by the authors. Many other papers have been published in the same field by using different optimization methods.

Optimization methods used in geotechnical engineering can be separated into three main groups as deterministic optimization techniques, nature-inspired search methods (stochastic) and hybrid optimization techniques (Yin et al., 2018). Gradient-based algorithms and Nelder-Mead Simplex algorithms (Ledesma et al., 1996; Gens and Ledesma, 1996; Lecampion et al., 2002; Calvello and Finno, 2004; Finno and Calvello, 2005) are two main deterministic optimization techniques. Gradient-based methods such as the steepest descent, the conjugate gradient, and the Newton method can expedite the progression of optimization due to the use of gradient information. However, it requires a derivative calculation which may be hard to implement. Besides, the initial trial solutions may change the results (Finno and Calvello., 2005). According to Yin et al. (2018), gradient-based methods are insufficient for complex nonlinear problems. Gradient-based methods cannot be used when the objective function is non-differentiable, discrete or discontinuous. These shortcomings limit the use of deterministic optimization methods especially in complex engineering problems. Nature-inspired search methods which are also called stochastics, genetic programming, evolutionary algorithms and swarm intelligence (Arora, 2004). They are also called as metaheuristic methods since there is no assumption about the optimization problems and having huge search spaces. Metaheuristics are designed for large scale, complex and challenging problems (Yang, 2010). These methods have a capability of escaping from local optimum and can solve multiple-objectives

problems, mixed design variables and problems having uncertainty in the model (Arora, 2004). Particle swarm optimization (PSO), differential evolutions (DE), evolution strategy (ES), genetic algorithms (GA), etc. (Pal et al., 1996; Samarajiva et al., 2005; Goh, 1999; Levasseur et al., 2007, 2008, 2009, 2010; Rechea et al., 2008; Miranda et al., 2010; Papon et al., 2012; Hashash et al., 2010) are the most common stochastic optimization techniques. Metaheuristics are applicable to most real-life problems. Unlike conventional optimization techniques, which have speed and local optimality problems, hybrid optimization techniques show high performance for convergence speed (Tsai et al., 2004). Some of the cases that hybrid optimization techniques can be applied are the optimization of pile groups, geotechnical parameter identification, slope stability problems, etc. (Yin et al., 2018). Since stochastic methods have robust search ability, they can be combined in hybrid methods. In the geotechnical engineering field, the use of hybrid optimization techniques may increase in the future.

More details about metaheuristic search methods and Particle Swarm Optimization used in this research are in the following section.

### **2.6.1.1. Nature-inspired (Metaheuristic) Search Methods**

Nature-inspired methods are developed by imitating natural phenomena and they have been developed over the past 20 years. These search methods may appear to be a random technique to reach an optimum solution; however, it makes use of a natural optimization or intelligent heuristic way to lead the search for the optimum solution. The technique starts with a collection of design points which is called the population. The method then attempts to generate a better design point throughout each iteration of the algorithm using specific stochastic procedures.

Stochastic search algorithms have recently been a highlight in solving adamant engineering optimization problems due to their apparent robust and efficient performance when compared to the deterministic algorithms (Saka and Dogan, 2012).

This is due to the fact that these methods travel in a restricted design domain randomly with the goal of reaching the optimum solution. Their objective is to proficiently explore the search space using certain governing mechanisms to provide an almost optimal solution if not a global optimum. They also exploit some approaches to evade getting stuck in limited areas of the search space. Additionally, they do not require an unambiguous affiliation between the objective function and the limitations. Metaheuristic methods are estimation techniques and there is no scientific evidence that the optimum answer obtained is the global one. Nonetheless, while they are not problem specific, they have demonstrated a highly effective and forceful way of procuring the solution of practical engineering design optimization problems with continuous as well as the discrete design variables.

The literature suggests that the metaheuristic techniques are proficient and reliable to an acceptable degree. Their performance is not affected by the complexity of optimization problems (Saka and Dogan, 2012). Voss (2000), states that in complex engineering design optimization problems with continuous and discrete variables, metaheuristic algorithms often achieve better results than the traditional approaches of the branch, bound and dynamic programming. Moreover, metaheuristics are relatively more malleable when compared to classical mathematical programming techniques due to the fact that they tackle the optimization problem directly without imposing any condition such as expressing objective function or design constraints.

The disadvantage of these algorithms is that they do not secure a global solution. However, this setback can be minimized by allowing the algorithm to run multiple times for longer periods (Arora, 2004).

#### **2.6.1.2. Particle Swarm Optimization (PSO)**

Swarm intelligence is a metaheuristic approach that is based on the collective behavior of insect swarm, bird flocking or fish schooling that is seen in nature. PSO turns this combined behavior of particles into a numerical optimization algorithm just like how

a swarm of bees works together to achieve a single optimum goal instead of the survival of the fittest idea.

It falls under the class of swarm intelligence methods and it is also a population-based stochastic optimization procedure presented by Kennedy and Eberhart in 1995. PSO initiates its process with a randomly generated set of solutions call the initial population. The optimization process is then implemented by searching for the optimum solution by updating the generations.

Considering other metaheuristic optimization methods, PSO has better search routine for some hard optimization problems with a faster solution (Kennedy and Eberhart, 2001). PSO offers quick implementation since the algorithm needs adjustment of few parameters only. Since the gradient data obtained from the error function is not essential for PSO, it can be used in optimization problems where the gradient information is either unobtainable or time consuming to derive (Bergh, 2001). Contrasting to evolutionary optimization techniques such as GA, binary number encoding is not a requirement for this algorithm making it simpler in terms of implementing it digitally. PSO has been implemented successfully on a number of problems such as mechanical and structural optimization problems, artificial neural network training and fuzzy system control (Arora, 2004).

Nguyen et al., (2016); Zhang et al., (2013); Knabe et al., (2013); Mulia A., (2012); Knabe et al., (2012); Sadoghi et al, (2011); Zhang et al., (2009); Meier et al., (2008); and Schanz et al., (2006) studied inverse analysis using Particle Swarm Optimization with the intention of parameter identification of constitutive models.

## CHAPTER 3

### BACK ANALYSIS PLATFORM

#### 3.1. Introduction

The stages of metaheuristics based back analysis platform in order to estimate geotechnical parameters based on the field measurements in deep excavations are explained in this chapter. The aim is to calibrate the soil parameters for selected construction stages by using back-calculation, thus to predict upcoming stages' behavior using calibrated parameters. Updated field data are added into the platform at every stage, therefore the predictions become more accurate for subsequent excavation phases.

Development of the back-analysis platform and its application to deep excavation problems is described in detail in the following sections.

#### 3.2. Development of Back-analysis Platform for Deep Excavation-induced Movements

Back-analysis platform established in this thesis consists of followings:

- (1) numerical modeling of deep excavation using the finite element method (FEM) in order to calculate the geo-structure's responses,
- (2) implementation of Particle swarm optimization (PSO) algorithm with the intention of modification of the soil material parameters in the light of observed field measurements.

In a typical deep excavation problem, construction sequence and geo-structure's response are defined by the numerical model. The deep excavation is first modeled by

taking the construction scenario into consideration in back-analysis platform. The initial design parameters are used in the first run. Back analysis platform enables multiple input parameters to be optimized simultaneously through the iterations. At each iteration, the optimization code compares the computed displacements and the measured field data. Iterative process repeats until the stopping criteria are met. The back-analysis procedure is shown in Figure 3-1.

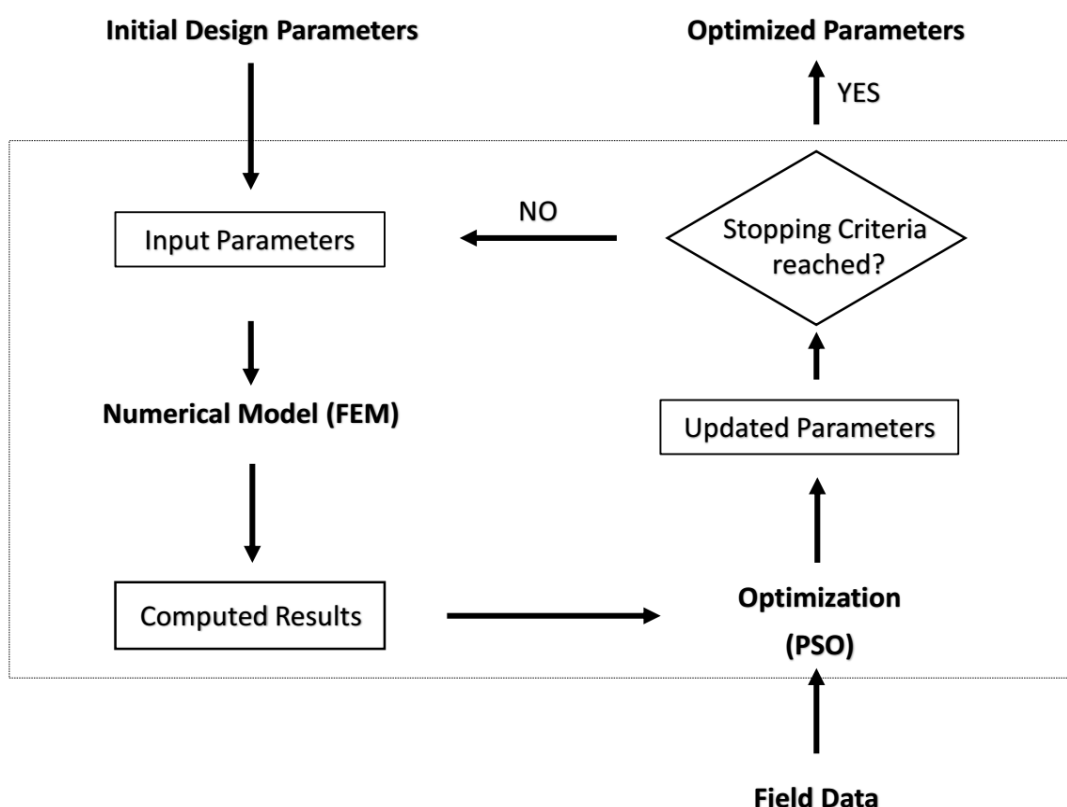


Figure 3.1. Back Analysis Platform Flowchart

In this research, the commercial finite element program PLAXIS is used to model the deep excavation and to compute the horizontal displacements. The discrepancy between computed displacements and the measured field data is minimized by the PSO algorithm, which is coded in Python 3.6.0 software. The optimization is

performed by coupling PLAXIS and Python code developed specifically for this purpose.

### 3.2.1. Finite Element Analysis Configuration

FEM enables solving the equilibrium equations of the geostructures through the discretization and provides the ability to model the complex nonlinear behavior of the soil through various geometries with diverse boundary limits and constitutive models. Plane strain assumption is made in 2D FEM while disregarding possible 3D effects on the results. The plane strain model implies that the strains in the longitudinal axis (out of plane direction) are ignored ( $\epsilon_z = 0$ ). This model is used where the length is considerably greater than the width of the excavation. The plane strain assumption is effective in the analysis of deep excavation and generally gives correct estimations of lateral deflections, especially away from the corners. Creating the geometry by considering the construction scenario is the first step of modeling the deep excavation. Coordinates of soil layers, structural elements (i.e. wall, anchors, struts), and excavation levels are entered. Next step is the definition of soil stratigraphy and properties of structural elements. Material parameters and interfaces are assigned to corresponding soil and structural elements. The interfaces are used to model the interaction between the soil and the wall and enable indication of the reduced wall friction as compared with soil friction. Strength reduction factor interface ( $R_{inter}$ ) value is entered in PLAXIS, which refers to the strength of the soil to the interface strength and is calculated using equation 3-1. The lowest value of  $R_{inter}=0.01$  which refers to non-friction between the soil and the wall, whereas the upper bound value of  $R_{inter}=1.0$  which means the soil and the wall is totally in contact.

$$R_{inter} = \frac{\tan\theta_{wall}}{\tan\theta_{soil}} \quad (3-1)$$

The soil is modeled as a continuum and decoupled into meshes (the specified number of elements) in different shape and size. Meshes are linked at nodal points, and the

stresses and deformations are computed at these points. Size of the mesh is not uniform throughout the model such that they become finer at soil-structure interaction points as shown in Figure 3-2.

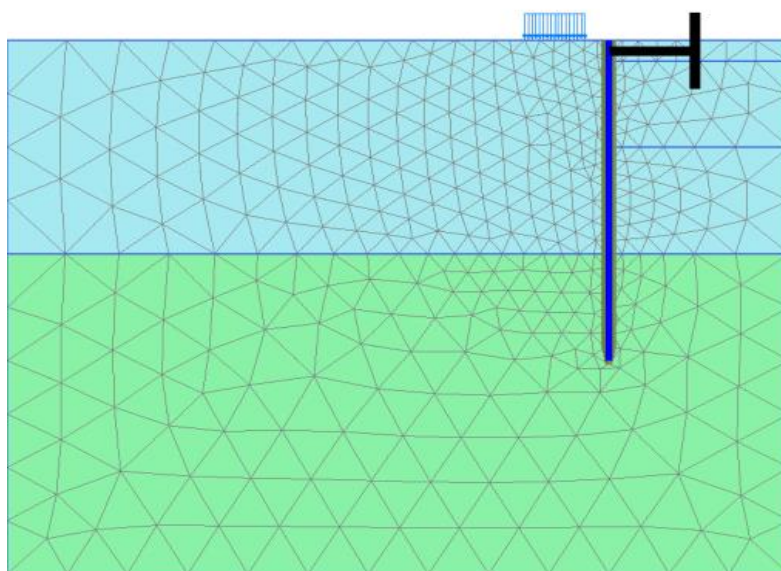


*Figure 3.2. Generated Mesh Example of Deep Excavation with Supported Wall*

Finally, in the calculation stage, the construction steps of deep excavation are defined in the software. The construction scenario is divided into phases. For instance, the first phase of the model includes the wall installation to the anticipated depth and the activation of external loads. At each phase, the soil is progressively extracted until the final excavation depth. In PLAXIS, this procedure is known as staged construction where the construction activities are defined step by step. Unless the failure has occurred, the calculation stage ends, and the results of the analysis can be viewed. Total displacements, total strains, effective stresses, total stresses, pore water pressures and internal forces of the structural elements results can be viewed in the results.

The successful use of FEM depends on the constitutive model selection. Constitutive models for soil behaviors are discussed in section 2.4.1.1. The behavior of soil layers is taken into account using Hardening-soil (HS) model in this research. Considering the theory of plasticity, including soil dilatancy, and yield cap make the HS model more thematic. This model is an elastoplastic type of hyperbolic model, expressed in the framework of shear hardening plasticity. Due to the fact that the stiffness of soil for isotropic loading, unloading/reloading, and shearing can be automatically provided by the HS model, it gives more accurate results for calculating horizontal displacements. The basic parameters used in the HS model is given in Table 3-1, and the formulation of the HS model is shown in Figure 3-3.

Table 3.1. *Parameters of Hardening Soil Model*

<b>Parameter</b>	<b>Description</b>
$c'_{ref}$	Effective cohesion
$\phi'$	Effective angle of friction
$\psi$	Angle of dilatancy
$E_{50}^{ref}$	Secant stiffness in standard drained triaxial test
$E_{oed}^{ref}$	Tangent stiffness for primary oedometer loading
$E_{ur}^{ref}$	Unloading-reloading stiffness ( $E_{ur}=3E_{50}$ )
$\nu_{ur}$	Poisson's ratio for unloading-reloading ( $\nu_{ur}=0.2$ )
$K_0$	$K_0$ value for normal consolidation ( $K_0=1-\sin\phi$ )
$m$	Power for the stress-level dependency of stiffness

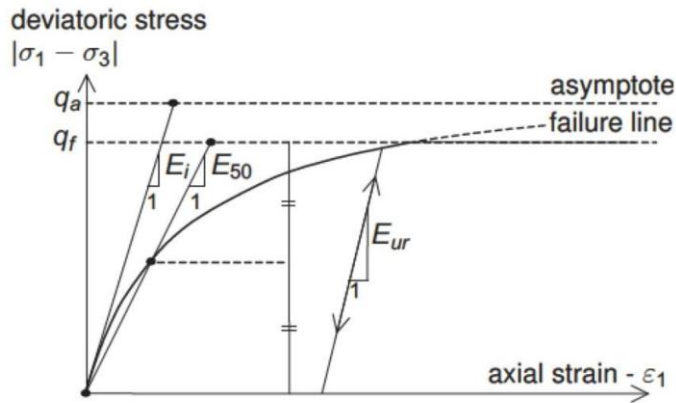


Figure 3.3. Hyperbolic Stress-Strain relation in Primary Loading for a Standard Drained Triaxial Test (PLAXIS 2D User's Manual, 2010)

$E_i$  = Initial Stiffness (Young's) Modulus

for

$$q < q_f ; - \varepsilon = \frac{1}{E_i} \frac{q}{1 - q/q_a} \quad (3-2)$$

$$E_i = \frac{2E_{50}}{2 - R_f} \quad (3-3)$$

$$R_f = \frac{q_f}{q_a} = 0.9 \quad (3-4)$$

The failure stress is defined by equation 3-8.

$$q_f = (c' \cot \theta' - \sigma'_3) \frac{2 \sin \theta'}{1 - \sin \theta'} \quad (3-5)$$

The stress dependency for secant stiffness ( $E_{50}$ ) and unloading/reloading ( $E_{ur}$ ) modulus can be expressed by equation 3-6.

$$E_{50} = E_{50}^{ref} \left( \frac{\sigma'_3 + a}{\sigma'_{3,ref} + a} \right)^m \quad (3-6)$$

or

$$E_{50} = E_{50}^{ref} \left( \frac{c' \cos \theta' - \sigma'_3 \sin \theta'}{c' \cos \theta' + P_{ref} \sin \theta'} \right)^m \quad (3-7)$$

Differently, oedometer modulus  $E_{oed}$  can be expressed by equation 3-8.

$$E_{oed} = E_{oed}^{ref} \left( \frac{c' \cos \theta' - \frac{\sigma'_3}{K_0} \sin \theta'}{c' \cos \theta' + P_{ref} \sin \theta'} \right)^m \quad (3-8)$$

where,

$P_{ref} = P_a = 100$  kPa (the atmospheric pressure)

$\sigma'_3$  = confining pressure

$$a = \frac{c}{\tan \theta'} \quad (3-9)$$

$m = 1$  for clays and 0.5 for sands (Gouw, 2012).

### 3.2.2. Particle Swarm Optimization Algorithm

Swarm intelligence is a metaheuristic approach that is based on the collective behavior of insect swarm, bird flocking or fish schooling that is seen in nature. Particle swarm optimizer (PSO) turns social behaviors of particles such as bird flocking or fish schooling into a numerical optimization algorithm just like how a swarm of bees works together to achieve a single optimum goal instead of the survival of the fittest idea. The PSO computational algorithm is described through the following terms:

Particle is used for identification of an individual in the swarm. Particle Position is the coordinates of the particle and denotes a design point (a vector of design variables). Particle Velocity simply answers the question “What is the moving rate of particles in the search space?” Swarm Leader presents the particle with the best position. It denotes a particle position (design point) having the lowest fitness value.

Fitness value is the difference between computed displacements and the measured field data. It represents the function that is being iteratively minimized during

optimization process by modification of soil parameters between predefined boundaries. The quality of solution is evaluated by defining the fitness function and different combination of fitness function is possible (Zhao and Yin, 2009; Tang et al, 2006; Vardakos, 2007; Knabe et al., 2013).

The fitness value for deep excavation problem in this research is calculated using equation 3-10.

$$\text{Fitness (f)} = \sqrt[10]{\sum_{i=1}^n (x_{measured}^i - x_{fem}^i)^2} \quad (3-10)$$

where, n is the number of selected points on the model (10 points in this study) and x is the lateral deflection.

The number of selected points on the model should not be chosen arbitrarily. The measured points in the field that are compared should be chosen according to FE mesh points since the displacements can only be computed at these mesh nodes.

In the PSO algorithm, each particle has a location (design point) which signifies a potential solution to an optimization problem. Each particle is specified by its own ID “i”. The following symbols  $X_i$  refers to the present position of the particle, and  $V_i$  is the present velocity of the particle.

Each particle in the swarm records its own present position and its finest position gained during the algorithm. The best position for the  $i^{\text{th}}$  particle is referred as (pBest) $_i$ . The best position that has been reached for all the particles in the swarm together is referred as gBest.

The f symbol refers to the fitness function that needs to be minimized and k is the iteration number. Equation 3-11 is used in order to update the personal best position.

$$(\text{pBest})_i (k+1) = \begin{cases} (\text{pBest})_i (k) & \text{if } f(x_i(k+1)) \geq f((\text{pBest})_i (k)) \\ x_i (k+1) & \text{if } f(x_i(k+1)) < f((\text{pBest})_i (k)) \end{cases} \quad (3-11)$$

Equation 3-11 states that if the new fitness value is not better than pBest, keep the previous pBest, if the new fitness value is better than pBest, set new position as pBest. At each iteration of the algorithm, each particle's velocity is updated according to its best and swarm's best position as shown in equation 3-12. This process is the accelerating the particle to the best-known position.

$$v_i(k + 1) = w * v_i(k) + r1 * c1[(pBest)_i(k) - x_i(k)] + r2 * c2[(gBest)_i(k) - x_i(k)]$$

(3-12)

where w is the inertia weight that is used in order to avoid the new velocity being affected by the previous velocity and generally less than 1. r1 and r2 are the arbitrarily selected numbers between 0 and 1. c1 and c2 are constant numbers that help to direct the particles to better position and generally equal to 2 (Knabe et al., 2013).

Equation 3-13 is used in order to update the new position of the particle.

$$x_i(k + 1) = x_i(k) + v_i(k + 1)$$

(3-13)

Equation 3-13 states that the updated position of each particle is calculated by adding new velocity to the current position.

The procedure presented above is repeated until the stopping criteria are satisfied. Figure 3-4 shows the vectorial drawing of the position update process. Figure 3-5 illustrates the PSO algorithm flow chart.

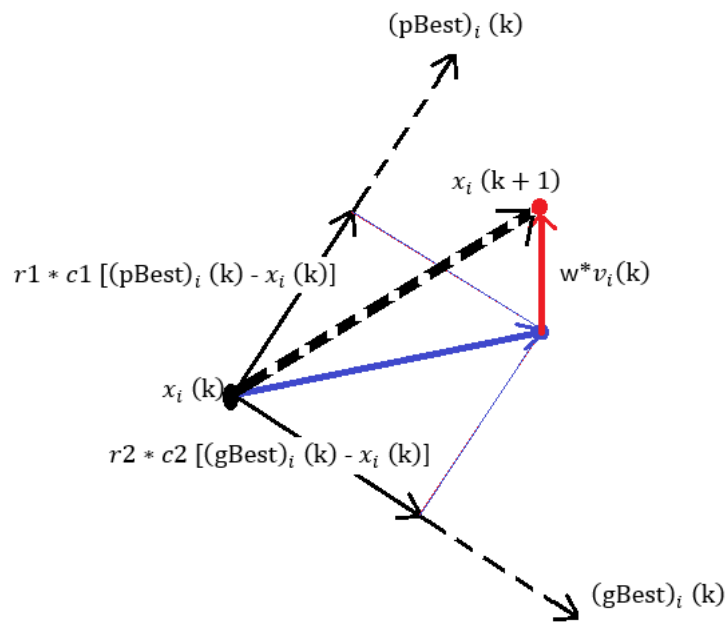


Figure 3.4. Position Update Process using PSO

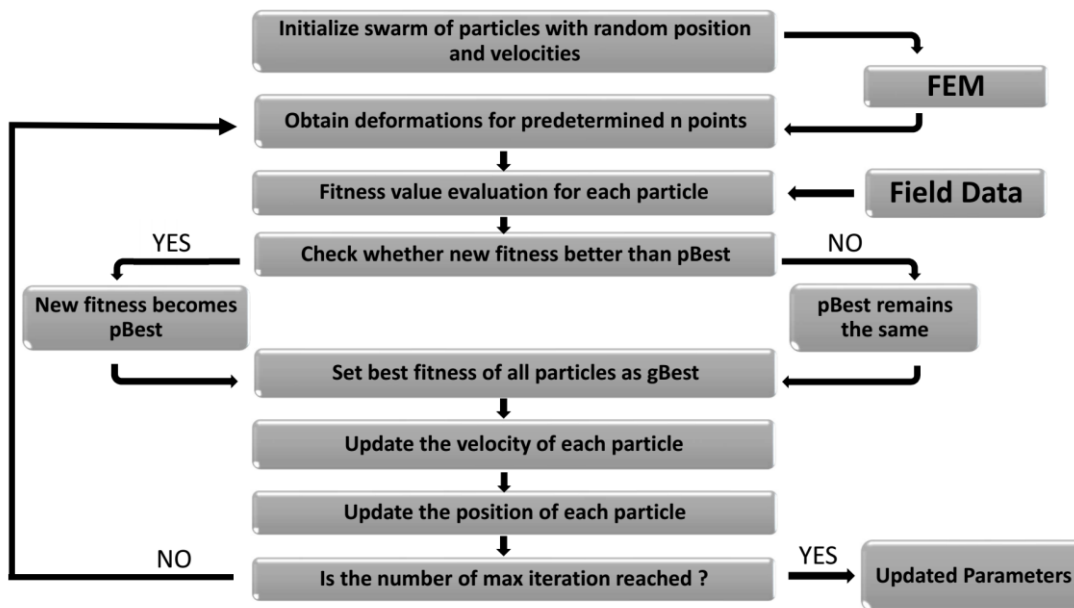


Figure 3.5. PSO Algorithm Flow Chart

The above framework is developed as a coupled software implementation where the Plaxis is run to obtain the FEM based realistic field deflections as realistically as possible, and PSO is then run to obtain the minimize the differences of the calculated deflections.



## **CHAPTER 4**

### **CASE STUDY:**

#### **DEEP EXCAVATION OF MAIDAN OFFICE – HOME OFFICE - SQUARE**

##### **4.1. Introduction**

In the present chapter, the application and the performance of the developed back analysis platform is explained and tested through a deep excavation case study, named Maidan Office-Home Office-Square project constructed in Ankara/Turkey. General information about Maidan Office-Home Office-Square Project including geological and geotechnical information, construction and monitoring processes are given in Section 4.2. Finite element model of deep excavation including detailed parameter settings is studied in Section 4.3. The application and the performance of Particle Swarm Optimization (PSO) algorithm for modification of the soil parameters related to observed field data are discussed in Section 4.4. Computed deformations of upcoming stages with back calculated parameters are compared with field data in order to see the prediction performance of the algorithm in Section 4.5. Finally, results and comparisons are presented in Section 4.6.

##### **4.2. Project Description**

Maidan Office-Home Office-Square Project was constructed in 2017 which includes 3 blocks of a 15-story commercial building with 3 basement levels, and a block of a car park with 3 basement levels. The project is in Ankara, which has the second highest population in Turkey with 5.5 million. The traffic density and structuring rate is very high at the location of the project, which necessitates deep excavation for many purposes such as car parking and water distribution networks. The location of the project is illustrated in Figure 4-1.

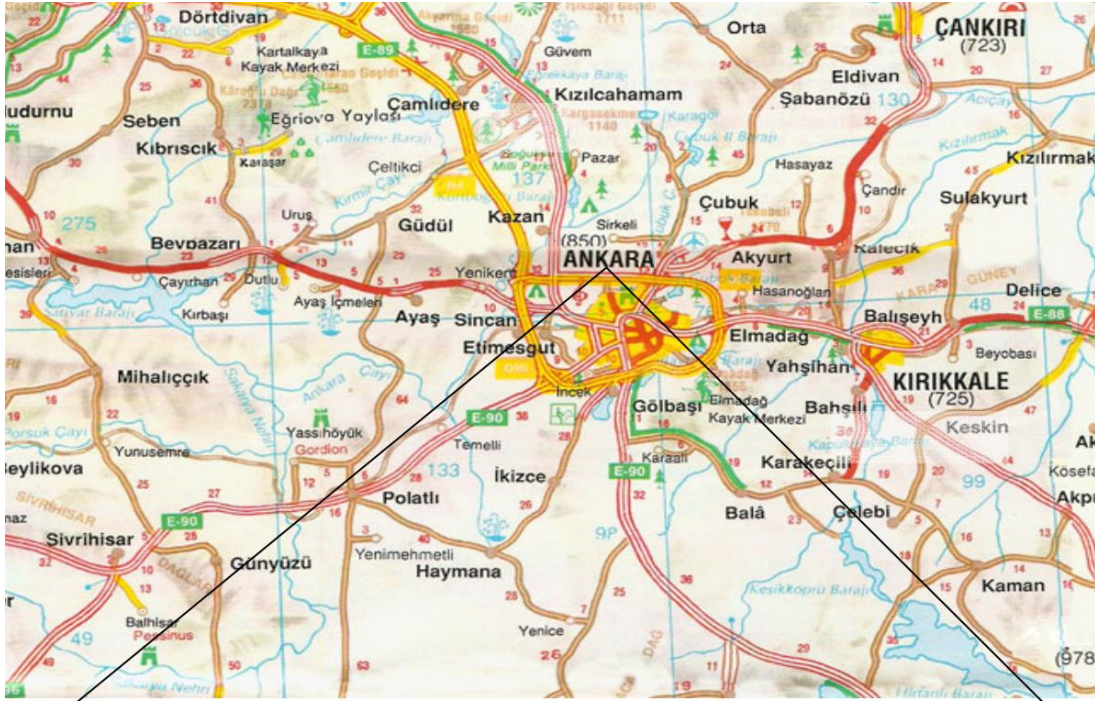


Figure 4.1. The location of the Project (retrieved from soil investigation report “Ankara İli, Çankaya İlçesi, 25389 Ada, 3 Parsel Jeolojik – Jeoteknik Etüt Raporu” by Toker Drilling and Construction Engineering Consultancy CO)

#### 4.2.1. Geological and Geotechnical Information

According to soil investigation report, named “Ankara İli, Çankaya İlçesi, 25389 Ada, 3 Parsel Jeolojik – Jeoteknik Etüt Raporu” and prepared by Toker Drilling and Construction Engineering Consultancy CO on May 2015, at the top of the excavation site, alluvial deposit up to 10 m in thickness which are deep brown – grey in color and includes medium-stiff / medium dense clay / gravelly clay / silty clay / sandy clayey gravel zones underlain by partly silty Gölbaşı Formation which are reddish fawn colored includes fine gravels, very stiff-hard clay zones. This clay layer partly includes very dense gravelly clayey sand / clayey gravel / clayey sand.

Geotechnical information such as idealized soil profile, initial estimations of geotechnical parameters of the soil and ground water table are determined in the light of laboratory and field tests. 17 boreholes, 559 m of total boring length, have been drilled in deep excavation site including standard penetration tests (SPT) and pressuremeter tests (PMT) boreholes. Initial design parameters of soil material are given in Table 4-1, which are determined using empirical correlations given in Equations 4.1 to 4.3, Table 4.2, Figures 4.2 and 4.3, are in the range of laboratory test findings (see Appendix C for laboratory test results).

Table 4.1. *Initial Design Parameters of Soil Materials*

Layer	Average SPT-N Value	PI (Plasticity Index)	Undrained Shear Strength $C_u$ (kPa)	$c'$ (kPa)	$\phi'$ (degree)	Deformation Modulus $E_s$ (MPa)
Alluvial Deposit Clay Layer	24	40	120	10	25	35
Hard Clay Layer	50	45	250	20	26	55

$$C_u = f_1 * N_{60} \quad (\text{Stroud, 1974}) \quad (4-1)$$

$$E_s = 100 - 300 * C_u \quad (\text{Duncan \& Buchignani, 1976}) \quad (4-2)$$

$$c' = \alpha' * \tan \phi' \quad (\text{Lunne, 1997}) \quad (4-3)$$

where  $\alpha'$  is in between 20-50 for hard clays.

Table 4.2.  $\alpha' - \tan \phi'$  Relationship (Lunne, 1997)

Type of soil	$\alpha^*$	$\tan \phi'$
Soft clay	5 – 10	0.35 – 0.45
Medium-stiff clay	10 – 20	0.40 – 0.55
Stiff clay	20 – 50	0.50 – 0.60

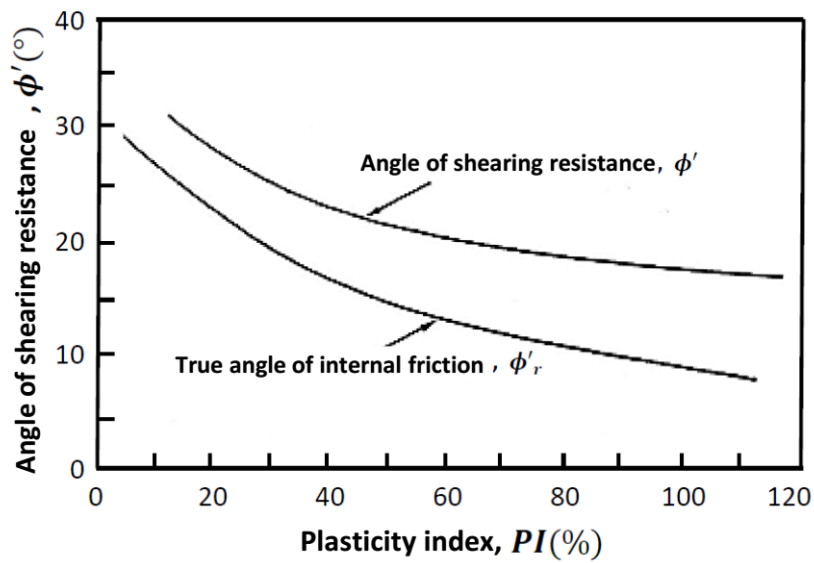


Figure 4.2.  $\phi'$ - $PI$  Relationship (Gibson, 1953)

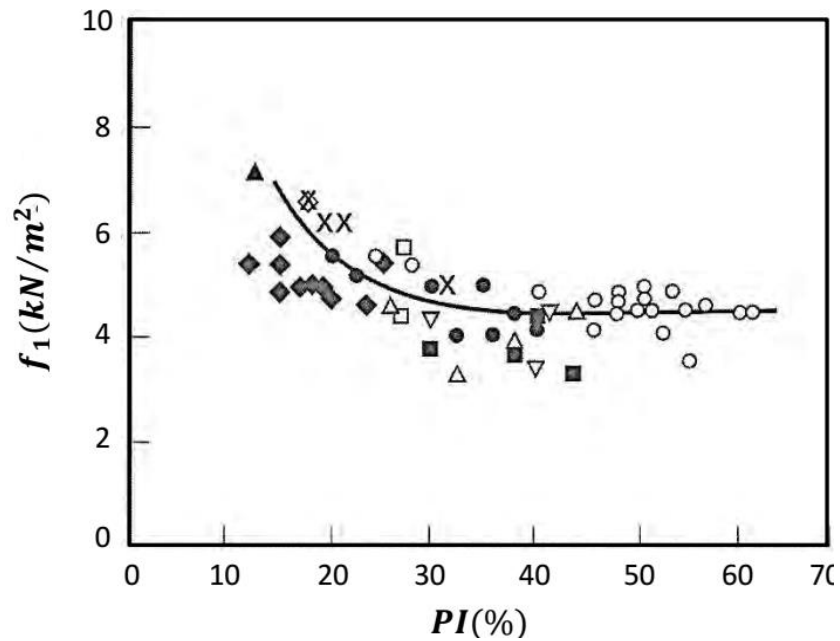


Figure 4.3. SPT- $N_{60}$  - $C_u$  – PI Relationship (Stroud,1974)

It took 100 days to complete the deep excavation construction, between 21.07.2015 – 31.10.2015. Total of 531 piles, having a total of 7477 m length,  $\text{Ø}60/100$  bored piles were constructed. Their depth changed between 12.2m and 15.2 m. In addition, total of 696 prestressed ground anchorages having 14,109 m total length were constructed as horizontal supports. The excavation site was well instrumented with 10 inclinometers in order to monitor the horizontal displacements of the pile wall periodically. Instrumentation plan and project layout are shown in Figure 4-4.

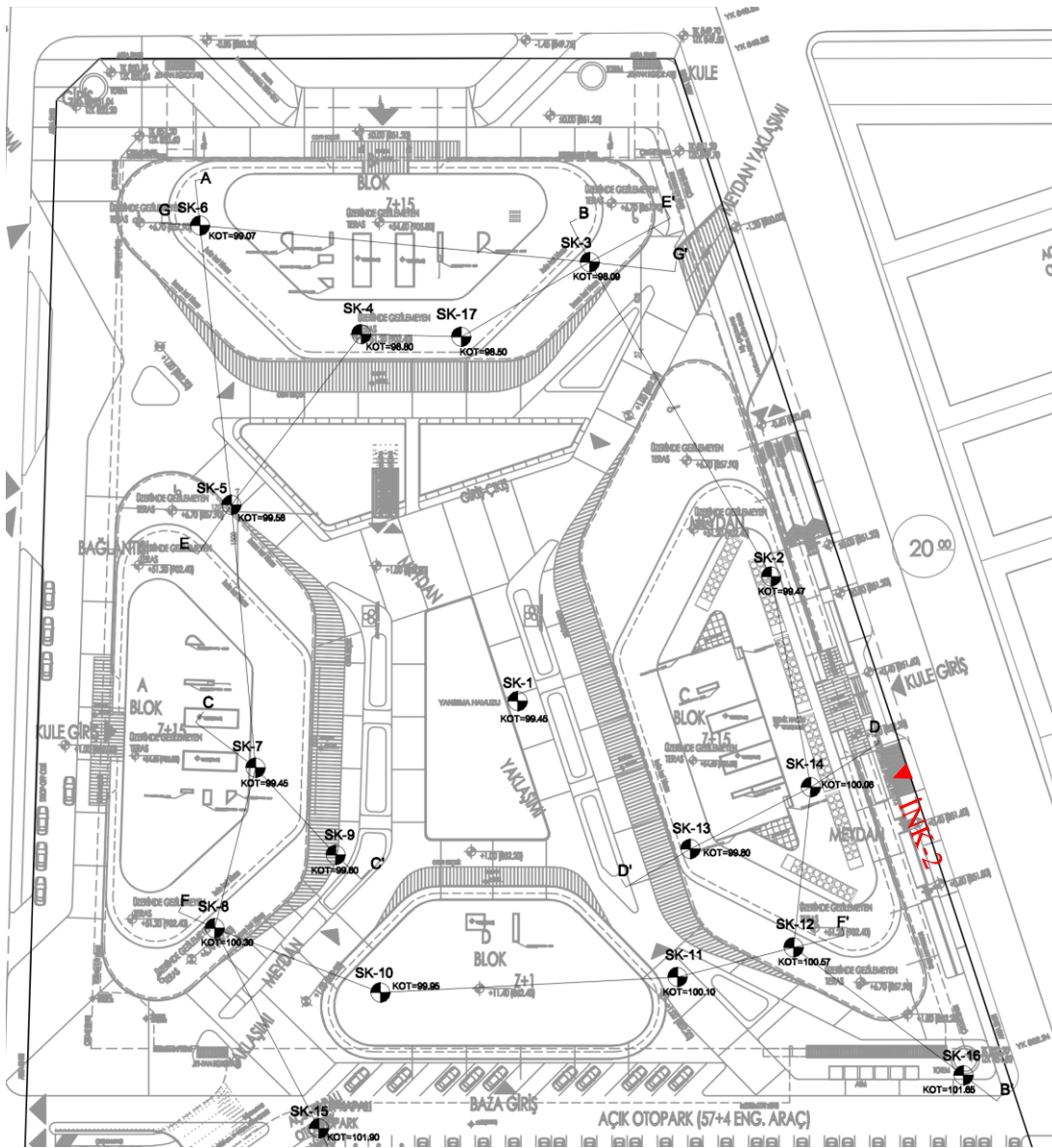


Figure 4.4. Project Layout and Instrumentation Plan (retrieved from soil investigation report “Ankara İli, Çankaya İlçesi, 25389 Ada, 3 Parsel Jeolojik – Jeoteknik Etüt Raporu” by Toker Drilling and Construction Engineering Consultancy CO)

In the scope of this thesis, deep excavation around C Block is studied. C block is a 15-story commercial building with 3 basement levels. The idealized soil profile is determined using SK-14 boring log. Figure 4-5 presents SPT-N values obtained from the SK-14 and a geological section of the soil underneath the C Block.



#### 4.2.2. Construction and Monitoring

A typical cross section and the deep excavation geometry with a support system are shown in Figure 4-6 in details. Ø60/100 bored piles were designed as structural elements which are 15.2 m deep. The wall was supported by three levels of 3x0.6” prestressed ground anchors. Drill diameter of anchorages is 140 mm. The final excavation depth was 9.8 m from the pile cap and 11.6 m from the original ground level. 1.8 m of the slope was designed between the original ground level and the top of the pile.

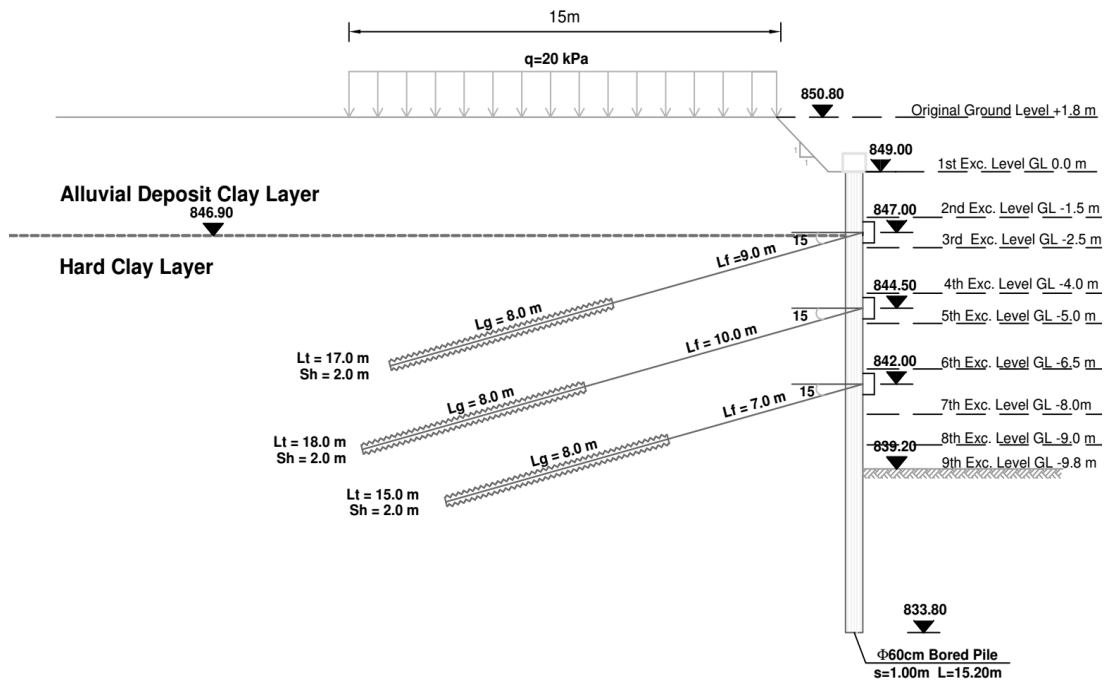


Figure 4.6. Ground Profile and Deep Excavation Geometry

Horizontal displacements of the studied case are monitored by Inclinator #2. In the light of these displacement measurements, optimization takes place with the intention of calibration of the soil material parameters. The cumulative deflection versus depth

plot during 7 weeks of Inclinator #2 is shown in Figure 4-7. In inclinometer readings, the deflection at the bottom is fixed to zero and the deflections are taken relative to this point cumulatively from bottom to top. The maximum cumulative movements are observed at the top of the pile and the deflection reached equilibrium after 7 weeks (Stage 5) as it can be seen from the figure.

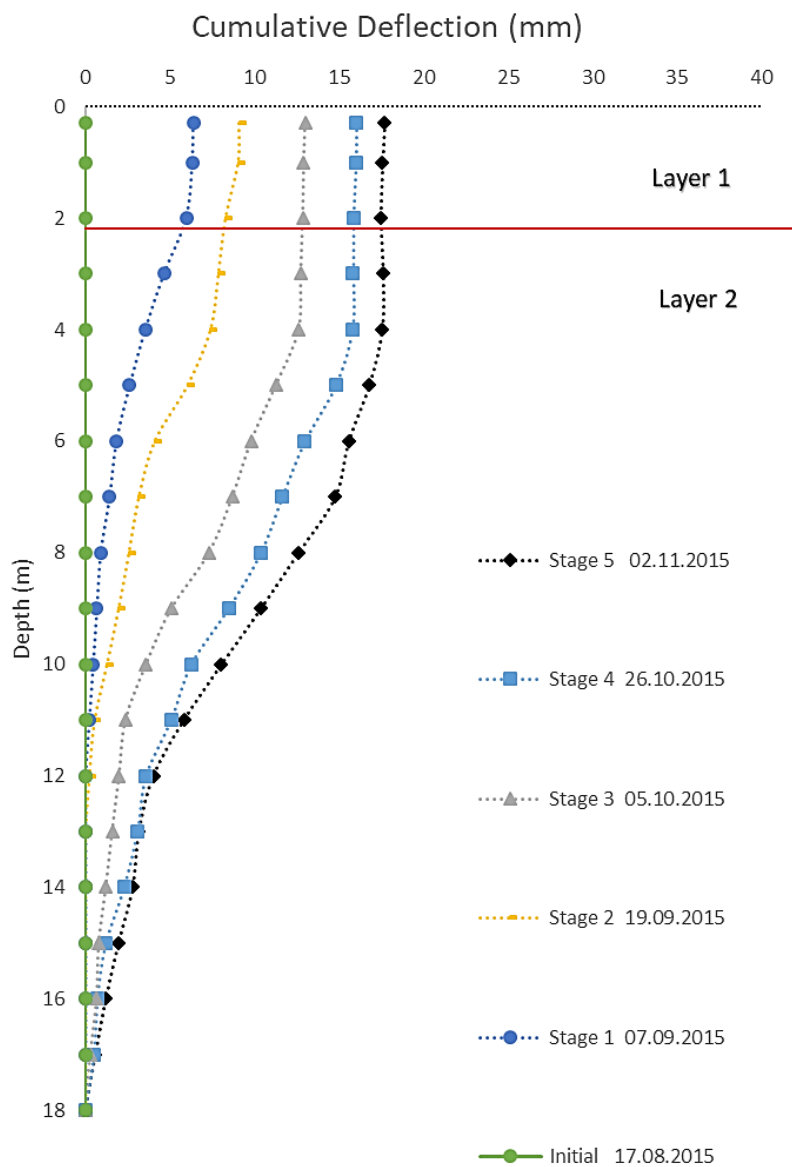


Figure 4.7. Inclinator #2 Cumulative Readings

### 4.3. Finite Element Model

The commercial finite element program PLAXIS is used to model the deep excavation and to compute displacements of the wall. The model creation started by defining project properties as illustrated in Figure 4-8. The procedure summarized in Chapter 3.2.1 was followed in order to model the deep excavation.

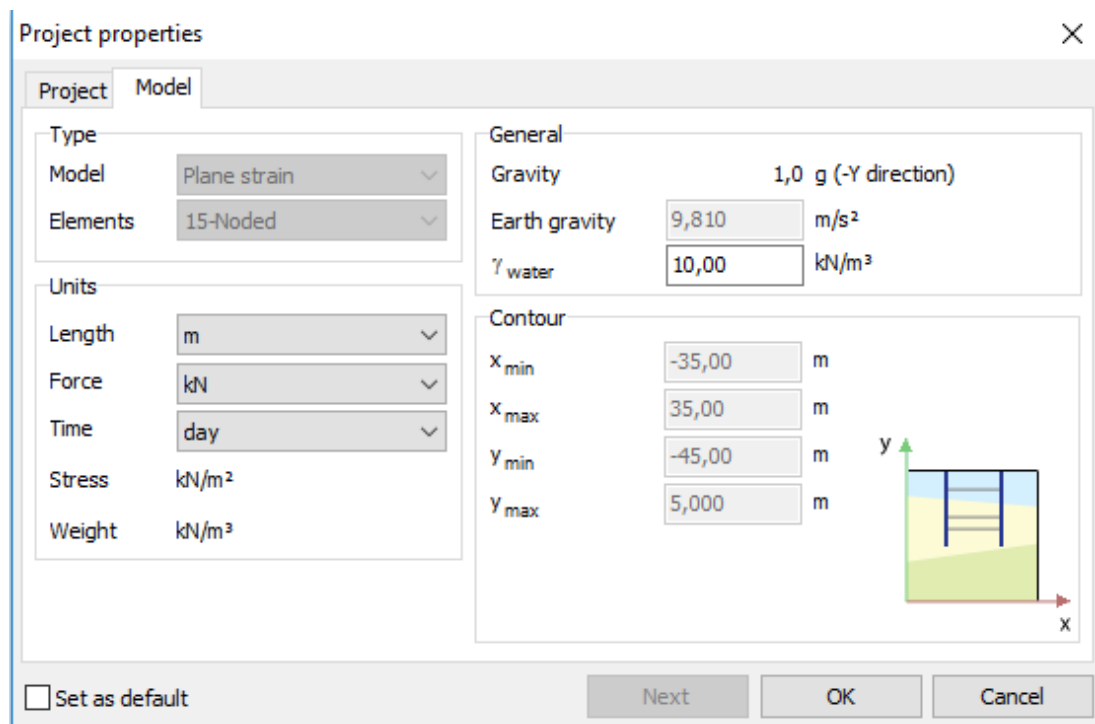


Figure 4.8. Numerical Model Properties

Constitutive parameters of soil layers are identified using Hardening-Soil model in this thesis. In Hardening soil model, the following material parameters must be defined for each soil layer:  $\gamma$ ,  $c$ ,  $\phi$ ,  $E_{50}^{ref}$ ,  $E_{oed}^{ref}$ ,  $E_{ur}^{ref}$ ,  $R_{inter}$ ,  $m$ . Three parameters ( $c$ ,  $\phi$ ,  $E_{50}^{ref}$ ) which are having a weighty effect on a horizontal deflection for two clay layers are calibrated during an optimization process. Table 4-3 shows the search range of parameters that are calibrated by the optimization algorithm. The rest of the

parameters were directly taken from the geotechnical investigations. Unit weight of top alluvial deposit clay layer and hard clay layer are taken as 19 kN/m<sup>3</sup> and 19.5 kN/m<sup>3</sup> respectively using laboratory test results retrieved from Toker Drilling and Construction Engineering Consultancy CO. Strength reduction factor interface ( $R_{inter}$ ) value is taken as 0.7 for both soil layer. “m” values are taken as 1 since both layers are clay layer (Tjie-Liong, 2014). Since  $E_{oed}^{ref}$  parameter is internally adjusted in PLAXIS, it cannot be optimized by back analysis (Calvello and Finno, 2004). The value of  $E_{oed}^{ref}$  is taken as the value of  $E_{50}^{ref}$ . Also, the value of  $E_{ur}^{ref}$  is taken as 3 times of  $E_{50}^{ref}$  value (Tjie-Liong, 2014). The finite element mesh is shown in Figure 4-9.

Table 4.3. Search Range of Optimized Parameters

	$E_{50}^{ref}$ (MPa)	$\varphi'$ (degree)	$c'_{ref}$ (kPa)
Alluvial Deposit Clay Layer	40 – 7.5	29 - 24	10 - 3
Hard Clay Layer	100 - 30	30 - 24	25 - 10

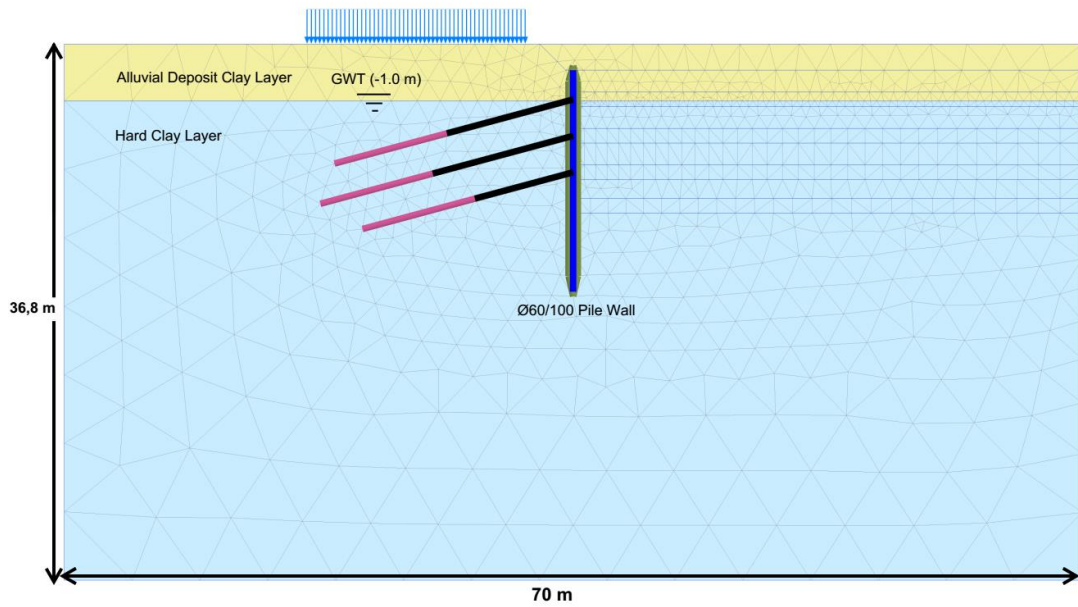


Figure 4.9. Finite Element Mesh

Wall structures are defined by plate elements in PLAXIS 2D. C25/30 type of concrete is used in the construction of piles which has the modulus of elasticity of 30.000 MPa.

$$A = \pi r^2; \quad (4-4)$$

$$I = \pi r^4 / 4 \quad (4-5)$$

for Ø60/100 piles

$$r = 0.3 \text{ m and } s = 1 \text{ m}$$

$$EA / s = 8.48 \times 10^6 \text{ kN/m; and}$$

$$EI / s = 1.91 \times 10^5 \text{ kN/m}^2/\text{m}$$

Prestressed anchors are defined by anchor and embedded pile row elements in PLAXIS 2D. For the free length of anchors 3x0.6” type of anchor is used in the construction. The modulus of elasticity of steel is 210,000 MPa, and the nominal steel area of 7 wire strand 6” is 139 mm<sup>2</sup>. For the bond length of anchors, C16 type of concrete is used in grout construction which has the modulus elasticity of 27,000 MPa

and unit weight ( $\gamma$ ) of 24 kN/m<sup>3</sup>. The diameter of the grout hole is designed as 14 cm and the anchor spacing is 2 m.

$$A_{\text{free}} = 3 \times 139 = 417 \text{ mm}^2$$

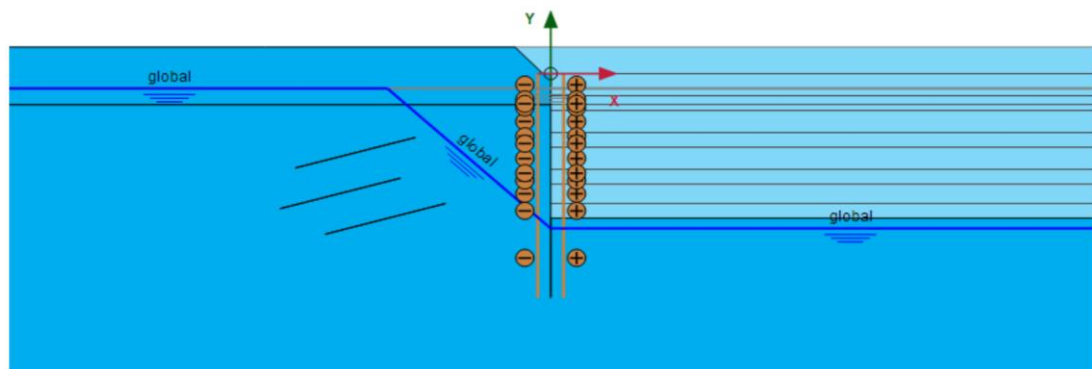
$$EA_{\text{free}} = 8.76 \times 10^4 \text{ kN}$$

for anchor capacity of 400 kN/m<sup>2</sup> and the bond length of 8 m, allowable skin resistance;

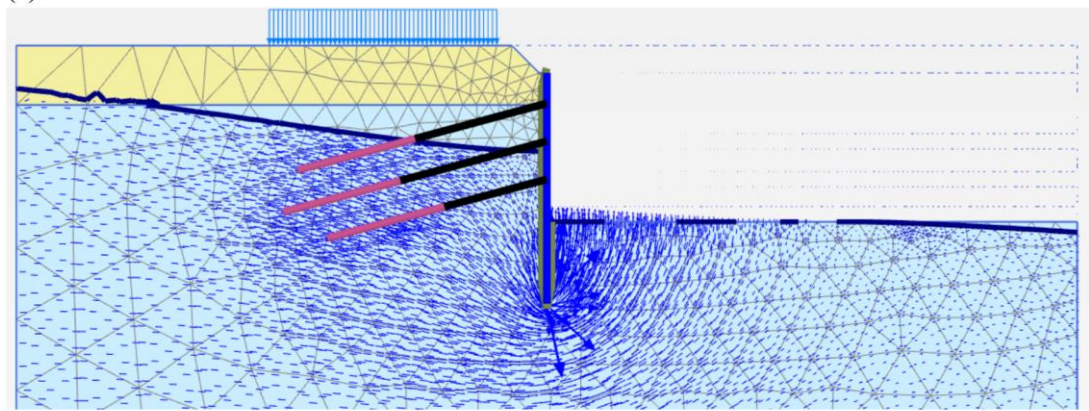
$$T_{\text{top, max}} = 50 \text{ kN/m}$$

Another important parameter in finite element modeling is to determine the level of ground water. Gouw (2012) states that improper modeling of ground water causes uncertainties in numerical analysis. According to soil investigation report, ground water was encountered in SK-14 borehole at depths between 2.5 m to 2.8 m below the existing ground level. However, it was stated that high potential of ground water was not observed in the site, and existing water groups can be drained by pumps during the excavation process. Therefore, drained conditions and long-term strength parameters ( $c'$ ,  $\phi'$ ,  $E'$ ) have been used in numerical analysis.

The structural element has been designed as an intermittent pile wall in this study. Permeable walls cause water drawdown on the unexcavated part. Especially for intermittent pile walls in clays and rocks, ground water is drained more in unexcavated part. Figure 4-10 shows the ground water level representation and ground water flow for the final calculation phase in the analysis.



(a)



(b)

Figure 4.10. (a) Groundwater Level Definition; (b) Groundwater Flow through the Pile

In the calculation step, the construction stages of excavation are defined in PLAXIS 2D. The finite element model consists of 12 calculation phases, which are shown in Figures 4.11 to 4.23.

- The initial phase shows the initial conditions of the field. Two different clay layers and the ground water table can be seen from the Figure 4.11.

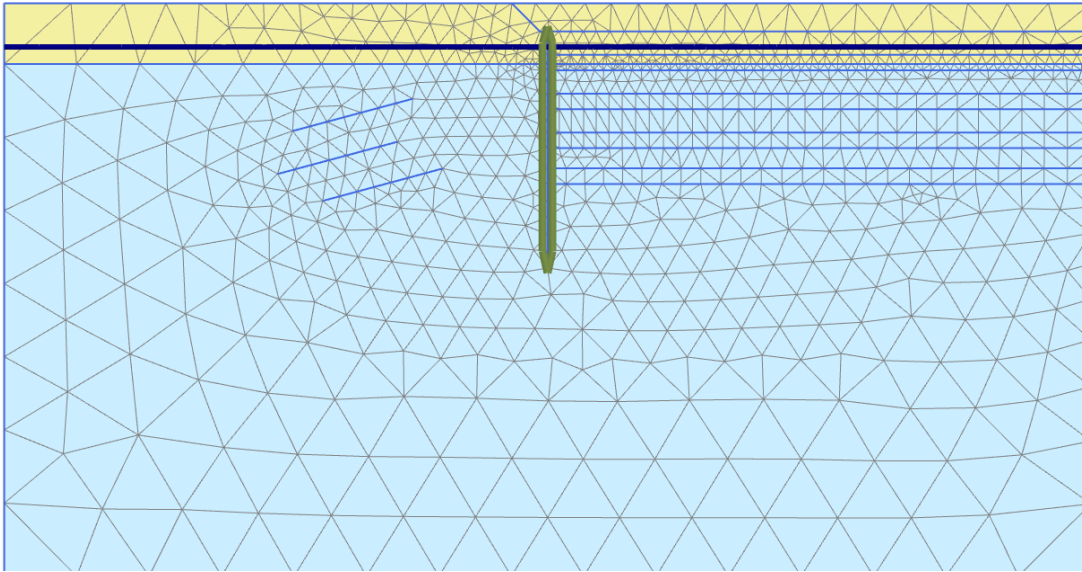


*Figure 4.11. Initial Phase*

- Phase 1: 1.8 m of slope (1:1) was excavated and 15.2 m length, Ø60/100 bored concrete pile was installed. 20 kPa surcharge load (construction vehicles and materials, and surrounding buildings) was activated.

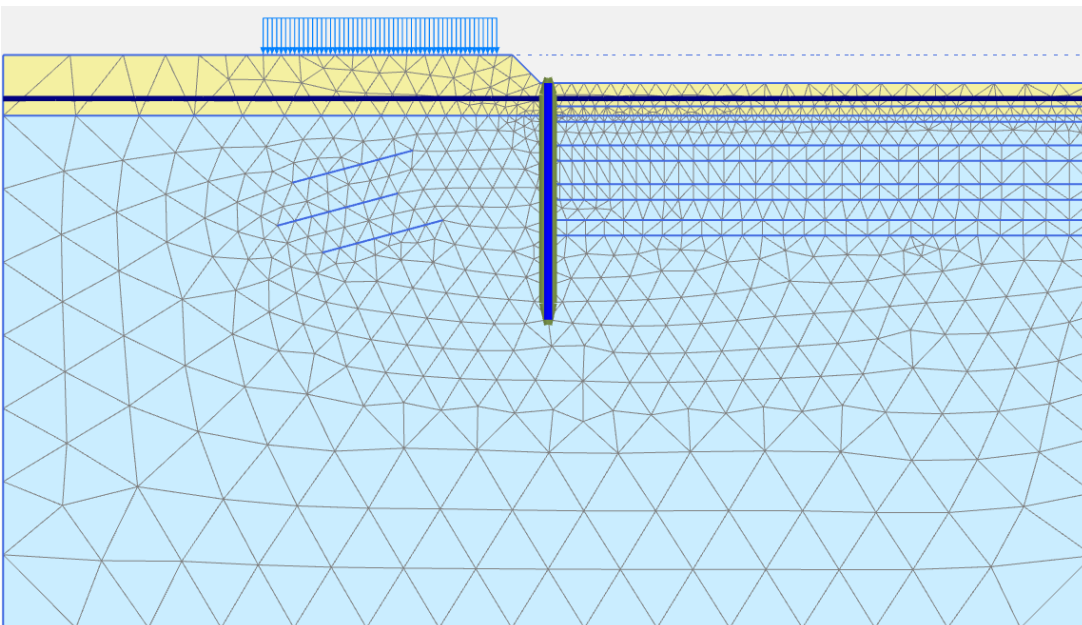


*Figure 4.12. Phase 1*

- Phase 2: 1<sup>st</sup> excavation to a depth of -1.50 m was activated.

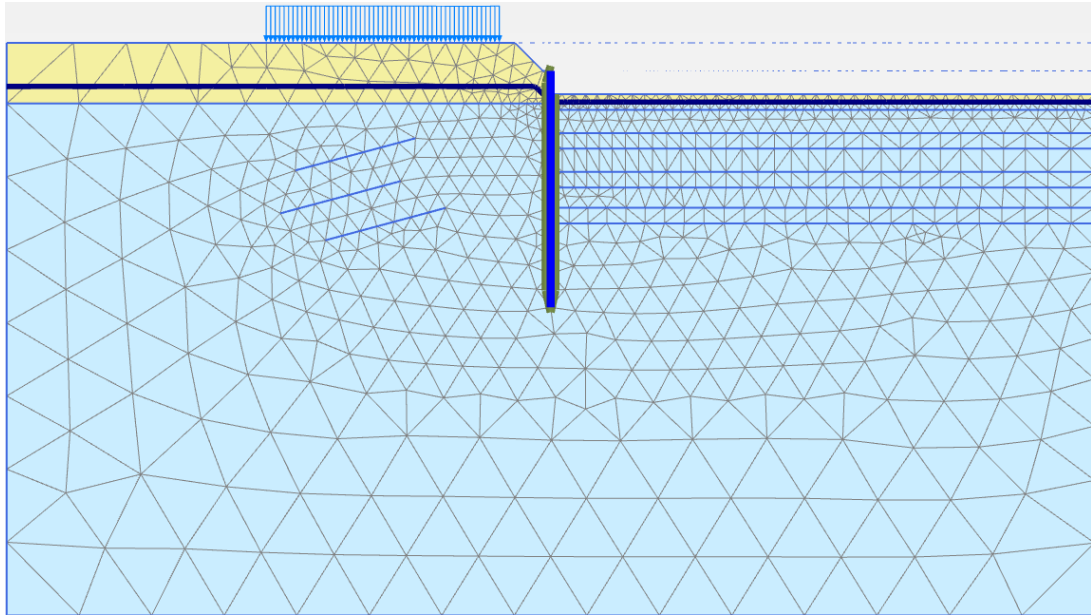


*Figure 4.13. Phase 2*

- Phase 3: 2<sup>nd</sup> excavation to a depth of -2.50 m was activated.

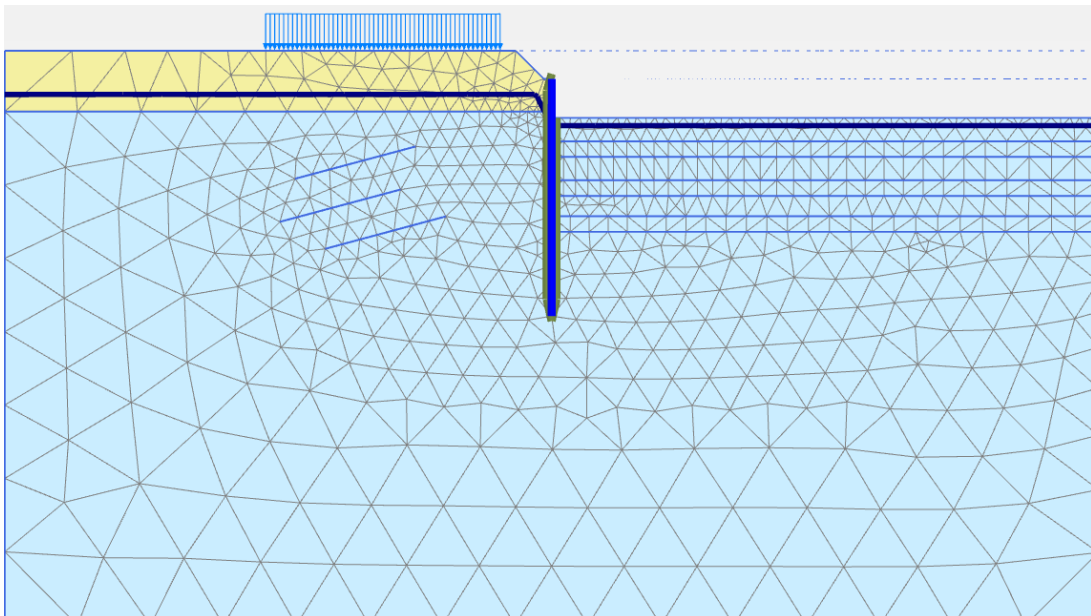


*Figure 4.14. Phase 3*

- Phase 4: 1<sup>st</sup> row prestressed anchorage was activated.

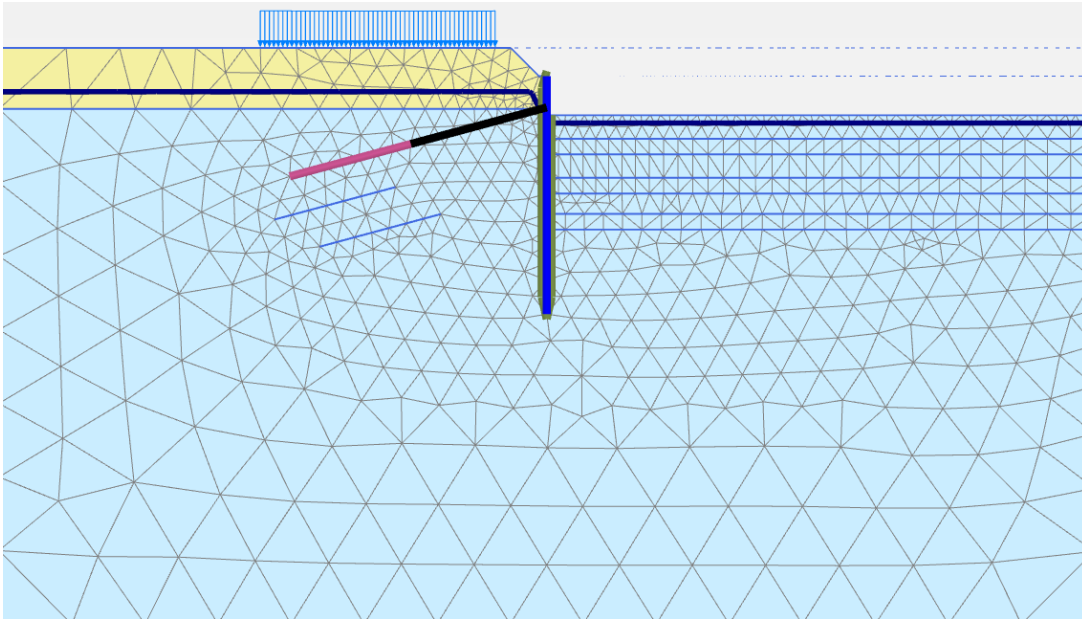


Figure 4.15. Phase 4

- Phase 5: 3<sup>rd</sup> excavation to a depth of -4.00 m was activated.

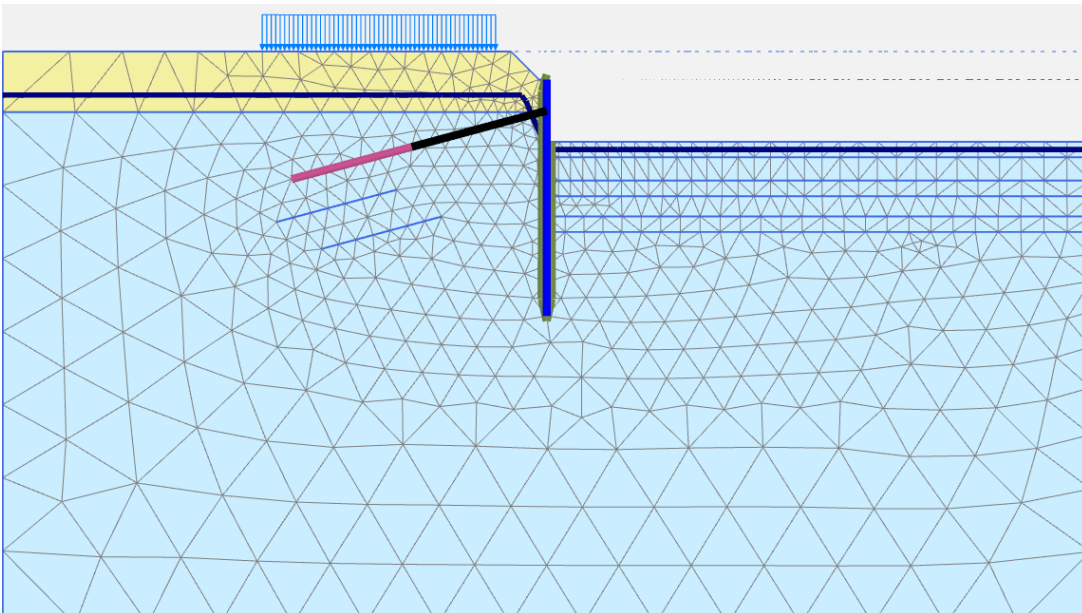


Figure 4.16. Phase 5

- Phase 6: 4<sup>th</sup> excavation to a depth of -5.00 m was activated.

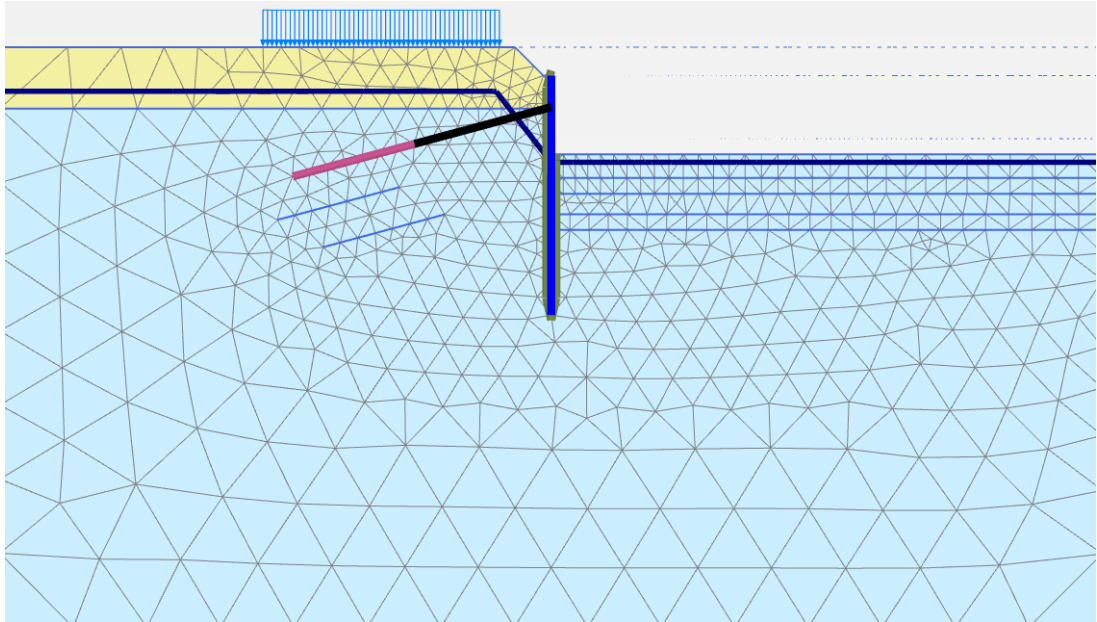


Figure 4.17. Phase 6

- Phase 7: 2<sup>nd</sup> row prestressed anchorage was activated.

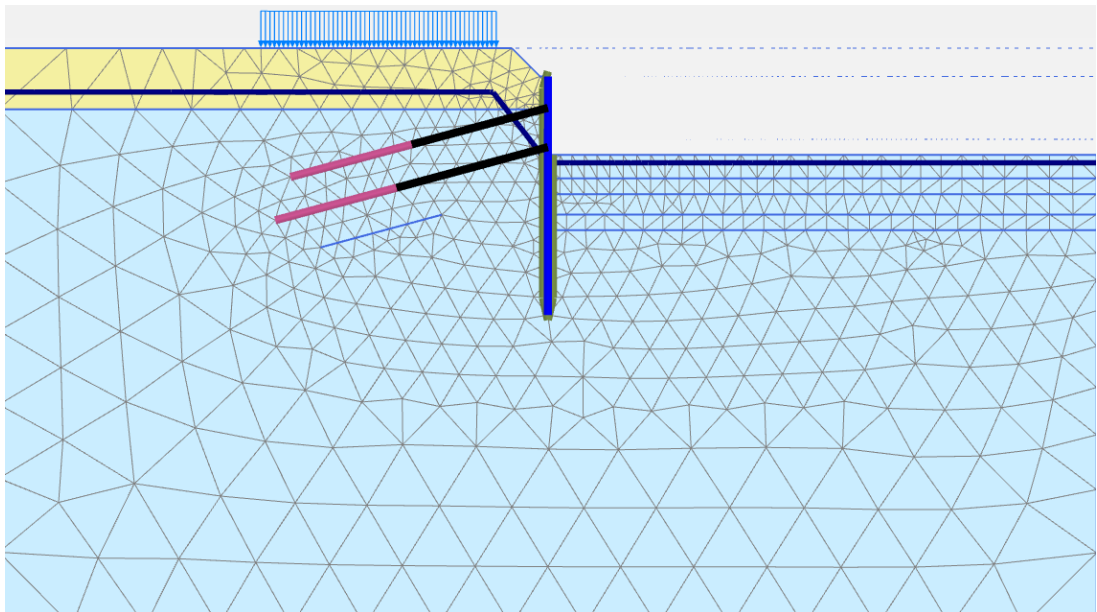


Figure 4.18. Phase 7

- Phase 8: 5<sup>th</sup> excavation to a depth of -6.50 m was activated.

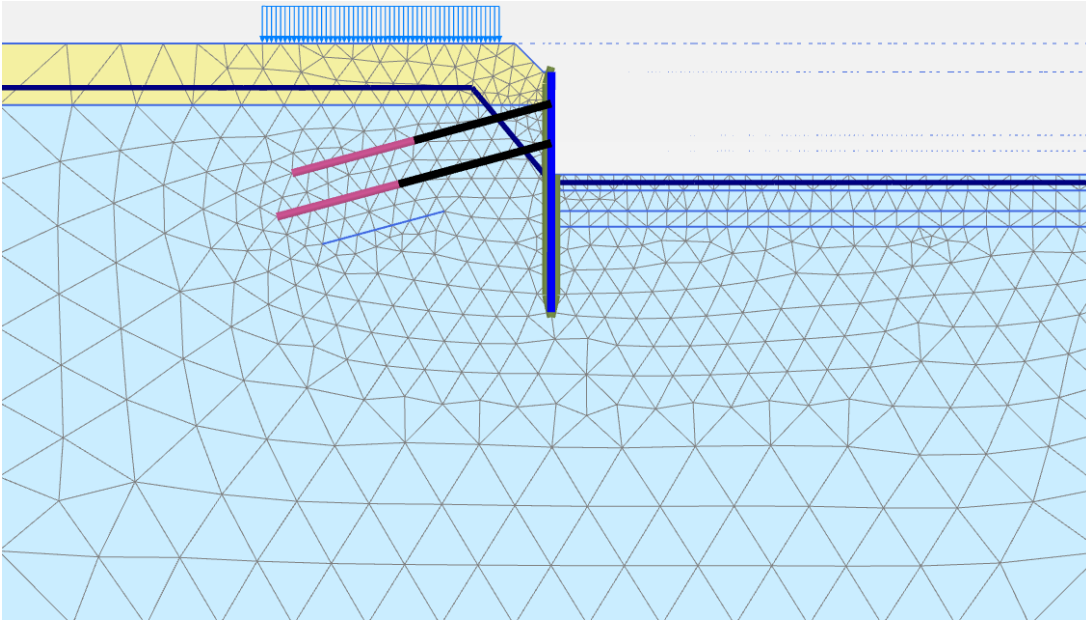


Figure 4.19. Phase 8

- Phase 9: 6<sup>th</sup> excavation to a depth of -8.00 m was activated.

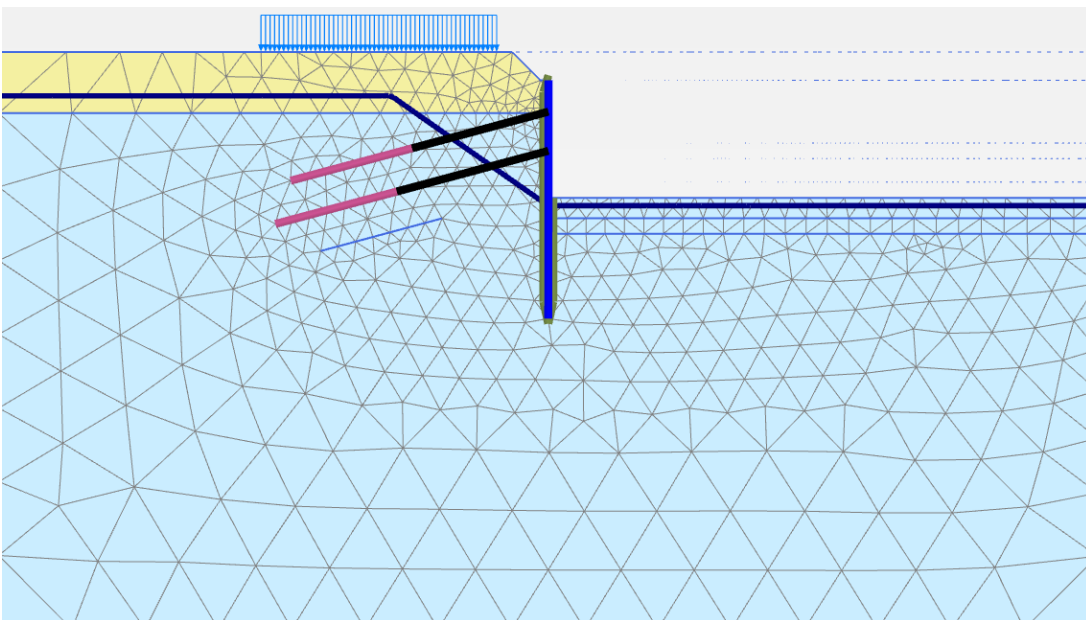


Figure 4.20. Phase 9

- Phase 10: 3<sup>rd</sup> row prestressed anchorage was activated.

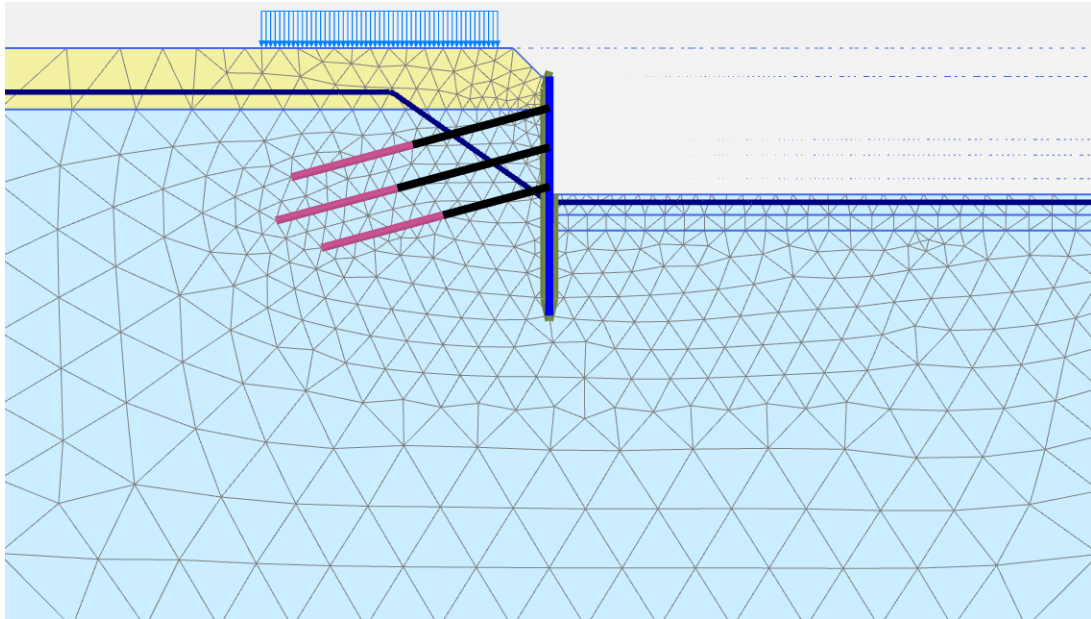


Figure 4.21. Phase 10

- Phase 11: 7<sup>th</sup> excavation to a depth of -9.00 m was activated.

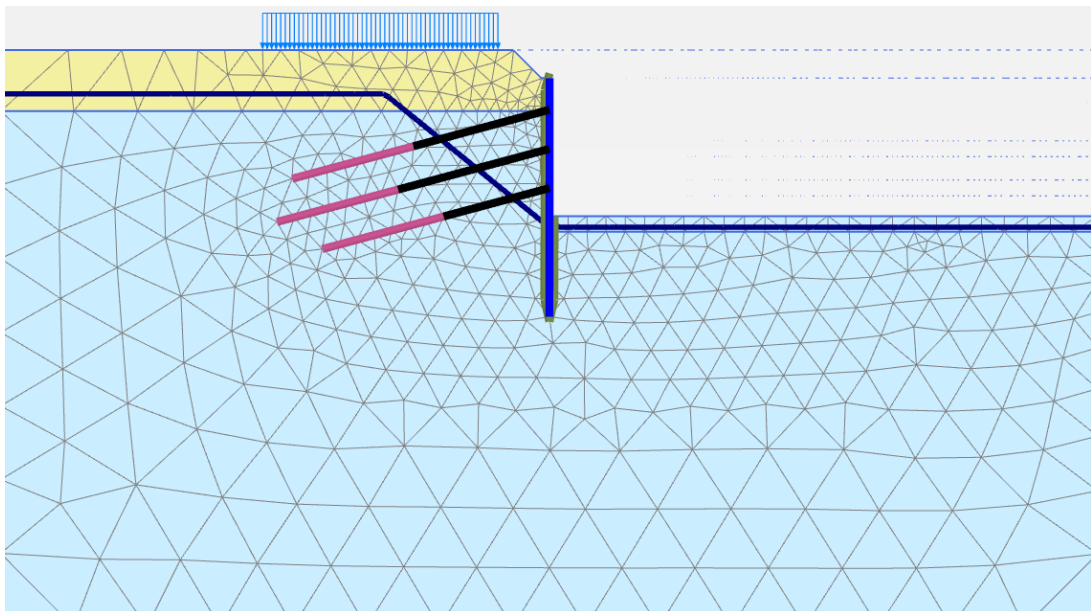


Figure 4.22. Phase 11



Table 4.4. Construction Stages and Calculation Phases in Numerical Model

Description	Calculation Phase	Construction Stage
At-rest (Before Construction)	0	Initial Conditions
Wall Installation	1	Slope excavation
		Construction of wall
Deep Excavation	2	Excavate until -1,50 m
	3	<b>Excavate [-2,50 m] (Stage 1)</b>
	4	First row anchorage prestressing
	5	Excavate [-4,00 m]
	6	<b>Excavate [-5,00 m] (Stage 2)</b>
	7	Second row anchorage prestressing
	8	Excavate [-6,50 m]
	9	<b>Excavate [-8.00m] (Stage 3)</b>
	10	Third row anchorage prestressing
	11	<b>Excavate [-9,00 m] (Stage 4)</b>
	12	<b>Excavate [-9,80 m] (Stage 5)</b>

#### 4.4. Application and the Performance of Particle Swarm Optimization

The purpose of this part is to calibrate 6 soil parameters ( $E_{50}^{ref}$ ,  $\phi'$  and  $c'_{ref}$ ) for two clay layers in the light of continuously entered field measurements assuming that the factual observed field measurements and well represented finite element model. With this intention, a well-known optimization algorithm Particle swarm optimization (PSO) was coded, which is used to fit the observed field measurements and FEM results. The procedure summarized in Chapter 3.2.2 was followed in order to apply PSO. 40 particles are used in the swarm and 20 maximum number of iterations are chosen during the analyses. Although 5-10 iterations are enough for PSO method to work well (Gedik, 2018), the maximum iteration number is set to 20 in order to see the performance of the algorithm. Inertia weight  $w$  is selected as 0.99 and as Knabe (2013) suggests, velocity constants  $c_1$  and  $c_2$  are selected as 2. The algorithm initializes the swarm of particles with random positions and velocities. PLAXIS calculates the lateral deformations at ten predetermined points for each 40 particles. Fitness values are calculated for each particle using Equation 3-1. The lowest fitness value becomes  $gBest$  for that iteration. After updating velocities and positions of the particles using Equations 3-12 and 3-13, new parameter sets are generated for the next

iteration. The same procedure is repeated for 20 iterations starting from the calculation of deformations at ten predetermined points for 40 new particles. Parameters with the best fitness value, which gives the minimum difference between inclinometer readings, and results estimated using PLAXIS are the optimized parameters.

The developed back-analysis platform is run for each stage, and parameters which give the lowest fitness value are found using the inclinometer results of the corresponding stage. Then, forward calculations with obtained parameters are performed to predict the upcoming stages' lateral deformations in order to see the performance of the back-analysis platform. With this, 6 soil material parameters are obtained in the light of inclinometer readings at each back-analysis run.

Reaching the maximum number of iterations is the stopping criteria for the optimization algorithm. Besides, there must be an acceptance criterion for the algorithm. It is considered that there may be measuring errors while taking inclinometer readings. The tolerance for the difference between inclinometer readings and results estimated using PLAXIS at 10 points is selected as 1.5 mm to overcome potential measurement errors. The corresponding maximum fitness value is calculated as 0.0019 m. Fitness value lower than 0.0019 is accepted as a feasible solution for this specific problem. Fitness values calculated by using initial design parameters are 0.0027; 0.0029; 0.0021; 0.0027 and 0.0096 for stages 1, 2, 3, 4 and 5 respectively. Results prior to any optimization and the results after each optimization process are presented in the following parts. Forward calculations and conformity with inclinometer measurements are also shown at the end of each run.

#### **4.4.1. Initial Design Performance**

Visual examination is the simplest way to demonstrate the difference between the computed and the measured results. Figure 4-24 illustrates the visual conformity between the inclinometer readings and FEM computed lateral deflections by initial design parameters for the selected five construction stages. The figures show that the computed deflections are lower than the inclinometer readings especially in the upper

clay layer for the first three stages. On the other hand, the initial design parameters are underestimated so that the computed deflections are considerably larger than the actual deflections which cause delusive deflection profiles in the final stage. This result shows that the site investigations and laboratory tests did not reflect the field conditions properly in this specific problem assuming that the factual observed field measurements and well represented finite element model.

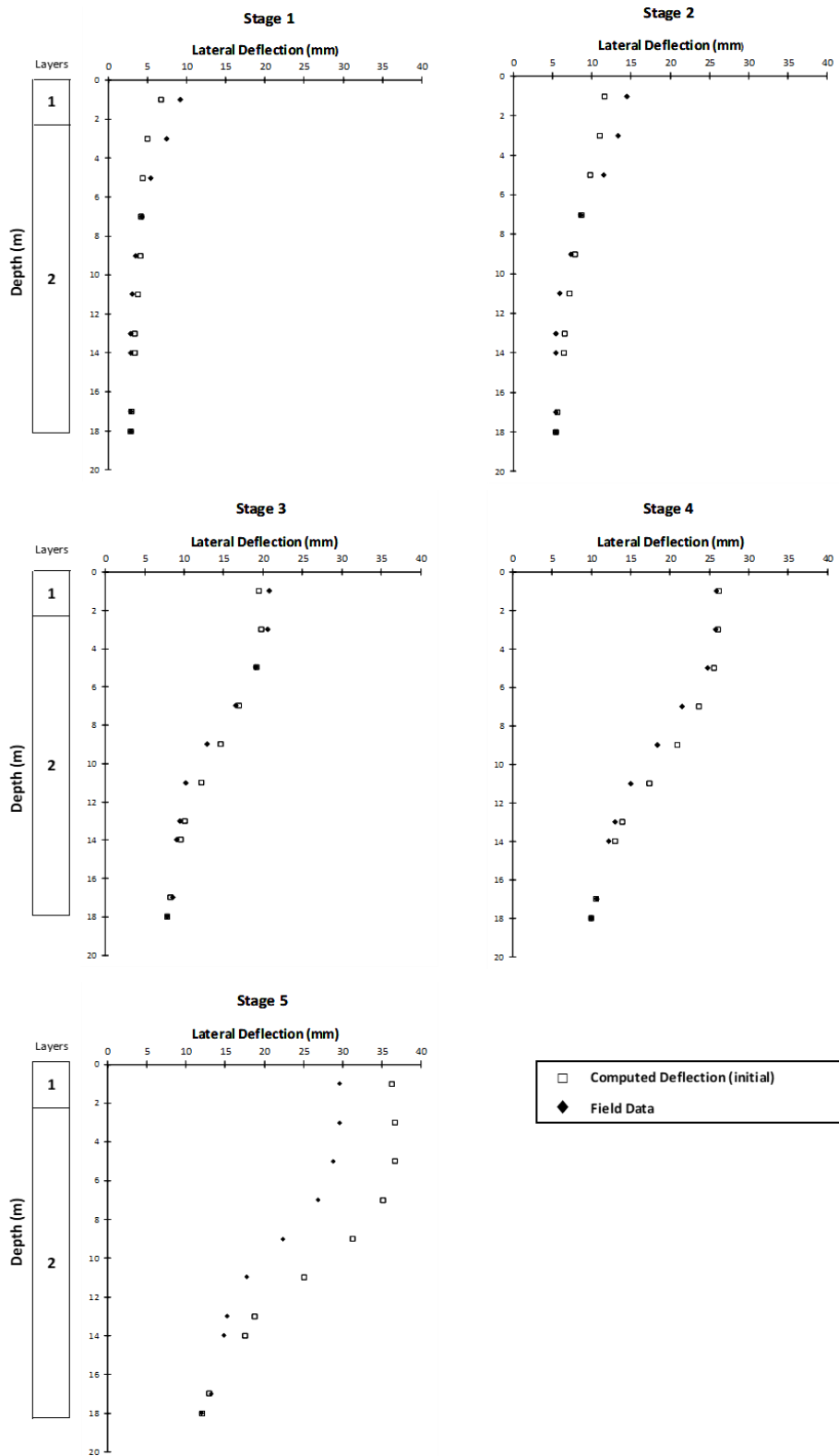


Figure 4.24. Measured versus Computed Deflections: Initial Design Parameters

#### 4.4.2. Optimization based on Stage 1 Observations

It took approximately 8 hours and 30 minutes to complete the optimization for Stage 1. Figure 4-25 illustrates the evolution of the particle's best position (pBest) for different iterations of the optimization process. Figure 4-25(a-d) show the best positions of particles at 1<sup>st</sup>, 10<sup>th</sup>, 15<sup>th</sup> and 20<sup>th</sup> iterations. These graphs illustrate the convergence of the particles towards the optimum solution. As can be seen from the graphs, the convergence is dramatic between the 1<sup>st</sup> and the 10<sup>th</sup> iterations. There is a no significant difference between 15<sup>th</sup> and 20<sup>th</sup> iterations. The optimum solution is found in the early iterations. Furthermore, gBest values of the best particle in the swarm in 20 iterations is shown in Figure 4-26. As it is seen in this Figure, gBest values decrease progressively towards the solution. The fitness value is 0.00104 at the end of the optimization process, which is considered a feasible solution.

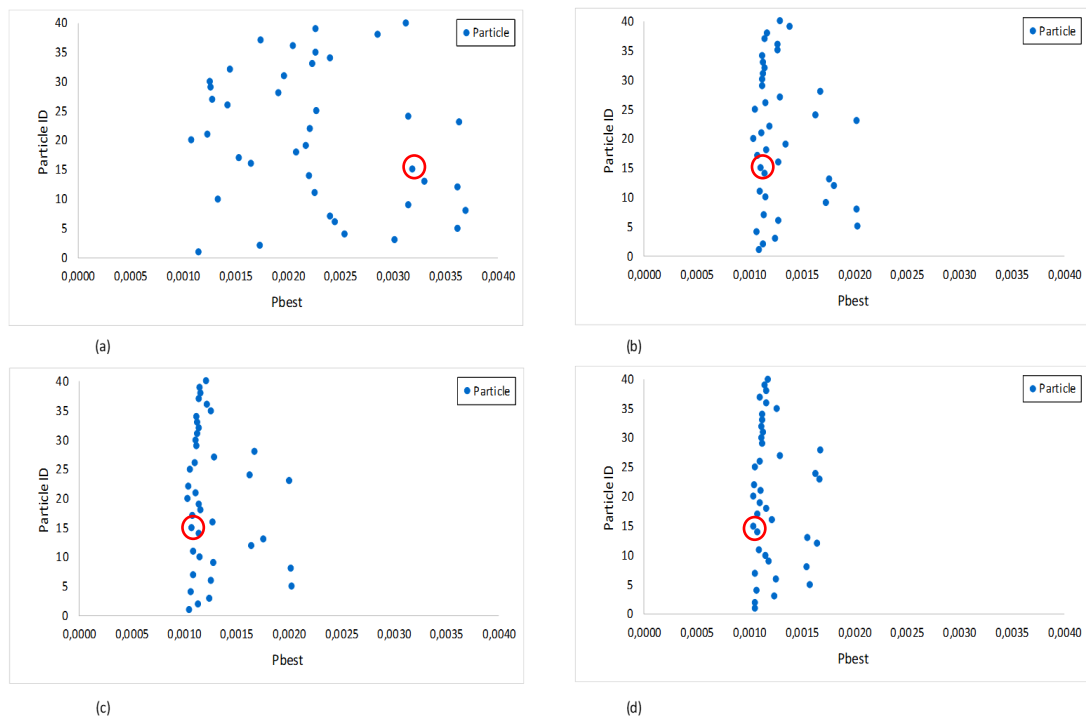


Figure 4.25. Evolution of Particle's Best Positions pBest in Different Iterations for Stage 1: (a) 1<sup>st</sup> iteration; (b) 10<sup>th</sup> iteration; (c) 15<sup>th</sup> iteration;(d) 20<sup>th</sup> iteration

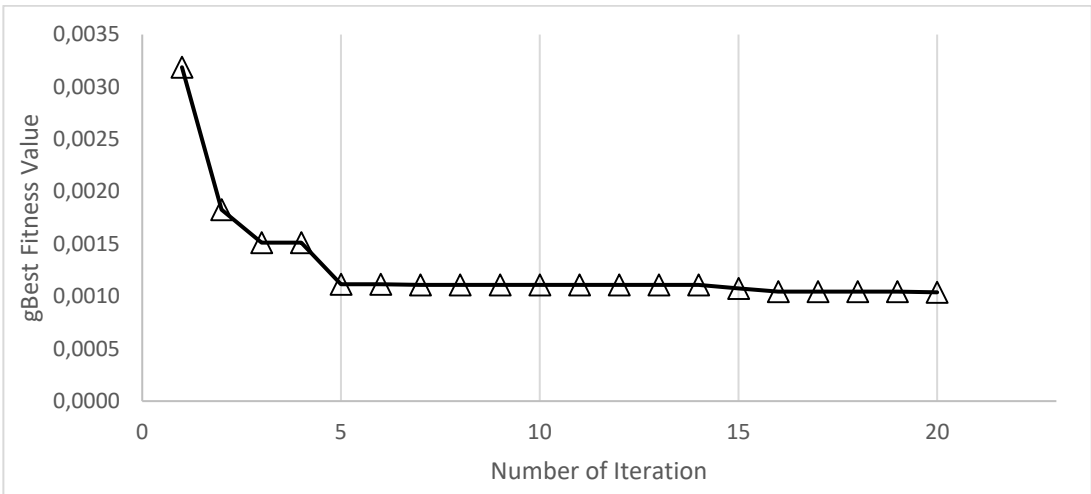


Figure 4.26. gBest Fitness Values of Best Parameter in 20 Iterations for Stage 1

Figure 4-27 illustrates the visual conformity between the inclinometer readings and FEM computed lateral deflections by optimized parameters based on Stage 1 observations. Optimization produced a good fit between the measured and computed deflections. The back calculated parameters by PSO are given in Table 4-5.

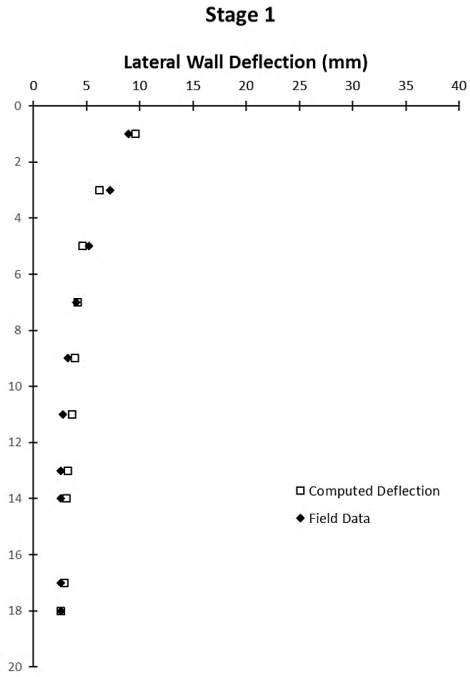


Figure 4.27. Measured versus Computed Deflections: Parameters Optimized based on Stage 1 Observations

Table 4.5. Optimized Parameters after Stage 1

	$E_{50}^{ref}$ (MPa)	$\phi'$ (degree)	$c'_{ref}$ (kPa)
Alluvial Deposit Clay Layer	22.9	26.8	6.2
Hard Clay Layer	61.2	25.2	10

#### 4.4.3. Optimization based on Stage 2 Observations

Optimization of Stage 2 took approximately 12 hours. Figure 4-28(a-d) show the best positions of particles at 1<sup>st</sup>, 10<sup>th</sup>, 15<sup>th</sup> and 20<sup>th</sup> iterations. The decrease of gBest values for 20 iterations is shown in Figure 4-29. The fitness value is 0.00135 at the end of the optimization process which is considered as feasible solution.

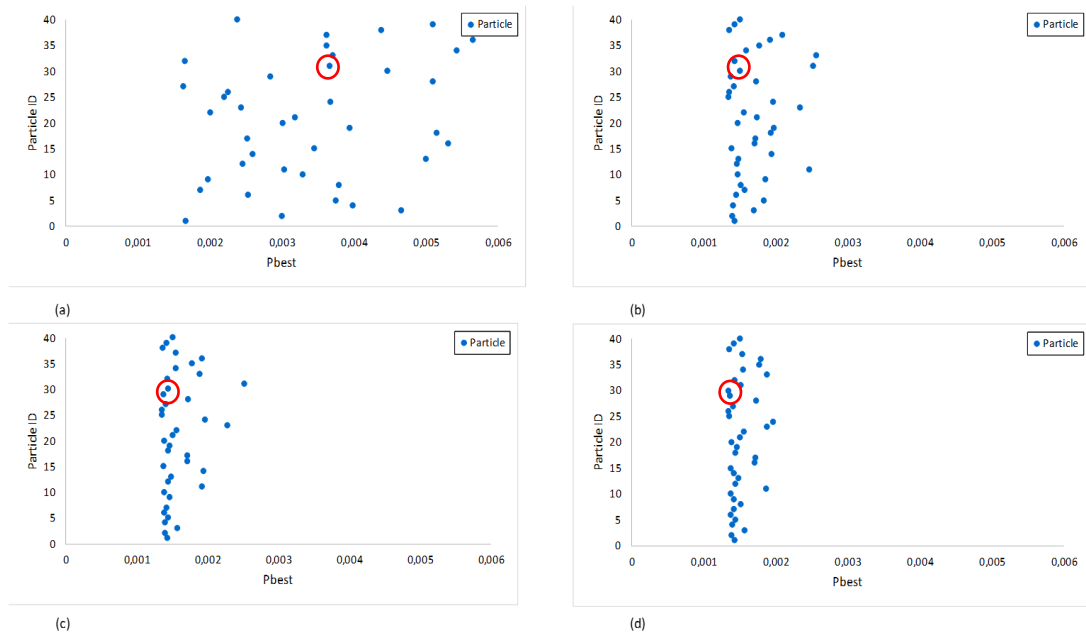


Figure 4.28. Evolution of Particle's Best Positions pBest in Different Iterations for Stage 2: (a) 1st iteration; (b) 10<sup>th</sup> iteration; (c) 15<sup>th</sup> iteration;(d) 20<sup>th</sup> iteration

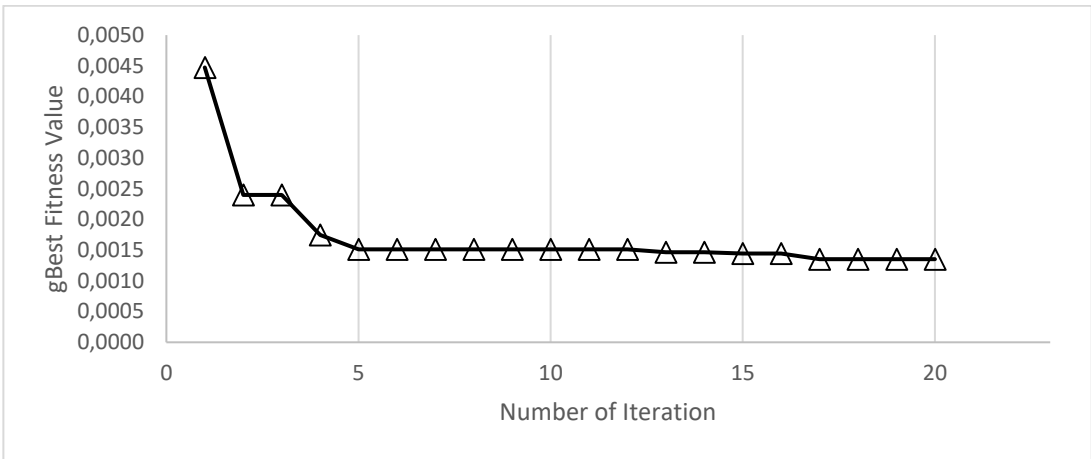


Figure 4.29. gBest Fitness Values of Best Parameter in 20 Iterations for Stage 2

Figure 4-30 illustrates the visual conformity between the inclinometer readings and FEM computed lateral deflections by optimized parameters based on Stage 2 observations. Optimization produced a good fit between the measured and computed deflections. The back calculated parameters by PSO are given in Table 4-6.

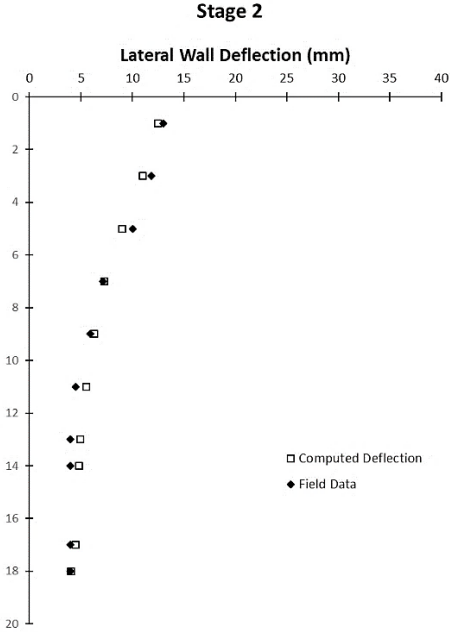


Figure 4.30. Measured versus Computed Deflections: Parameters Optimized based on Stage 2 Observations

Table 4.6. Optimized Parameters after Stage 2

	$E_{50}^{ref}$ (MPa)	$\phi'$ (degree)	$c'_{ref}$ (kPa)
Alluvial Deposit Clay Layer	22.5	26.0	6.1
Hard Clay Layer	74.2	27.9	10.7

#### 4.4.4. Optimization based on Stage 3 Observations

It took approximately 15 hours and 30 minutes to complete the optimization for Stage 3. Figure 4-31(a-d) show the best positions of particles at 1<sup>st</sup>, 10<sup>th</sup>, 15<sup>th</sup> and 20<sup>th</sup> iterations. The decrease of gBest values for twenty iterations is shown in Figure 4-32. The fitness value is 0.00128 at the end of the optimization process which is considered as feasible solution.

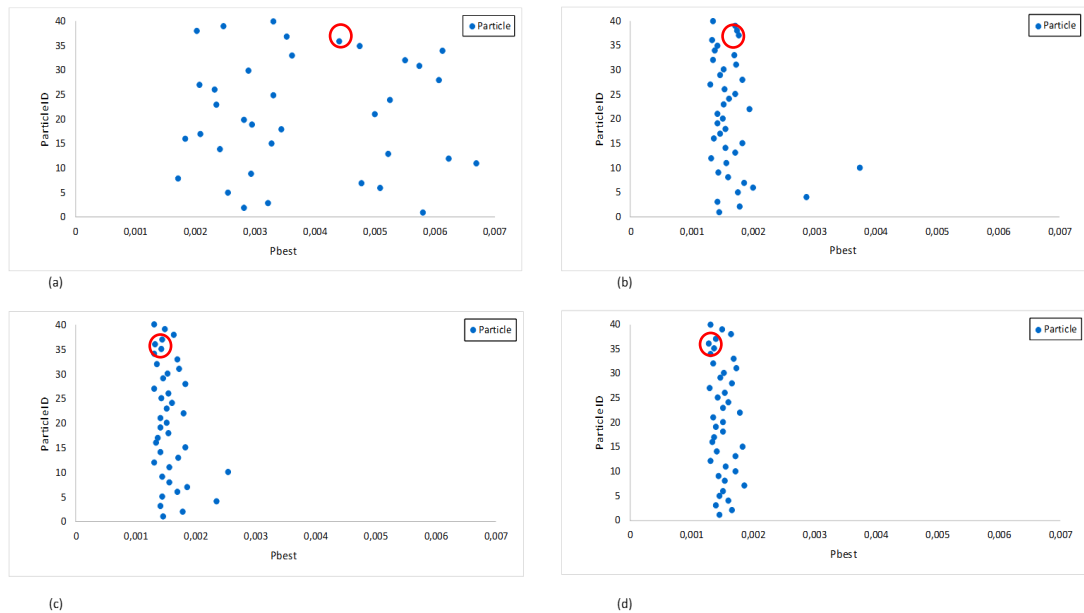


Figure 4.31. : Evolution of Particle's Best Positions pBest in Different Iterations for Stage 3: (a) 1st iteration; (b) 10th iteration; (c) 15th iteration;(d) 20th iteration

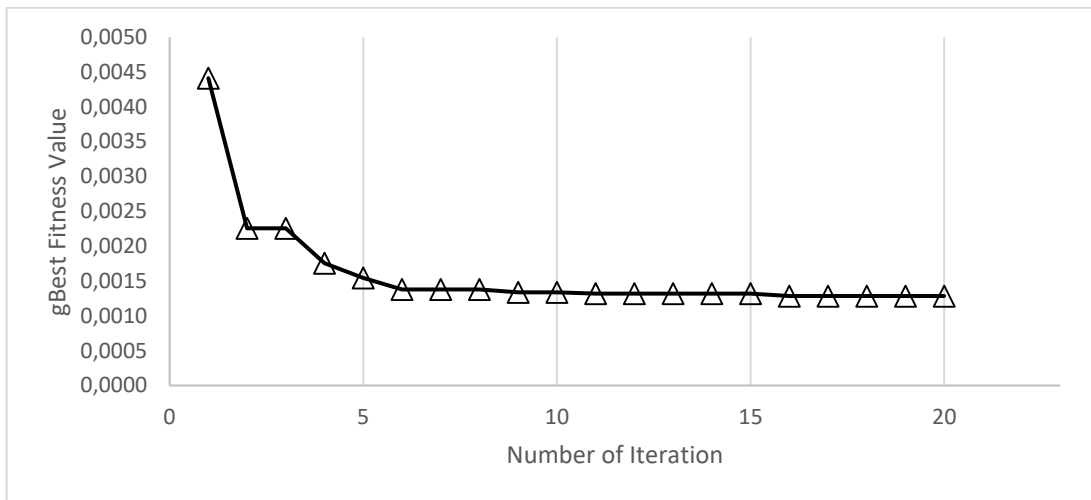


Figure 4.32. gBest Fitness Values of Best Parameter in 20 Iterations for Stage 3

Figure 4-33 illustrates the visual conformity between the inclinometer readings and FEM computed lateral deflections by optimized parameters based on Stage 3 observations. Optimization produced a good fit between the measured and computed deflections. The back calculated parameters by PSO are given in Table 4-7.

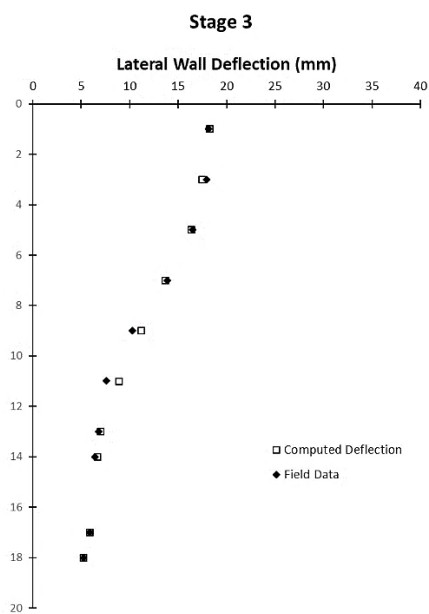


Figure 4.33. Measured versus Computed Deflections: Parameters Optimized based on Stage 3 Observations

Table 4.7. Optimized Parameters after Stage 3

	$E_{50}^{ref}$ (MPa)	$\phi'$ (degree)	$c'_{ref}$ (kPa)
Alluvial Deposit Clay Layer	11.3	26.6	3.8
Hard Clay Layer	82.4	28.0	11.2

#### 4.4.5. Optimization based on Stage 4 Observations

It took approximately 18 hours and 30 minutes to complete the optimization for Stage 4. Figure 4-34(a-d) show the best positions of particles at 1<sup>st</sup>, 10<sup>th</sup>, 15<sup>th</sup> and 20<sup>th</sup> iterations. The decrease of gBest values for twenty iterations is shown in Figure 4-35. The fitness value is 0.00130 at the end of the optimization process which is considered as feasible solution.

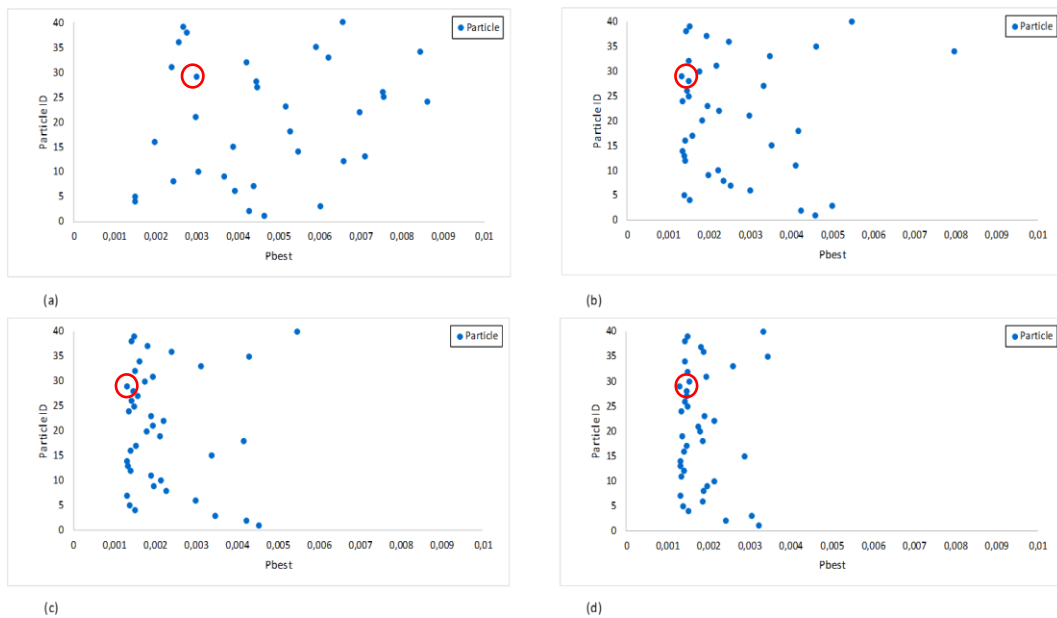


Figure 4.34. Evolution of Particle's Best Positions pBest in Different Iterations for Stage 4: (a) 1<sup>st</sup> iteration; (b) 10<sup>th</sup> iteration; (c) 15<sup>th</sup> iteration;(d) 20<sup>th</sup> iteration

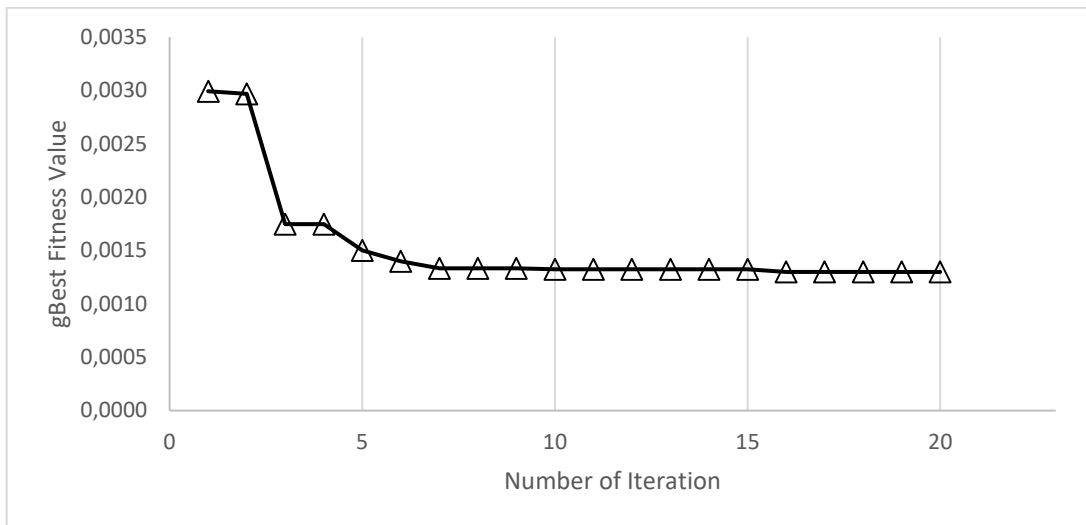


Figure 4.35. gBest Fitness Values of Best Parameter in 20 Iterations for Stage 4

Figure 4-36 illustrates the visual conformity between the inclinometer readings and FEM computed lateral deflections by optimized parameters based on Stage 4 observations. Optimization produced a good fit between the measured and computed deflections. The back calculated parameters by PSO are given in Table 4-8.

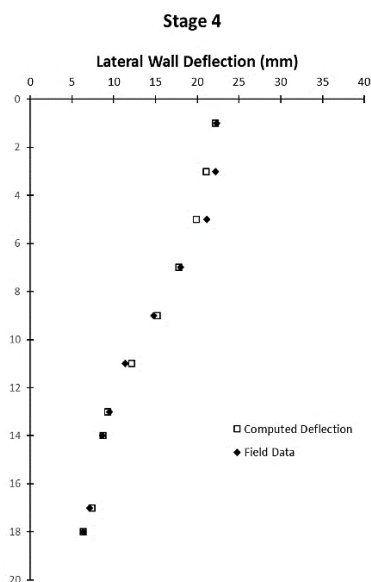


Figure 4.36. Measured versus Computed Deflections: Parameters Optimized based on Stage 4 Observations

Table 4.8. Optimized Parameters after Stage 4

	$E_{50}^{ref}$ (MPa)	$\phi'$ (degree)	$c'_{ref}$ (kPa)
Alluvial Deposit Clay Layer	8.4	25.9	6.9
Hard Clay Layer	85.1	28.8	11.5

#### 4.4.6. Optimization based on Stage 5 Observations

It took approximately 20 hours to complete the optimization for Stage 5. Figure 4-37(a-d) show the best positions of particles at 1<sup>st</sup>, 10<sup>th</sup>, 15<sup>th</sup> and 20<sup>th</sup> iterations. The decrease of gBest values for twenty iterations is shown in Figure 4-38. The fitness value is 0.00183 at the end of the optimization process which is considered as feasible solution.

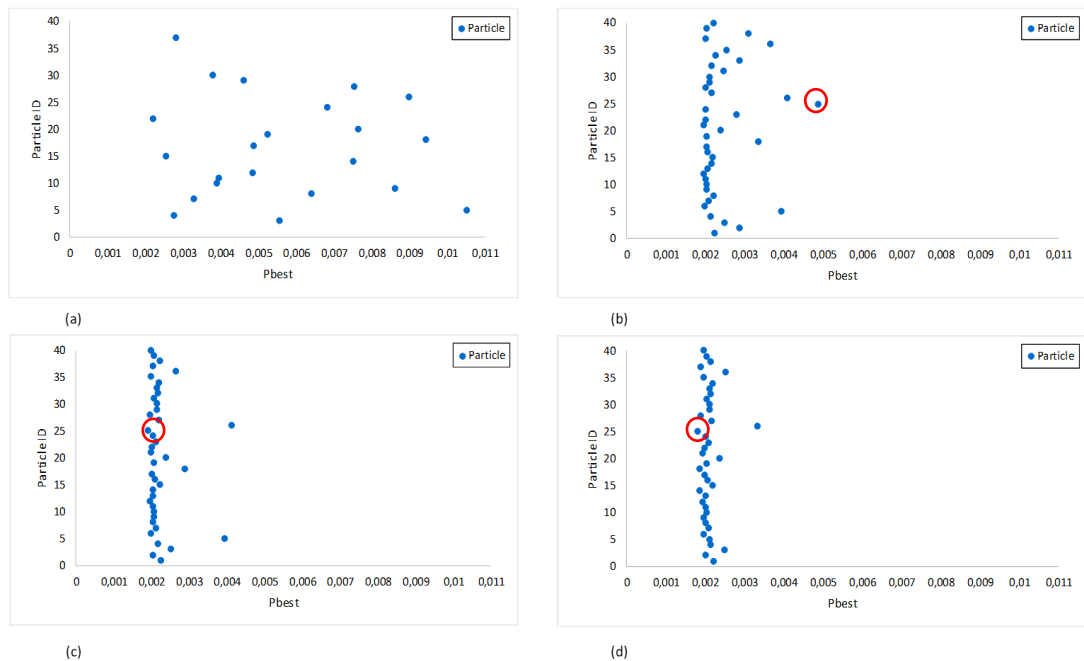


Figure 4.37. Evolution of Particle's Best Positions pBest in Different Iterations for Stage 5: (a) 1<sup>st</sup> iteration; (b) 10<sup>th</sup> iteration; (c) 15<sup>th</sup> iteration; (d) 20<sup>th</sup> iteration

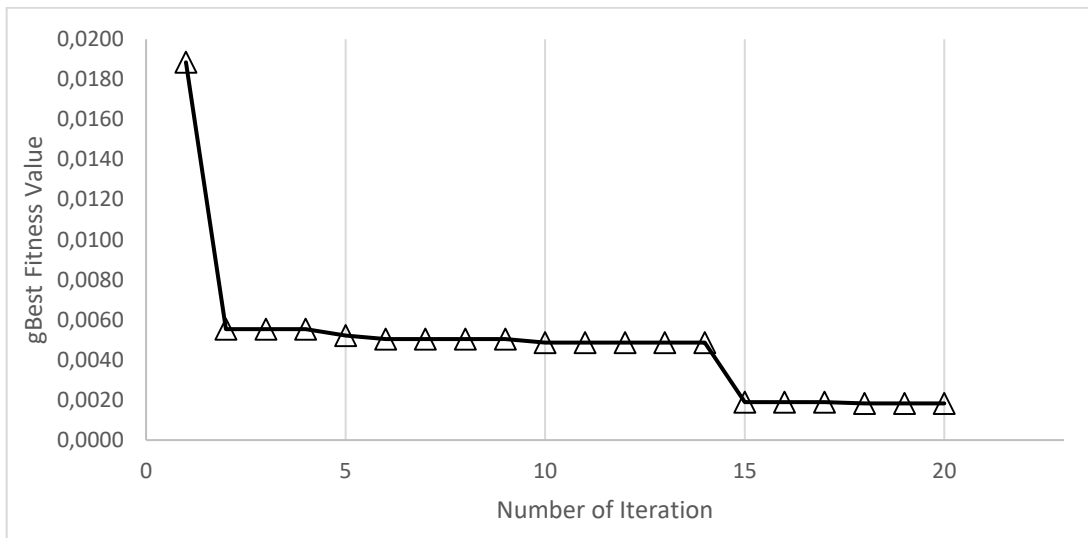


Figure 4.38. gBest Fitness Values of Best Parameter in 20 Iterations for Stage 5

Figure 4-39 illustrates the visual conformity between the inclinometer readings and FEM computed lateral deflections by optimized parameters based on Stage 5 observations. Optimization produced a good fit between the measured and computed deflections. The back calculated parameters by PSO are given in Table 4-9.

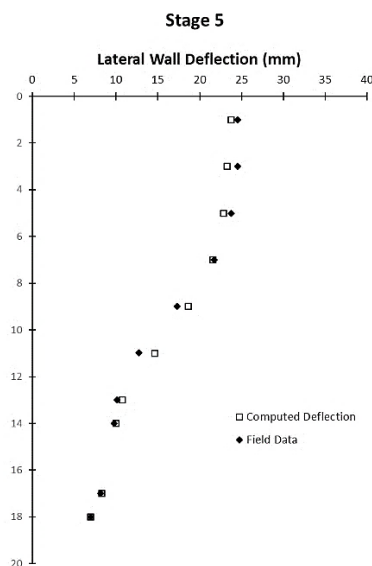


Figure 4.39. Measured versus Computed Deflections: Parameters Optimized based on Stage 5 Observations

Table 4.9. *Optimized Parameters after Stage 5*

	$E_{50}^{ref}$ (MPa)	$\phi'$ (degree)	$c'_{ref}$ (kPa)
Alluvial Deposit Clay Layer	9.0	26.2	5.3
Hard Clay Layer	91.9	28.8	15.8

#### **4.5. Forward Predictions with Optimized Parameters**

In this part of the thesis, the prediction performance of optimized parameters is examined by applying a forward calculation process for each stage. For this purpose, back calculated parameters are fed to the PLAXIS as inputs to obtain the next stage's lateral deformations at ten predetermined points. The comparison of measured inclinometer readings and the predicted horizontal deflections for each stage are presented.

##### **4.5.1. Horizontal Displacement Prediction of Stage 2**

Back calculated parameters obtained from Stage 1 is used to predict the horizontal deflection behavior of Stage 2. The comparison of measured inclinometer readings and the predicted horizontal deflections is illustrated in Figure 4-40. The fitness value is calculated as 0.0021 by optimized parameters which was calculated as 0.0029 by initial design parameters.

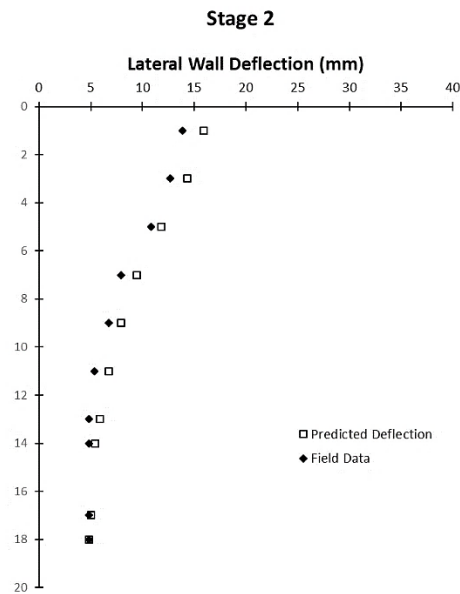


Figure 4.40. Measured versus Predicted Deflections of Stage 2: Parameters Optimized based on Stage 1 Observations

#### 4.5.2. Horizontal Displacement Prediction of Stage 3

Back calculated parameters obtained from Stage 2 is used to predict the horizontal deflection behavior of Stage 3. The comparison of measured inclinometer readings and the predicted horizontal deflections is illustrated in Figure 4-41. The fitness value is calculated as 0.0014 by optimized parameters which was calculated as 0.0021 by initial design parameters.

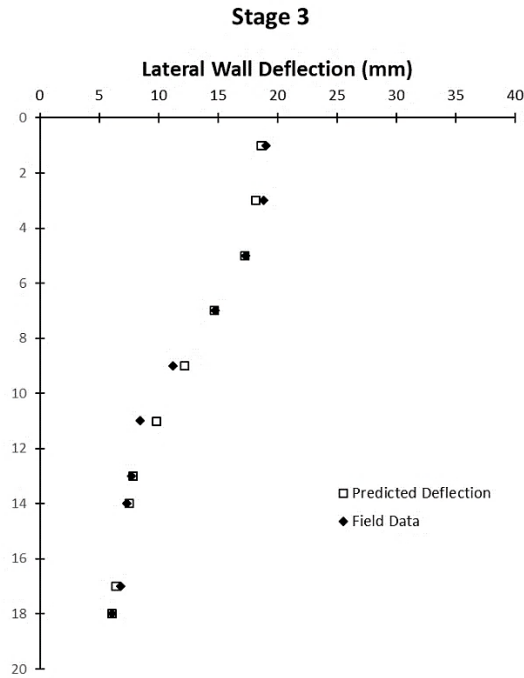


Figure 4.41. Measured versus Predicted Deflections of Stage 3: Parameters Optimized based on Stage 2 Observations

#### 4.5.3. Horizontal Displacement Prediction of Stage 4

Back calculated parameters obtained from Stage 3 is used to predict the horizontal deflection behavior of Stage 4. The comparison of measured inclinometer readings and the predicted horizontal deflections is illustrated in Figure 4-42. The fitness value is calculated as 0.0011 by optimized parameters which was calculated as 0.0027 by initial design parameters.

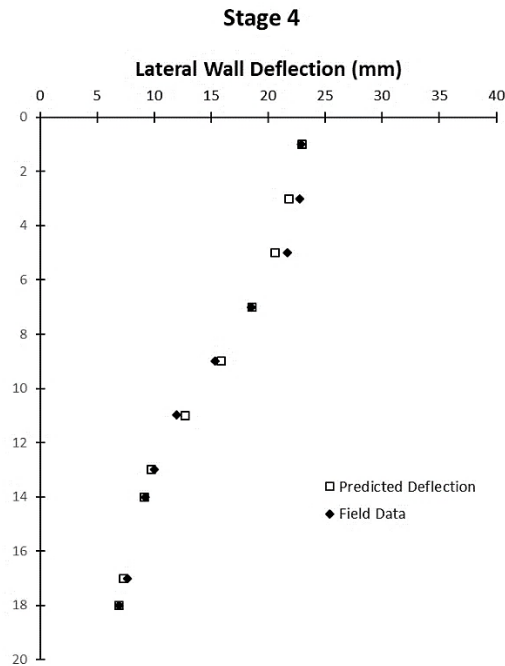


Figure 4.42. Measured versus Predicted Deflections of Stage 4: Parameters Optimized based on Stage 3 Observations

#### 4.5.4. Horizontal Displacement Prediction of Stage 5

Back calculated parameters obtained from Stage 4 is used to predict the horizontal deflection behavior of Stage 5. The comparison of measured inclinometer readings and the predicted horizontal deflections is illustrated in Figure 4-43. The fitness value is calculated as 0.0043 by optimized parameters which was calculated as 0.0096 by initial design parameters.

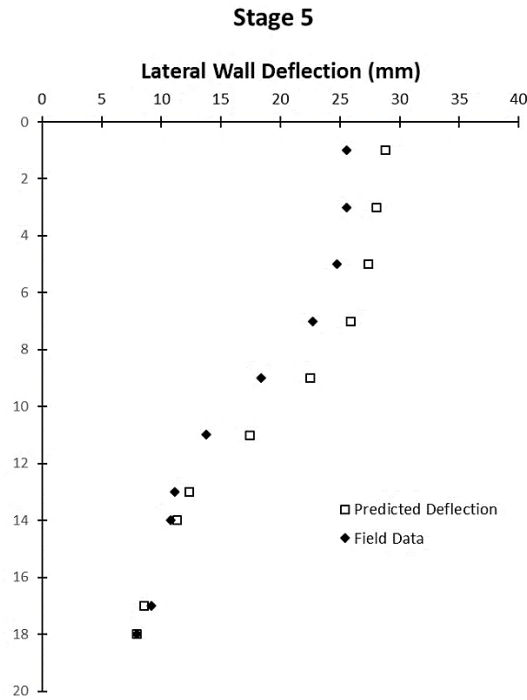


Figure 4.43. Measured versus Predicted Deflections of Stage 5: Parameters Optimized based on Stage 4 Observations

These results are satisfying since the observations used in the analyses give comparable predictions for subsequent stages. Back calculations based on PSO could predict the inclinometer results reasonably.

#### 4.6. Results and Comparisons

Calibration of soil parameters for selected stages by comparing measured field data and FEM results and thus extracting constitutive model parameters that reflect the soil behavior in a deep excavation case study is the primary interest of this thesis. The evolution of soil parameters is tabulated in Table 4-10 for each optimization stage. It is experienced that the parameter change in the hard clay layer has more effect on the behavior of the deep excavation than the upper clay layer for the abovementioned case

study as it is expected. The hard clay layer is the layer where the bottom of the excavation exists. Moreover, it is the firm clay layer where the pile tip is located.

The stiffness and the strength properties of the soil have an important impact on deformations. However, it is highly problematic to decide these parameter values precisely. Due to discontinuities in soil, its stress-strain response is inconstant (Marulanda, 2005). Available site investigations and laboratory tests may not be adequate in quantitative determinations especially for stiffness parameter ( $E_{50}^{ref}$ ) at smaller strains due to sampling disturbance. Moreover, there are number of factors that may affect the accuracy of results of numerical analyses including initial conditions on the ground such as at-rest in-situ stresses, ground water activities, complex pre-history of the construction, etc. Therefore, initial design parameters are contrasting with optimized parameters as illustrated in Table 4-10. These results indicated that the field conditions could not be reflected properly by site investigations and laboratory tests especially at small strains levels assuming that the factual observed field measurements and well represented finite element model.

Table 4.10. *Best-fit Values of Parameters at Each Optimization Stages*

	Alluvial Deposit Clay Layer			Hard Clay Layer		
	$E_{50}^{ref}$ (MPa)	$\phi'$ (degree)	$c'_{ref}$ (kPa)	$E_{50}^{ref}$ (MPa)	$\phi'$ (degree)	$c'_{ref}$ (kPa)
Initial	35	25	10	55	26	20
Stage 1	22.9	26.8	6.2	61.2	25.2	10.0
Stage 2	22.5	26.0	6.1	74.2	27.9	10.7
Stage 3	11.3	26.6	3.8	82.4	28.0	11.2
Stage 4	8.4	25.9	6.9	85.1	28.8	11.5
Stage 5	9.0	26.2	5.3	91.9	28.8	15.8

The conformity of the physical and numerical model shows the success of the optimization. In order to see the performance of the back-analysis platform, lateral deflections prior to any optimization and the lateral deflections computed by using optimized parameters are plotted and compared with the inclinometer results in Figure 4-44. In almost all the stages, the deflections computed by the initial design parameters are higher than the observed field deflections. On the other hand, the results using optimized parameters have high convergence rates in fitting the observed lateral deflections for all the stages. It can be deduced that; the back calculated parameters can simulate the lateral deflections. Comparing the fitness values is another way of examining the performance of the optimization as shown in Table 4-11. Calculated fitness values by optimized parameters are accepted as a feasible solution since they are lower than the threshold fitness value which is calculated as 0.0019 m.

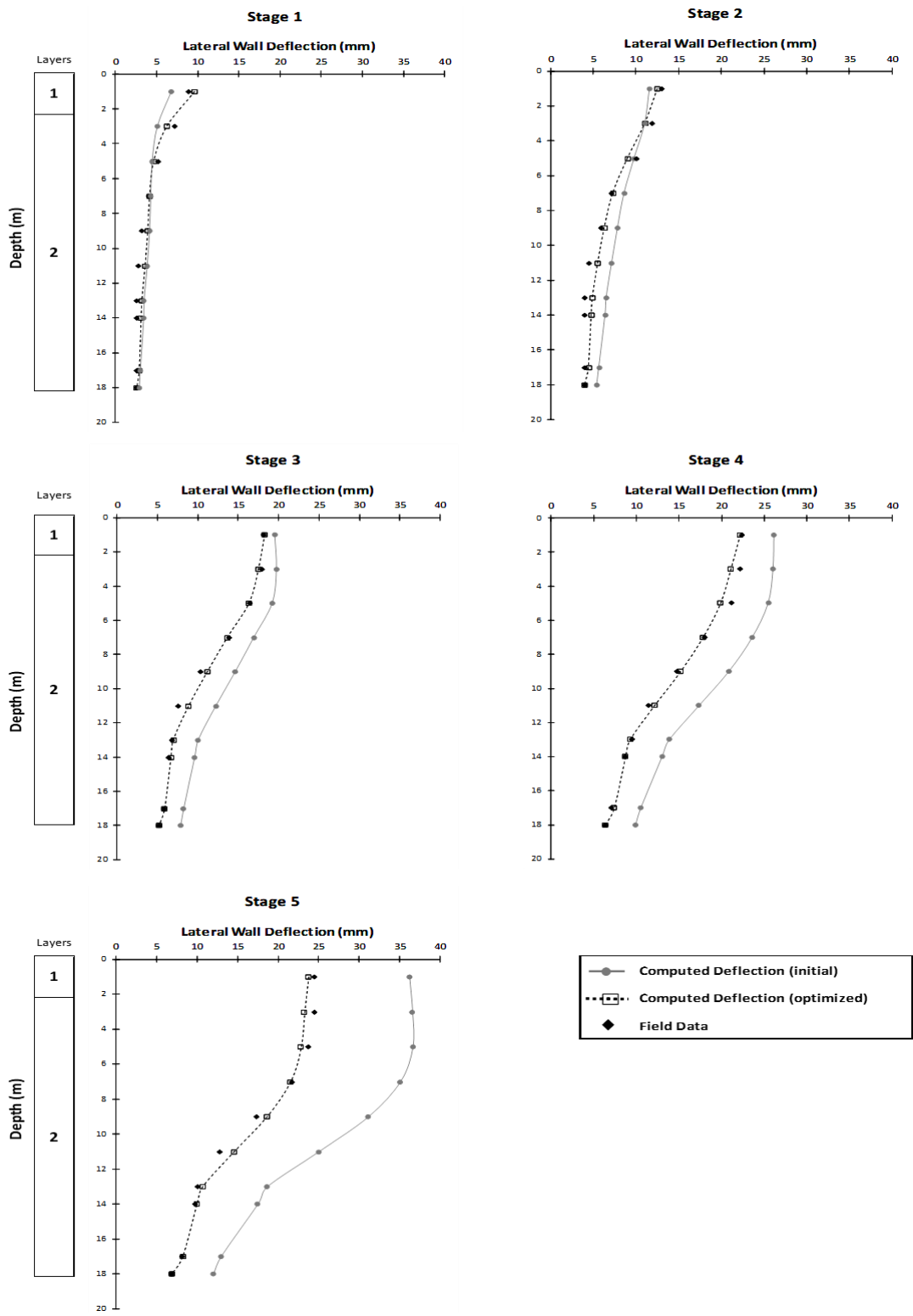


Figure 4.44. Comparison of Field Observed and Computed Deflections at each Stage using Initial Design Parameters and Best-fit Estimates of Parameters

Table 4.11. *Calculated Fitness Values at Each Optimization Stages*

	Fitness Values (m)				
	Stage 1	Stage 2	Stage 3	Stage 4	Stage 5
Initial Design Parameters	0.0027	0.0029	0.0021	0.0027	0.0096
Optimized Parameters	0.0010	0.0014	0.0013	0.0013	0.0018

Considering these comparisons, estimating soil geotechnical properties from the actual site conditions rather than initial investigations would be beneficial in the numerical analysis of deep excavations. Computed deflections by using back calculated parameters are in good agreement with the actual deflections. Additionally, the optimized material parameters can be used in the prediction of following stages' lateral deformations. Comparison of observed and the predicted deflections using parameters from the previous stage and initial estimates of parameters are illustrated in Figure 4-45. The discrepancy between these deflections are reasonable. Predicted results using optimized parameters have solid convergence rates in fitting actual deflections at Stages 2,3 and 4. The maximum difference is observed in Stage 5 and is less than %26 of actual horizontal displacement. These results show that back calculated parameters are not only used in lateral deflection computation at the observation stage but also beneficial in the prediction of horizontal deflections during/after construction. The predictions enable designers to understand a deep excavation's behavior even if not perfectly estimated. The design is updated throughout the excavation period due to continuously entered field measurements. Hence, any variation from the original design will be noticeable and possibly dealt with.

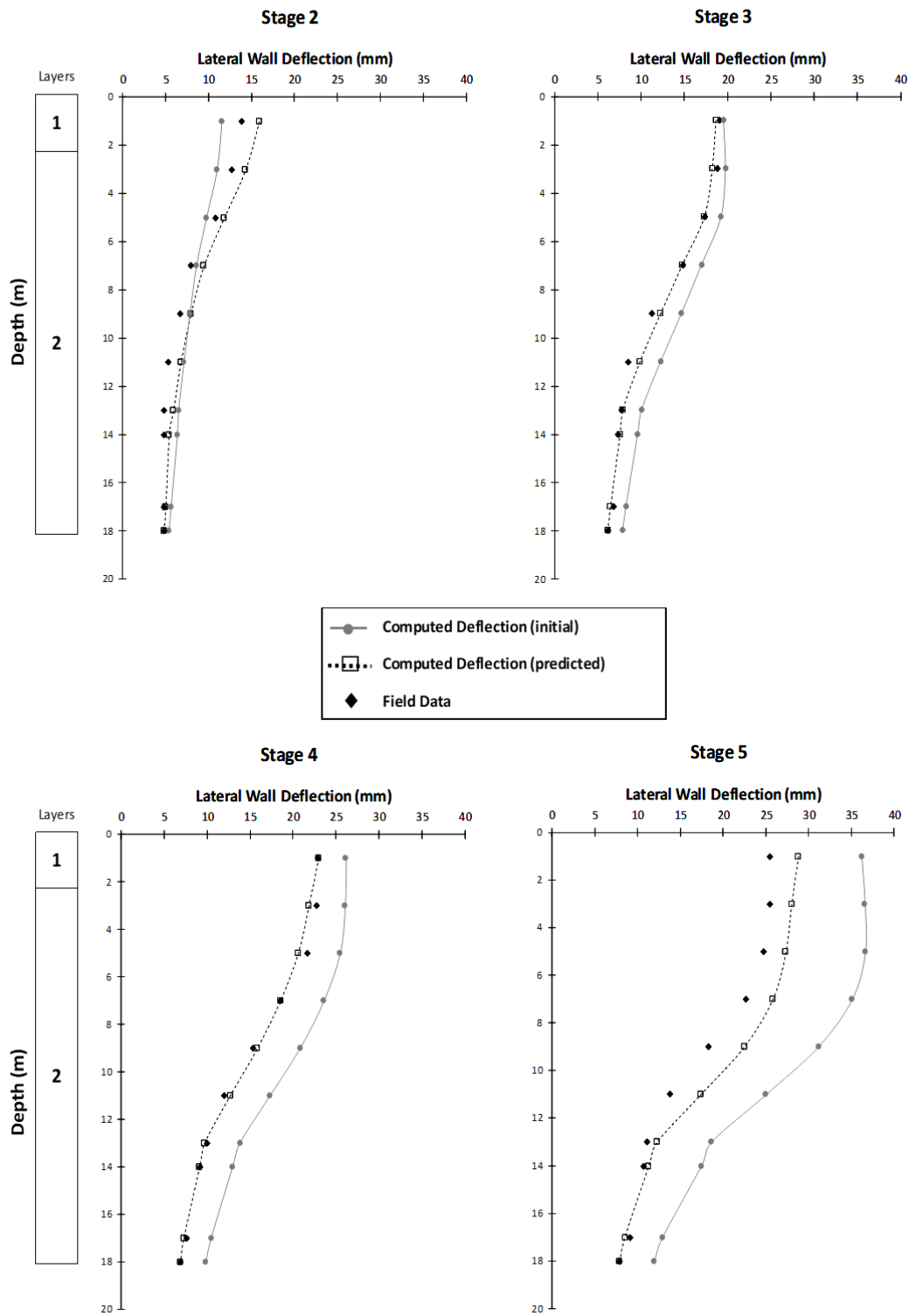


Figure 4.45. Comparison of Field Observed and Predicted Deflections for Stages 2-5 using Optimized Parameters from the Previous Stage and Initial Design Parameters

In the present study, both the lateral deflection computations at the observation stage and the deflection predictions of the subsequent stage are physically and numerically reasonable. However, as can be seen in Table 4-12, completion time of the optimization process is considered as a disadvantage. It takes around 25 minutes to complete one iteration at Stage 1 while it takes approximately 1 hour for Stage 5. 800 FEM runs need to be completed in the optimization of one stage. Nevertheless, the results obtained from the back analysis platform are valuable from the point of safety assurance and economy. It enables designers to modify geotechnical design during the deep excavation construction. Thus, the back calculation can be regarded as a required part of the geotechnical design. The completion period of optimization process can be reduced either by decreasing the number of iterations or the number of particles in the swarm. As it can be observed from the gBest values' evolution, 10 iterations are enough for optimization method to work well in the first four stages while the best fitness value is reached at 15<sup>th</sup> iteration at Stage 5. Separately, the number of particles in the swarm may be reduced. Although decreasing the number of particles in the swarm reduces the completion period, it may affect the performance of the optimization process adversely. One way to overcome this problem is that an experienced designer should decide the number of particles in the swarm after a few trials. Another way is to update the stopping criteria of optimization algorithm so that the process must stop when the fitness value is low enough until the discrepancy between the observed and calculated lateral displacements is an acceptable range.

Table 4.12. Completion Period of Each Optimization Stages

<b>FEM Calculation Phase</b>	<b>Construction Phase</b>	<b>Optimization Completion Period</b>
3/12	Excavate [-2,50 m] (Stage 1)	8 hours 30 minutes
6/12	Excavate [-5,00 m] (Stage 2)	12 hours
9/12	Excavate [-8,00 m] (Stage 3)	15 hours and 30 minutes
11/12	Excavate [-9,00 m] (Stage 4)	18 hours and 30 minutes
12/12	Excavate [-9,80 m] (Stage 5)	20 hours

## CHAPTER 5

### SUMMARY AND CONCLUSION

#### 5.1. Summary

The aim of this study was to develop a back analysis platform to obtain accurate geotechnical parameters of materials surrounding the deep excavations for safer and more economical designs. Developed platform consists of finite element based numerical modeling of deep excavation, optimization scheme and deflection monitoring throughout the excavation period. The commercial software, PLAXIS, is used to model the deep excavation and to compute the horizontal displacements. Material parameters are obtained by fitting the horizontal deflections obtained from the software and inclinometer data for selected construction stages through the widely used optimization technique named Particle Swarm Optimization (PSO) algorithm, coded using Python (version 3.6.0.). Obtained material parameters are then used to predict the upcoming stages' deformations. Periodically taken inclinometer readings are entered into the back analysis platform at the corresponding stages to calibrate the soil parameters.

The developed platform is applied to identify the soil parameters in a deep excavation project named Maidan Office-Home Office-Square project constructed in Ankara/Turkey. These parameters are then used for future predictions of deep excavation response. Firstly, deep excavation was numerically modeled by considering the actual construction scenario. Then, the back analysis was applied to identify the geotechnical parameters for Stage 1 by using the recorded inclinometer readings during the construction of Stage 1. The same procedure applied to Stages 2,3,4 and 5 as well. At the end of each run, geotechnical parameters are calibrated against newly entered field data. In addition, obtained parameters are used to predict

the next stage's lateral deflections. This is done by comparing the FEM results with the inclinometer readings. In conclusion, the evolution of soil parameters is observed, and it is clarified that the upcoming stages' behavior can be predicted during the excavation process by using calibrated parameters.

## 5.2. Findings of the Study

The reliability of results acquired from this study depends on many factors including factuality of the developed numerical model, accurate monitoring, etc. Firstly, true monitoring is the most essential component of a back analysis platform. Material parameters are obtained by fitting the FEM results and monitored inclinometer data. In other words, incorrect field monitoring causes improper material parameter identification through the back analysis platform. Secondly, the actual construction scenario and the behavior of soil surrounding the deep excavation should be represented by the numerical model. The deep excavation should be numerically modeled with the actual construction scenario in order to compare the corresponding inclinometer and FEM results. A selected constitutive model for soil behavior also has a significant share of the results. The back calculated parameters do not converge the actual values if the selected constitutive model is not appropriate. For instance, the hardening soil model is suitable for reflecting deep excavation response due to consideration of stress dependency whereas; stress dependency is not considered in the Mohr-Coulomb soil model. Another important factor is the number of parameters that are subjected to the optimization process. Every layer is defined by at least 8 different soil parameters in the hardening soil model, and some of them are highly correlated parameters such as  $E_{50}^{ref}$  and  $m$ . This number increased to 16 when two soil layers are existing in the analyses. It is almost impossible to optimize all the parameters at the same time since the number of available field data must be higher than the number of optimized parameters. Therefore, the designer should choose appropriate parameters to optimize in accordance with the available measurement

data. To exemplify, it would not be practical to optimize Poisson's ratio ( $\nu$ ) in linear elasticity model. In brief, not only PSO used in the present work but also all the metaheuristics-based optimization algorithms combined with FEM analysis concept do not secure a precise solution. For instance, numerous amalgamations of material properties may cause similar estimates of field deformations which in turn lead to a non-unique or non-converged solution. However, these setbacks can be minimized by increasing the number of selected points in the model and allowing the algorithm to run multiple times for longer periods as Nguyen (2011) suggests. Additionally, the geotechnical designer should be able to judge the consistency of optimized parameters by using engineering intuition.

Based on the performed finite element based back analyses and the literature, the following conclusions are inferred:

- This study shows that it is possible to increase the effectiveness of the geotechnical design of deep excavations in light of field monitoring data. Actual soil material parameters can be identified by the developed back analysis platform with true monitoring and numerical model. The results prove that geotechnical parameters were successfully obtained by using monitored inclinometer results through the back analysis platform. Back calculated parameters are then succeeded in the prediction of subsequent stage's horizontal deflections. The predictions enable designers to understand the global response of the deep excavation. The design is updated throughout the excavation period due to continuously entered field measurements. Hence, any variation from the original design will be noticeable and possibly dealt with at early stages of construction. The importance of uncertain factors including initial conditions on the ground such as at-rest in-situ stresses, groundwater activities, complex pre-history of the construction, etc. is highly reduced. Back analysis combined with finite element analysis and optimization algorithm forms an efficient numerical tool that provides safer and more economical design over the conventional methods. Conventional analysis presumes that

the excavation proceeds as it is designed while the design is always updateable in the back analysis.

- The field conditions could not be reflected properly by site investigations and laboratory tests. Available site investigations and laboratory tests may not be adequate in the quantitative determination of actual soil material parameters due to sample disturbance, construction effects, etc. These uncertainties were minimized by back calculation method by considering the continuous monitoring.
- It was observed that PSO is a highly prospering global optimization method. PSO demonstrated an effective and forceful way of procuring the solution in the early iterations of the optimization process. The method showed the high performance of solving a complex deep excavation problem even if the design variables are correlated. It was concluded that the PSO algorithm is suitable and applicable for parameter identification in deep excavation problems.
- The stiffness parameter ( $E_{50}^{ref}$ ) and the failure parameters ( $c'$  and  $\phi'$ ) have an impact on horizontal deformations. It is observed from the analyses that the stiffness parameter is more effective in controlling the horizontal deformations. It was also approved (Pakbaz et al. 2013) that the stiffness parameter (E) has more effect for small deformations at lower depths while failure parameters ( $c$  and  $\phi$ ) are more effective for significantly larger deformations because of soil's plastic behavior at greater depths.
- In the back calculation of material parameters of multiple soil layers, the layer's sensitivity to input parameters on excavation behavior shows an alteration. For instance, parameter change in a layer where the bottom of the excavation exists or layer where the pile tip is located has more effect on horizontal deformations. In the light of this information, in the case of multiple layer problems (more than 2 layers), it would be a good idea to combine two layers and analyze it as one layer when one of the layers has a considerably lower influence on the results. In this way, the number of parameters that are

subjected to optimization will be reduced, and the performance of the optimization process will be increased.

- The completion period of the optimization process is considered as a disadvantage. It takes around 8 hours and 30 minutes to complete Stage 1 optimization while it takes approximately 20 hours for Stage 5. In order to complete the optimization process of one stage, 800 FEM runs need to be completed in the present study. Reducing the number of iterations will shorten the completion period. Another alternative is decreasing the number of particles in the swarm to a certain extent since it may affect the performance of the optimization process adversely. The geotechnical designer should be able to judge the optimum number of particles and the iteration number. It would be more practical and user-friendly to update the stopping criteria of optimization algorithm so that the process stops when the fitness value is low enough until the discrepancy between the observed and calculated lateral displacements is in an acceptable range.

In the present work, metaheuristic-based soil parameter identification in deep excavation is studied. Back-analysis platform is established which combines the finite element model and the particle swarm optimization algorithm. The application and the sufficiency of the technique were presented. The benefits over the conventional methods of the platform were demonstrated. It enables designers to reassess the estimations, enhance the quality of the design and redesign in case of any variation from the design predictions during the construction. It is also applicable to complex deep excavation problems with multiple soil layers and input parameters. Consequently, the back analysis should be involved in field investigations for safe and economical geotechnical design.

### **5.3. Recommendations for Future Study**

- The back analysis platform developed in this thesis can be applied in different case studies involving deep excavation to validate the applicability of the method.
- Inclinometer readings are the only monitoring data used in this study. It would be more sophisticated and reliable if the stress inputs such as the load cell readings are also included in monitored data.
- In order to reduce the execution time of the optimization process, one of the best alternatives is to use popular machine learning technique “Artificial Neural Network (ANN)” instead of running FEM analyses for all the iterations. Hashash et. al, (2003) state that neural network based constitutive models are adopted to “learn or evolve” methodology and provide an insight into material behavior. ANN is operated by using previously attained artificial data from FEM analyses; they are used to find deflections once appropriate input values are provided

## REFERENCES

- Arora, J. S. (2004). *Introduction to optimum design*. Elsevier.
- Aungkulanon, P., Chaiead, N., & Luangpaiboon, P. (2010, March). Simulated manufacturing process improvement via particle swarm optimisation an firefly algorithms. In World Congress on Engineering 2012. July 4-6, 2012. London, UK. (Vol. 2189, pp. 1123-1128). International Association of Engineers.
- Becker, P., Gebreselassie, B., & Kempfert, H. G. (2008). Back analysis of a deep excavation in soft lacustrine clays.
- Bhatkar, T., Barman, D., Mandal, A., & Usmani, A. (2017). Prediction of behavior of a deep excavation in soft soil: a case study. *International Journal of Geotechnical Engineering*, 11(1), 10-19.
- Brinkgreve, R.B.J., Broere, W. and Waterman, D. (2009). *Plaxis 2D V9, Tutorial Manual and Material Models Manual*, Plaxis bv.
- Calvello, M., & Finno, R. J. (2004). Selecting parameters to optimize in model calibration by inverse analysis. *Computers and Geotechnics*, 31(5), 410-424.
- Cividini, A., Jurina, L., & Gioda, G. (1981, December). Some aspects of 'characterization' problems in geomechanics. In *International Journal of Rock Mechanics and Mining Sciences & Geomechanics Abstracts* (Vol. 18, No. 6, pp. 487-503). Pergamon.
- Clough, G. W. (1990). Construction induced movements of in situ walls. Design and performance of earth retaining structures, 439-470.
- Clough, G. W., & Duncan, J. M. (1971). Finite element analyses of retaining wall behavior. *Journal of Soil Mechanics & Foundations Div.*
- Clough, G.W., and O'Rourke, T.D., "Construction Induced Movements of Insitu Walls", *Design and Performance of Earth Retaining Structures*, ASCE, pp. 439-470, 1990
- Clough, G. W., & Tsui, Y. (1974). Performance of tied-back walls in clay. *Journal of Geotechnical and Geoenvironmental Engineering*, 100(Proc. Paper 11028).
- Clough, G. W., Smith, E. M., & Sweeney, B. P. (1989). Movement control of excavation support systems by iterative design. In *Foundation engineering: current principles and practices* (pp. 869-884). ASCE.
- Doğan, E., & Saka, M. P. (2012). Optimum design of unbraced steel frames to LRFD AISC using particle swarm optimization. *Advances in Engineering Software*, 46(1), 27-34.

- Du, H., Chi, S., & Wang, F. (2006, December). Using an Improved Particle Swarm Optimization for Back Analysis of Geotechnical Parameters of Concrete Face Rock-fill Dams. In 2006 Sixth International Conference on Hybrid Intelligent Systems (HIS'06) (pp. 66-66). IEEE
- Eberhart, R. C., Shi, Y., & Kennedy, J. (2001). Swarm intelligence. Elsevier.
- Finno RJ, Harahap IS. Finite element analyses of HDR-4 excavation. *Journal of Geotechnical and Geoenvironmental Engineering*, ASCE 1991; 117(10):1590–1609.
- Finno, R. J., & Calvello, M. (2005). Supported excavations: Observational method and inverse modeling. *Journal of Geotechnical and Geoenvironmental Engineering*, 131, 826–836
- Fletcher, R., & Reeves, C. M. (1964). CM: Function minimization by conjugate gradients. *Comput. j*, 7, 149-154.
- Fourie, P. C., & Groenwold, A. A. (2002). The particle swarm optimization algorithm in size and shape optimization. *Structural and Multidisciplinary Optimization*, 23(4), 259-267.
- Gens, A., Ledesma, A., & Alonso, E. E. (1996). Estimation of parameters in geotechnical backanalysis—II. Application to a tunnel excavation problem. *Computers and Geotechnics*, 18(1), 29-46.
- Ghaboussi, J., Pecknold, D. A., Zhang, M., & Haj-Ali, R. M. (1998). Autoprogressive training of neural network constitutive models. *International Journal for Numerical Methods in Engineering*, 42(1), 105-126.
- Gioda, G. (1985). Some remarks on back analysis and characterization problems in geomechanics. In 5th international conference on numerical methods in geomechanics (pp. 47-61). AA Balkema Publishers.
- Gioda, G., & Locatelli, L. (1999). Back analysis of the measurements performed during the excavation of a shallow tunnel in sand. *International Journal for Numerical and Analytical Methods in Geomechanics*, 23(13), 1407-1425.
- Gioda, G., & Maier, G. (1980). Direct search solution of an inverse problem in elastoplasticity: identification of cohesion, friction angle and in situ stress by pressure tunnel tests. *International Journal for Numerical Methods in Engineering*, 15(12), 1823-1848.
- Gioda, G., & Sakurai, S. (1987). Back analysis procedures for the interpretation of field measurements in geomechanics. *International Journal for Numerical and Analytical Methods in Geomechanics*, 11(6), 555-583.
- Goh, A. T. (1999). Genetic algorithm search for critical slip surface in multiple-wedge stability analysis. *Canadian Geotechnical Journal*, 36(2), 382-391.

- Goldberg, D. T., Jaworski, W. E., & Gordon, M. D. (1976). Lateral support systems and underpinning.
- Gouw, T. L. (2014). Common Mistakes on the Application of Plaxis 2D in Analyzing Excavation Problems. *International Journal of Applied Engineering Research*.
- Hasançebi, O., Çarbaş, S., & Saka, M. P. (2010). Improving the performance of simulated annealing in structural optimization. *Structural and Multidisciplinary Optimization*, 41(2), 189-203.
- Hasançebi, O., Çarbaş, S., Doğan, E., Erdal, F., & Saka, M. P. (2009). Performance evaluation of metaheuristic search techniques in the optimum design of real size pin jointed structures. *Computers & Structures*, 87(5-6), 284-302.
- Hashash, Y. (1992). Analysis of deep excavations in clay (Doctoral dissertation, Massachusetts Institute of Technology).
- Hashash, Y. M., & Whittle, A. J. (1996). Ground movement prediction for deep excavations in soft clay. *Journal of geotechnical engineering*, 122(6), 474-486.
- Hashash, Y. M., Fu, Q., & Butkovich, J. (2004). Generalized strain probing of constitutive models. *International journal for numerical and analytical methods in geomechanics*, 28(15), 1503-1519.
- Hashash, Y. M., Levasseur, S., Osouli, A., Finno, R., & Malecot, Y. (2010). Comparison of two inverse analysis techniques for learning deep excavation response. *Computers and geotechnics*, 37(3), 323-333.
- Hashash, Y. M., Marulanda, C., Ghaboussi, J., & Jung, S. (2003). Systematic update of a deep excavation model using field performance data. *Computers and Geotechnics*, 30(6), 477-488.
- Hashash, Y. M., Marulanda, C., Ghaboussi, J., & Jung, S. (2006). Novel approach to integration of numerical modeling and field observations for deep excavations. *Journal of Geotechnical and Geoenvironmental Engineering*, 132(8), 1019-1031.
- Hill, R. (1950). *The mathematical theory of plasticity*, Caledron Press, Oxford
- Horodecki, G. A., Bolt, A. F., & Dembicki, E. (2004). Deep excavation braced by diaphragm wall in Gdańsk (Poland).
- Hsiung, B. C. B. (2009). A case study on the behaviour of a deep excavation in sand. *Computers and Geotechnics*, 36(4), 665-675
- Jardine, R. J., Potts, D. M., Fourie, A. B., & Burland, J. B. (1986). Studies of the influence of non-linear stress-strain characteristics in soil-structure interaction. *Geotechnique*, 36(3), 377-396.

- Keidser, A., & Rosbjerg, D. (1991). A comparison of four inverse approaches to groundwater flow and transport parameter identification. *Water Resources Research*, 27(9), 2219-2232.
- Knabe, T., Datcheva, M., Lahmer, T., Cotecchia, F., & Schanz, T. (2013). Identification of constitutive parameters of soil using an optimization strategy and statistical analysis. *Computers and Geotechnics*, 49, 143-157.
- Knabe, T., Schweiger, H. F., & Schanz, T. (2012). Calibration of constitutive parameters by inverse analysis for a geotechnical boundary problem. *Canadian Geotechnical Journal*, 49(2), 170-183.
- Lecampion, B., Constantinescu, A., & Nguyen Minh, D. (2002). Parameter identification for lined tunnels in a viscoplastic medium. *International Journal for Numerical and Analytical Methods in Geomechanics*, 26(12), 1191-1211.
- Ledesma, A., Gens, A., & Alonso, E. E. (1996). Estimation of parameters in geotechnical backanalysis—I. Maximum likelihood approach. *Computers and Geotechnics*, 18(1), 1-27.
- Levasseur, S., Malécot, Y., Boulon, M., & Flavigny, E. (2008). Soil parameter identification using a genetic algorithm. *International Journal for Numerical and Analytical Methods in Geomechanics*, 32(2), 189-213.
- Levasseur, S., Malecot, Y., Boulon, M., & Flavigny, E. (2009). Statistical inverse analysis based on genetic algorithm and principal component analysis: method and developments using synthetic data. *International journal for numerical and analytical methods in geomechanics*, 33(12), 1485-1511.
- Levasseur, S., Malecot, Y., Boulon, M., & Flavigny, E. (2010). Statistical inverse analysis based on genetic algorithm and principal component analysis: applications to excavation problems and pressuremeter tests. *International journal for numerical and analytical methods in geomechanics*, 34(5), 471-491.
- Lunne, T., Powell, J. J., & Robertson, P. K. (2002). *Cone penetration testing in geotechnical practice*. CRC Press.
- Ma, J. Q., Berggren, B. S., Bengtsson, P. E., Stille, H., & Hintze, S. (2006, August). Back analysis on a deep excavation in Stockholm with finite element method. In *Proc. 6th European Conference on Numerical Methods in Geotechnical Engineering*, Graz, Austria (pp. 423-429).
- Mana, A. I., & Clough, G. W. (1981). Prediction of movements for braced cuts in clay. *Journal of Geotechnical and Geoenvironmental Engineering*, 107(ASCE 16312 Proceeding).
- Ma'ruf, M. F., & Darjanto, H. (2017). Back Calculation of Excessive Deformation on Deep Excavation. *Procedia Engineering*, 171, 502-510.

- Marulanda, C. (2005). Integration of numerical modeling and field observations of deep excavations. University of Illinois at Urbana-Champaign.
- Meier, J., Schaedler, W., Borgatti, L., Corsini, A., & Schanz, T. (2008). Inverse parameter identification technique using PSO algorithm applied to geotechnical modeling. *Journal of Artificial Evolution and Applications*, 2008, 3.
- Mikkelsen, P. E. (1996). Landslides: Investigation and mitigation. Chapter 11-Field instrumentation. Transportation Research Board Special Report, (247).
- Miranda, T., Dias, D., Eclaircy-Caudron, S., Correia, A. G., & Costa, L. (2011). Back analysis of geomechanical parameters by optimisation of a 3D model of an underground structure. *Tunnelling and Underground Space Technology*, 26(6), 659-673.
- Miranda, T., Dias, D., Eclaircy-Caudron, S., Correia, A. G., & Costa, L. (2011). Back analysis of geomechanical parameters by optimisation of a 3D model of an underground structure. *Tunnelling and Underground Space Technology*, 26(6), 659-673.
- Moreira, N., Miranda, T., Pinheiro, M., Fernandes, P., Dias, D., Costa, L., & Sena Cruz, J. (2013). Back analysis of geomechanical parameters in underground works using an Evolution Strategy algorithm. *Tunnelling and Underground Space Technology*, 33, 143-158.
- Mulia, A. (2012). Identification of Soil constitutive soil model parameters using multi objective particle swarming optimization (Doctoral dissertation, Master thesis, National Taiwan University of Science and Technology, Taipei, Taiwan).
- Nelder, J. A., & Mead, R. (1965). A simplex method for function minimization. *The computer journal*, 7(4), 308-313.
- Nguyen-Tuan, L., Lahmer, T., Datcheva, M., Stoimenova, E., & Schanz, T. (2016). A novel parameter identification approach for buffer elements involving complex coupled thermo hydro-mechanical analyses. *Computers and Geotechnics*, 76, 23-32.
- Osouli, A., & Hashash, Y. M. (2009). The Relationship between Field Measurements and Soil Behavior in TNEC Deep Excavation. In *Contemporary Topics in Ground Modification, Problem Soils, and Geo-Support* (pp. 169-176).
- Ou, C. Y., & Tang, Y. G. (1994). Soil parameter determination for deep excavation analysis by optimization. *Journal of the Chinese Institute of Engineers*, 17(5), 671-688.
- Ou, C. Y., Chiou, D. C., & Wu, T. S. (1996). Three-dimensional finite element analysis of deep excavations. *Journal of Geotechnical Engineering*, 122(5), 337-345.

- Pal, S., Wathugala, G. W., & Kundu, S. (1996). Calibration of a constitutive model using genetic algorithms. *Computers and Geotechnics*, 19(4), 325-348.
- Papon, A., Riou, Y., Dano, C., & Hicher, P. Y. (2012). Single-and multi-objective genetic algorithm optimization for identifying soil parameters. *International Journal for Numerical and Analytical Methods in Geomechanics*, 36(5), 597-618.
- Peck, R. B. (1969). Deep excavations and tunneling in soft ground. *Proc. 7th ICSMFE*, 1969, 225-290.
- PLAXIS 2D 2010 Material Models Manual (2010). Delft University of Technology & PLAXIS B.V.
- PLAXIS 2D 2010 Reference Manual (2010). Delft University of Technology & PLAXIS B.V.
- Poeter, E. P., & Hill, M. C. (1997). Inverse models: A necessary next step in ground water modeling. *Groundwater*, 35(2), 250-260.
- Poeter, E. P., & Hill, M. C. (1998). Documentation of UCODE, a computer code for universal inverse modeling. DIANE Publishing.
- Potts, D. M., & Fourie, A. B. (1984). The behaviour of a propped retaining wall: results of a numerical experiment. *Geotechnique*, 34(3), 383-404.
- Powell, M. J. (1964). An efficient method for finding the minimum of a function of several variables without calculating derivatives. *The computer journal*, 7(2), 155-162.
- Prevost, J. H., & Popescu, R. (1996). Constitutive relations for soil materials. *Electronic journal of geotechnical engineering*, 1.
- Rechea, C., Levasseur, S., & Finno, R. (2008). Inverse analysis techniques for parameter identification in simulation of excavation support systems. *Computers and Geotechnics*, 35(3), 331-345.
- Sadoghi Yazdi, J., Kalantary, F., & Sadoghi Yazdi, H. (2011). Calibration of soil model parameters using particle swarm optimization. *International Journal of Geomechanics*, 12(3), 229-238.
- Saka, M. P. (2007). Optimum design of steel frames using stochastic search techniques based on natural phenomena: a review. *Civil engineering computations: tools and techniques*, 6, 105-147.
- Saka, M. P., & Dogan, E. (2012). Recent developments in metaheuristic algorithms: a review. *Comput Technol Rev*, 5(4), 31-78.

- Sakurai, S. (1993). Back analysis in rock engineering. In: J. A. Hudson, T. Brown, C. Fairhurst and E. Hoek (Eds.) *Comprehensive Rock Engineering*, (4) Pergamon Press, pp. 543-569.
- Sakurai, S. (1997). Lessons learned from field measurements in tunneling. *Tunneling and underground space technology*, 12(4), 453-460.
- Sakurai, S., Akutagawa, S., Takeuchi, K., Shinji, M., Shimizu, N. (2003). Back analysis for tunnel engineering as a modern observational method. *Tunnelling and Underground Space Technology* 18, 185–196
- Sakurai, S., & Takeuchi, K. (1983). Back analysis of measured displacements of tunnels. *Rock mechanics and rock engineering*, 16(3), 173-180.
- Sakurai, S., Abe, S. (1981). Direct strain evaluation technique in construction of underground opening. *Proceedings, 22nd U.S Symposium on Rock Mechanics: Rock Mechanics from Research to Application*, MIT, Cambridge, Massachusetts, pp. 278- 282.
- Samarajiva, P., Macari, E. J., & Wathugala, W. (2005). Genetic algorithms for the calibration of constitutive models for soils. *International Journal of Geomechanics*, 5(3), 206-217.
- Schanz, T. (1999). Formulation and verification of the Hardening-Soil Model. *RBJ Brinkgreve, Beyond 2000 in Computational Geotechnics*, 281-290.
- Schanz, T., Zimmerer, M. M., Datcheva, M., & Meier, J. (2006). Identification of constitutive parameters for numerical models via inverse approach. *Felsbau*, 24(2), 11-21.
- Shao, Y. C. (1999). *Information feedback analysis in deep excavations* (Doctoral dissertation, Georgia Institute of Technology).
- Shao, Y., & Macari, E. J. (2008). Information feedback analysis in deep excavations. *International Journal of Geomechanics*, 8(1), 91-103.
- Simpson, A. R., & Priest, S. D. (1993). The application of genetic algorithms to optimization problems in geotechnics. *Computers and Geotechnics*, 15(1), 1-19.
- Sloan, S. W., & Randolph, M. F. (1982). Numerical prediction of collapse loads using finite element methods. *International Journal for Numerical and Analytical Methods in Geomechanics*, 6(1), 47-76.
- Tang, Y. G., Kung, T. C., & Hsieh, P. G. (2006). Identification of soil parameters for excavation using optimum method.
- Tarantola, A. (2005). *Inverse problem theory and methods for model parameter estimation* (Vol. 89). siam.

- Tjie-Liong, G. O. U. W. (2014). Common mistakes on the application of Plaxis 2D in analyzing excavation problems. *International Journal of Applied Engineering Research*, 9(21), 8291-8311.
- Totsev, A., & Jelle, J. (2009). Slope stability analysis using conventional methods and FEM. In *17th International Conference on Soil Mechanics and Geotechnical Engineering*.
- Tsai, J. T., Liu, T. K., & Chou, J. H. (2004). Hybrid Taguchi-genetic algorithm for global numerical optimization. *IEEE Transactions on evolutionary computation*, 8(4), 365-377.
- Van Den Bergh, F. (2001). An analysis of particle swarm optimizers (Doctoral dissertation, University of Pretoria).
- Vardakos, S. (2007). Back-analysis methods for optimal tunnel design (Doctoral dissertation, Virginia Tech).
- Venter, G., & Sobieszczanski-Sobieski, J. (2004). Multidisciplinary optimization of a transport aircraft wing using particle swarm optimization. *structural and Multidisciplinary optimization*, 26(1-2), 121-131.
- Vogt, N., & Totsev, A. (2006). Back-analysis of collapsed excavation. *Zeitschrift "Stroitelstvo"*, (3).
- Voss, S. (2000, August). Meta-heuristics: The state of the art. In *Workshop on Local Search for Planning and Scheduling* (pp. 1-23). Springer, Berlin, Heidelberg.
- Wang, J. H., Xu, Z. H., & Wang, W. D. (2009). Wall and ground movements due to deep excavations in Shanghai soft soils. *Journal of Geotechnical and Geoenvironmental Engineering*, 136(7), 985-994.
- Whittle, A. J., Hashash, Y. M., & Whitman, R. V. (1993). Analysis of deep excavation in Boston. *Journal of geotechnical engineering*, 119(1), 69-90.
- Yang, X. S. (2010). *Engineering optimization: an introduction with metaheuristic applications*. John Wiley & Sons.
- Yin, Z. Y., Jin, Y. F., Shen, J. S., & Hicher, P. Y. (2018). Optimization techniques for identifying soil parameters in geotechnical engineering: comparative study and enhancement. *International Journal for Numerical and Analytical Methods in Geomechanics*, 42(1), 70-94.
- Yoo, C. (2001). Behavior of braced and anchored walls in soils overlying rock. *Journal of Geotechnical and Geoenvironmental Engineering*, 127(3), 225-233.
- Yoo, C., & Lee, D. (2008). Deep excavation-induced ground surface movement characteristics—A numerical investigation. *Computers and Geotechnics*, 35(2), 231-252.

- Zentar, R., Hicher, P. Y., & Moulin, G. (2001). Identification of soil parameters by inverse analysis. *Computers and Geotechnics*, 28(2), 129-144.
- Zhang, C., Shao, H., & Li, Y. (2000, October). Particle swarm optimisation for evolving artificial neural network. In *Smc 2000 conference proceedings. 2000 IEEE international conference on systems, man and cybernetics. 'cybernetics evolving to systems, humans, organizations, and their complex interactions'*(cat. no. 0 (Vol. 4, pp. 2487-2490). IEEE.
- Zhang, Y., Gallipoli, D., & Augarde, C. (2013). Parameter identification for elasto plastic modelling of unsaturated soils from pressuremeter tests by parallel modified particle swarm optimization. *Computers and Geotechnics*, 48, 293-303.
- Zhang, Y., Gallipoli, D., & Augarde, C. E. (2009). Simulation-based calibration of geotechnical parameters using parallel hybrid moving boundary particle swarm optimization. *Computers and Geotechnics*, 36(4), 604-615.
- Zhao, H. B., & Yin, S. (2009). Geomechanical parameters identification by particle swarm optimization and support vector machine. *Applied Mathematical Modelling*, 33(10), 3997-4012.
- Zhao, B. D., Zhang, L. L., Jeng, D. S., Wang, J. H., & Chen, J. J. (2015). Inverse analysis of deep excavation using differential evolution algorithm. *International Journal for Numerical and Analytical Methods in Geomechanics*, 39(2), 115-134.



## APPENDICES

### A. Borehole Logs

TOKER DRILLING and CONSTRUCTION ENGINEERING CONSULTING CO		<b>SONDAJ LOGU</b> <b>BOREHOLE LOG</b>		SONDAJ NO / BOREHOLE NO <b>SK-14</b> SAYFA NO / PAGE NO <b>1 of 3</b>												
PROJE ADI / PROJECT:		EGE GRUP 25389 ADA 3 PARSEL ZEMİN ETÜDÜ														
KOORDİNATLAR / COORDINATES:		X: 479962.2824	Y: 4419659.0696													
SONDAJ KOTU / ELEVATION (m):		853.76														
SONDAJ DERİNLİĞİ / BORING DEPTH (m):		40.1		YERALTI SUYU DURUMU / GROUND WATER DATA												
BAŞLAMA TARİHİ / DATE STARTED:		25.09.2013		DERİNLİK / DEPTH (m):	TARİH / DATE:											
BİTİŞ TARİHİ / DATE COMPLETED:		28.09.2013		6.16m	09.10.2013											
SONDAJ MAKİNESİ / DRILLING RIG:		PSM-4		5.9m	10.10.2013											
SONDÖR / FOREMAN:		M. Güneş														
MÜHENDİS / ENGINEER:		M. Dinçer														
DERİNLİK / DEPTH (m)	NİHAZ (BOZULUŞ) / ELEVATION (m)	TOZ (N)	BOZ (N)	RÖZ (N)	NAMINE DERİNLİĞİ / SAMPLE DEPTH	ZEMİN TANIMLAMASI / SOIL DESCRIPTION	ZEMİN SUYU / SOIL MOISTURE (%)	ZEMİN SUYU / SOIL MOISTURE (%)	ZEMİN SUYU / SOIL MOISTURE (%)	ZEMİN SUYU / SOIL MOISTURE (%)	ZEMİN SUYU / SOIL MOISTURE (%)	ST. PENETRASYON DENENİ / ST. PENETRATION TEST			N <sub>60</sub>	
												0-10	10-30	30-45		
1	99					BITKİSEL TOPRAK										
2	98				SPT-1	1.5	1.95						7	9	10	N=19
3	97				UD-1	3	3.3									
4	96				SPT-2	3.3	3.75						18	34	11	N=45
5	95				UD-2	4.5	4.9									
6	94				SPT-3	4.9	5.35						5	11	24	N=35
7	93				SPT-4	6	6.45						4	4	8	N=12
8	92				UD-3	7.5	7.75									
9	91				SPT-5	7.75	8.2						12	19	24	N=43
10	90				SPT-6	9	9.45									
11	89				UD-4	10.5	10.75									
12	88				SPT-7	10.75	11.08						48	45	50/3	50+
13	87				SPT-8	12	12.21						49	50/6		50+
14	86				UD-5	13.5	13.95									
15	85				SPT-9	13.95	14.4						13	19	15	N=34
KIVAM DURUM / STIFFNESS		SİKLİK / DENSITY		GRANLAR / DISCONTINUITIES		KIRIKLAR / 30 cm - FRACTURES / 30 cm										
N = 0-2 Çok yumuşak	Very Soft	N = 0-4 Çok gevşek	Very Loose	0-10 % Pek az (Seyrek)	Trace	> 1 Seyrek	Little (M)									
N = 3-4 Yumuşak	Soft	N = 5-10 Gevşek	Loose	10-20 % Az	Little	1-2 Orta	Moderate (M)									
N = 5-9 Orta katı	Mid. Stiff	N = 11-30 Orta sıkı	Mid. Dense	20-35 % Sıfır	Adjective (some)	2-10 Sık	Close (C)									
N = 9-15 Katı	Stiff	N = 31-50 Sıkı	Dense	35-50 % Ve	And	10-20 Çok sık	Intense (I)									
N = 15-30 Çok katı	Very Stiff	N > 50 Çok Sıkı	Very Dense			> 30 Parçalı	Crushed (C)									
N > 30 Sert	Hard															
DAYANIMLILIK / STRENGTH		AYRISMA / WEATHERING		KAYA KALİTESİ TANIMI / RQD		AÇIKLAMALAR / REMARKS										
R0: Aşırı derinde zayıf	Extremely weak	I Taze	Fresh	0-25 % Çok zayıf	Very poor	UD: Örselememiş Numune / Undist. Sample										
R1: Çok zayıf	Very weak	II Az ayrılmış	Slightly weathered	25-50 % Zayıf	Fair	D: Örselemiş Numune / Disturbed Sample										
R2: Zayıf	Weak	III Orta ayrılmış	Mod. weathered	50-75 % Orta	Good	SPT: Standart Frez. Deneyi / St. Penet. Test										
R3: Orta dayanımlı	Medium	IV Çok ayrılmış	Highly weathered	75-90 % İyi	Excellent	VST: Vane Deneyi / Vane Shear Test										
R4: Dayanıklı	Strong	V Tamamen ayrılmış	Comp. weathered	90-100 % Çok İyi		P: Presiyometre Deneyi / Press. Test										
R5: Çok Dayanıklı	Very strong					K: Karot Numunesi / Core Sample										
R6: Aşırı dayanıklı	Extremely strong															

Figure A.1. Borehole Log 1/3





## B. Inclinometer #2 Readings

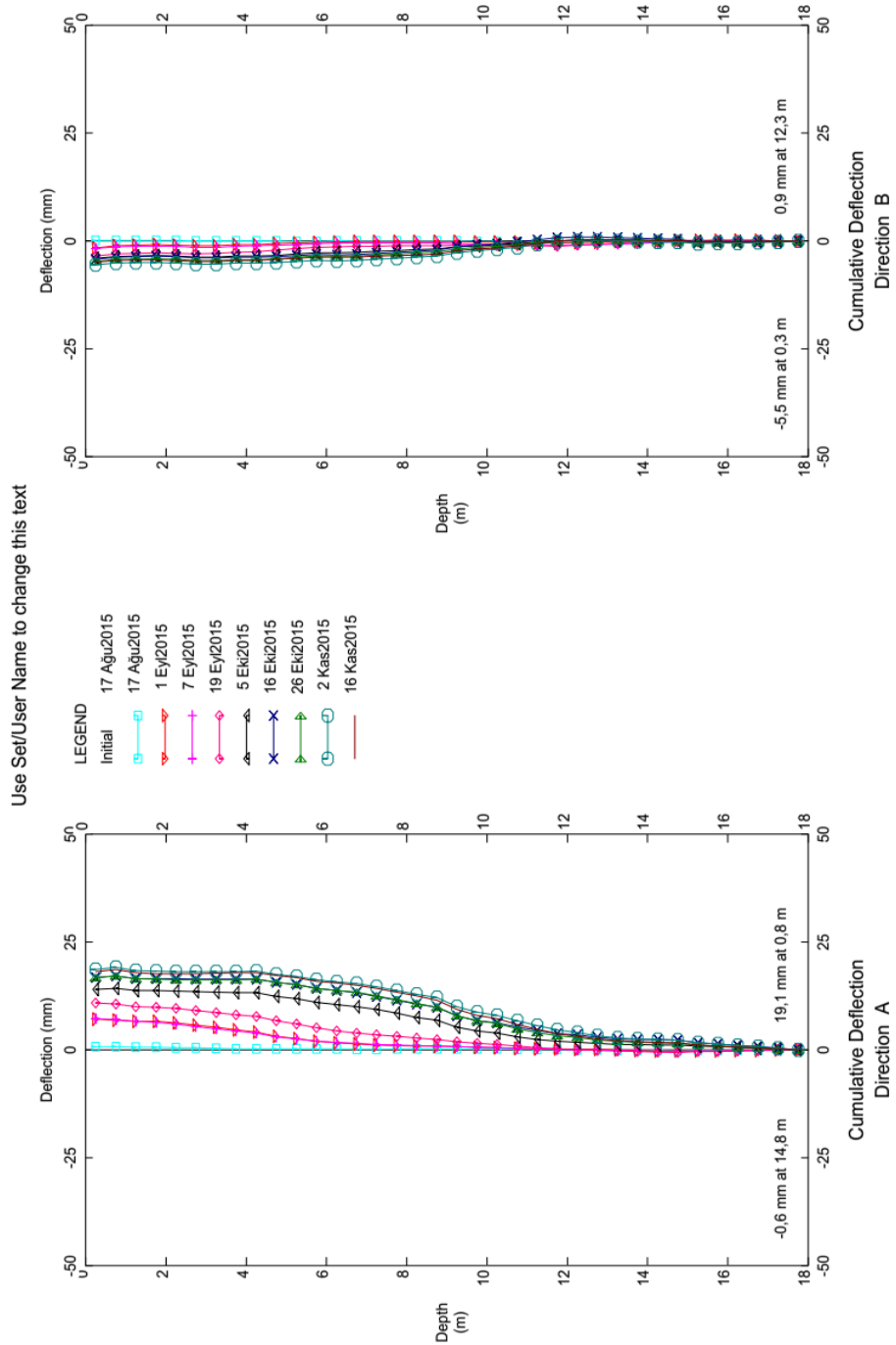


Figure B.1. Inclinometer #2 Readings

## C. Laboratory Test Results

7OKER		Zemin Mekaniği Laboratuvarı Soil Mechanics Laboratory		DENEY SONUÇLARI TABLOSU TABLE OF TEST RESULTS		Rapor/Rapor No:0716/ 2013 Sayfa/Page: 9		Firma/Date: 30.08.2013		Bakanlık Rapor No:2525669												
Örnek/Şantiye/Sitesi /Zem. No:38 TEL:3546433		OSTİM - ANKARA		Ege Grup- 25389 ADA 3 PARSEL Zemin Etüdü		Ege Grup		MÜŞTERİ / CLIENT:		Ege Grup												
SONDAJ BÖRİNG NO	NUMUNE SAMPLE NO	DERİNLİK DEPTH (m)	W <sub>n</sub> (%)	Y <sub>a</sub> KN/m <sup>3</sup>	C <sub>u</sub>	ATTERBERG LİMİTLERİ ATTERBERG LIMITS			ELEK ANALİZİ SİEVE ANALYSIS (% <sub>60</sub> Çapına Kadar Geçen)				U <sub>c</sub>	S <sub>c</sub>	S <sub>u</sub>	M <sub>v</sub>	DİREKT KESME DENEYİ SHEAR TEST	ÜÇ EKSENLİ BASINCI DENEYİ TRIAxIAL COMPRESSION TEST	SİRİŞTİRİLMİŞ DENEYİ UNCONSOLIDATED COMPRESSION TEST	KONSOLIDASYON DENEYİ CONSOLIDATION TEST		
						LL	PL	PI	4	10	40	200									c	ø
SK-14	SPT-1	1,50-1,95	22,5			56,9	23,4	33,5	100,0	99,7	99,0	96,3	CH									
SK-14	UD-2	4,50-4,90	21,0	19,60	2,52	67,3	24,3	43,0	100,0	98,4	96,0	92,2	CH	X								
SK-14	SPT-5	7,75-8,20	33,4			71,5	26,9	44,7	100,0	100,0	99,8	99,3	CH									
SK-14	UD-4	10,50-10,75	29,0		2,65	39,3	21,0	18,3	85,9	84,4	82,9	80,5	CL									X
SK-14	UD-5	13,50-13,95	23,5	19,01		93,8	30,0	63,8	95,0	91,1	86,3	81,0	CH									
SK-14	UD-6	16,50-16,90	31,7	18,98	2,61	79,6	24,2	55,4	97,8	96,8	94,3	89,6	CH									X
SK-14	SPT-13	19,50-19,90	30,2			72,6	27,3	45,3	99,8	98,5	96,2	90,1	CH									
SK-14	UD-7	22,50-22,60	27,9			85,7	32,5	63,2	99,7	99,0	96,9	92,4	CH									
SK-14	SPT-16	24,00-24,09	17,9			55,2	21,6	33,7	60,5	52,6	40,3	25,3	GC									
SK-14	SPT-18	27,00-27,35	29,6			71,0	24,3	46,7	100,0	99,6	98,6	94,1	CH									
SK-14	UD-8	28,50-28,60	31,4			84,4	29,4	55,0	95,8	92,1	90,4	85,3	CH									
SK-14	SPT-21	31,50-31,62	31,9			75,1	23,7	51,5	100,0	99,1	96,5	90,5	CH									
SK-14	SPT-23	34,50-34,64	29,4			69,8	26,1	43,7	96,0	93,5	87,6	80,7	CH									
SK-14	SPT-25	38,00-38,12	30,4			77,4	28,5	48,9	99,7	99,2	97,9	95,6	CH									
SK-15	SPT-1	1,50-1,95	22,1			52,5	20,0	32,6	60,8	52,5	42,7	29,3	GC									
SK-15	UD-1	4,50-4,90	29,3	19,87		65,8	23,8	42,0	100,0	100,0	99,8	96,9	CH									
SK-15	SPT-5	7,50-8,00	29,4			63,2	23,9	39,3	100,0	100,0	99,7	96,1	CH									
SK-15	UD-3	10,50-10,95	13,7	19,32	2,56	70,9	28,3	42,6	100,0	100,0	98,6	94,7	CH									X
SK-15	UD-4	13,50-14,00	29,1	18,94		91,3	27,4	63,9	96,7	95,0	92,1	86,7	CH									
SK-15	SPT-11	16,50-17,00	23,0			52,6	23,7	28,9	99,4	98,5	94,0	79,4	CH									
SK-15	UD-6	19,50-19,75	33,0	18,43	2,64	65,3	24,5	40,9	100,0	96,4	89,2	81,1	CH									X
SK-15	UD-7	22,50-22,70	23,3			57,1	19,8	37,3	92,6	90,4	87,0	78,6	CH									
SK-15	SPT-17	26,00-26,45	12,2			31,5	15,5	16,0	68,8	47,5	25,8	12,7	SC									

Laboratuvarımızın izni olmadan çoğaltılamaz.  
Çoğaltılması gerektiğinde adı, gibidir, kağıdı ve lab. Deneyinin imzası gereklidir.  
Deneyi Yapan/Etüt: TUC  
Laboratuvar Deneyselçisi  
Emrahullah K.ULUM  
Jen. AMB.  
Doküman No: T.Den.017

Figure C.1. Laboratory Test Results